

Adjacent-Bits-Swapped Polar codes: A new code construction to speed up polarization

Guodong Li

Min Ye

Sihuang Hu

Abstract

The construction of polar codes with code length $n = 2^m$ involves m layers of polar transforms. In this paper, we observe that after each layer of polar transforms, one can swap certain pairs of adjacent bits to accelerate the polarization process. More precisely, if the previous bit is more reliable than its next bit under the successive decoder, then switching the decoding order of these two adjacent bits will make the reliable bit even more reliable and the noisy bit even noisier.

Based on this observation, we propose a new family of codes called the Adjacent-Bits-Swapped (ABS) polar codes. We add a permutation layer after each polar transform layer in the construction of the ABS polar codes. In order to choose which pairs of adjacent bits to swap in the permutation layers, we rely on a new polar transform that combines two independent channels with 4-ary inputs. This new polar transform allows us to track the evolution of every pair of adjacent bits through different layers of polar transforms, and it also plays an essential role in the Successive Cancellation List (SCL) decoder for the ABS polar codes. Extensive simulation results show that ABS polar codes consistently outperform standard polar codes by 0.15 dB—0.6 dB when we use CRC-aided SCL decoder with list size 32 for both codes. The implementations of all the algorithms in this paper are available at <https://github.com/PlumJelly/ABS-Polar>

I. INTRODUCTION

Polar codes and Reed-Muller (RM) codes are two closely related code families in the sense that their generator matrices are formed of rows from the same square matrix. Although RM codes were discovered several decades earlier than polar codes, the capacity-achieving property of RM codes was established very recently. Specifically, polar codes were proposed by Arikan in [1] and were shown to achieve capacity on all Binary Memoryless Symmetric (BMS) channels in the same paper. In contrast, RM codes were proposed back in 1950s [2], [3], but the question of whether RM codes achieve capacity remains open for more than 60 years until the recent breakthroughs. It was shown in [4] that RM codes achieve capacity on Binary Erasure Channels (BEC) under the block-MAP decoder. More recently, Reeves and Pfister proved that RM codes achieve capacity on all BMS channels under the bit-MAP decoder [5].

While both code families achieve capacity of BMS channels, simulation results [6], [7] and theoretical analysis [8], [9] suggest that RM codes have better finite-length performance than polar codes. It was conjectured in [10] that this is because RM codes polarize even faster than polar codes. More precisely, in polar coding framework, we multiply a message vector consisting of $n = 2^m$ message bits with the matrix $\mathbf{G}_n^{\text{polar}} = (\mathbf{G}_2^{\text{polar}})^{\otimes m}$ and transmit the resulting codeword vector through a BMS channel. Here $\mathbf{G}_2^{\text{polar}} = \begin{bmatrix} 1 & 0 \\ 1 & 1 \end{bmatrix}$, and \otimes is the Kronecker product. The message bits are divided into information bits and

Research partially funded by National Key R&D Program of China under Grant No. 2021YFA1001000, National Natural Science Foundation of China under Grant No. 12001322, Shandong Provincial Natural Science Foundation under Grant No. ZR202010220025, and a Taishan scholar program of Shandong Province.

Guodong Li is with School of Cyber Science and Technology, Shandong University, Qingdao, Shandong, 266237, China. Email: guodongli@mail.sdu.edu.cn

Min Ye is with Tsinghua-Berkeley Shenzhen Institute, Tsinghua Shenzhen International Graduate School, Shenzhen 518055, China. Email: yeemmi@gmail.com

Sihuang Hu is with Key Laboratory of Cryptologic Technology and Information Security, Ministry of Education, Shandong University, Qingdao, Shandong, 266237, China and School of Cyber Science and Technology, Shandong University, Qingdao, Shandong, 266237, China. Email: hushuang@sdu.edu.cn

frozen bits according to their reliability under the successive decoder. This polar coding framework can also be used to analyze RM codes. To that end, we replace the recursive relation $\mathbf{G}_n^{\text{polar}} = \mathbf{G}_{n/2}^{\text{polar}} \otimes \mathbf{G}_2^{\text{polar}}$ in the standard polar code construction with $\mathbf{G}_n^{\text{RM}} = \mathbf{P}_n^{\text{RM}}(\mathbf{G}_{n/2}^{\text{RM}} \otimes \mathbf{G}_2^{\text{polar}})$. Here \mathbf{P}_n^{RM} is an $n \times n$ permutation matrix which reorders the rows of $\mathbf{G}_{n/2}^{\text{RM}} \otimes \mathbf{G}_2^{\text{polar}}$ according to their Hamming weights. It was conjectured in [10] that for the matrix \mathbf{G}_n^{RM} , the reliability of each message bit under the successive decoder becomes completely ordered, i.e., each message bit is always more reliable than its previous bit. If this conjecture were true, then one can show that RM codes polarize faster than polar codes, which leads to a better finite-length performance.

Inspired by the recursive relation $\mathbf{G}_n^{\text{RM}} = \mathbf{P}_n^{\text{RM}}(\mathbf{G}_{n/2}^{\text{RM}} \otimes \mathbf{G}_2^{\text{polar}})$ of RM codes, we propose a new family of codes called the Adjacent-Bits-Swapped (ABS) polar codes. In the construction of ABS polar codes, we use a similar recursive relation $\mathbf{G}_n^{\text{ABS}} = \mathbf{P}_n^{\text{ABS}}(\mathbf{G}_{n/2}^{\text{ABS}} \otimes \mathbf{G}_2^{\text{polar}})$. The matrix $\mathbf{P}_n^{\text{ABS}}$ is an $n \times n$ permutation matrix which swaps two adjacent rows if the two corresponding message bits are “unordered”, i.e., if the previous bit is more reliable than its next bit under the successive decoder. Swapping such two adjacent rows always accelerates polarization because it makes the reliable bit even more reliable and the noisy bit even noisier. While the permutation matrix \mathbf{P}_n^{RM} for RM codes involves a large number of swaps of adjacent rows, we limit the number of swaps in $\mathbf{P}_n^{\text{ABS}}$ so that the overall structure of ABS polar codes is still close to standard polar codes. In this way, we are able to devise a modified Successive Cancellation List (SCL) decoder to efficiently decode ABS polar codes.

Recall that both the code construction and the decoding algorithm of standard polar codes rely on a recursive relation between the bit-channels, which are the channels mapping from a message bit to the previous message bits and all the channel outputs. Since we swap certain pairs of adjacent bits in the ABS polar code construction, there is no explicit recursive relation between bit-channels. Instead, we introduce the notion of adjacent-bits-channels, which are 4-ary-input channels mapping from two adjacent message bits to the previous message bits and all the channel outputs. As the main technical contribution of this paper, we derive a recursive relation between the adjacent-bits-channels. This recursive relation serves as the foundation of efficient code construction and decoding algorithms for ABS polar codes.

We conduct extensive simulations to compare the performance of ABS polar codes and the standard polar codes over the binary-input AWGN channels for various choices of parameters. In particular, we have tested the performance for code length 256, 512, 1024, 2048. For each choice of code length, we test 3 code rates 0.3, 0.5 and 0.7. When we set the list size to be 32 for the CRC-aided SCL decoders of both code families, ABS polar codes consistently outperform standard polar codes by 0.15 dB—0.6 dB, but the decoding time of ABS polar decoder is longer than that of standard polar codes by roughly 60%. If we use list size 20 for ABS polar codes and keep the list size to be 32 for standard polar codes, then the decoding time is more or less the same for these two codes, and ABS polar codes still outperform standard polar codes for all choices of parameters. In this case, the improvement over standard polar codes is up to 0.5 dB.

The organization of this paper is as follows: In Section II, we describe the main idea behind the ABS polar code construction and explain why ABS polar codes polarize faster than standard polar codes. In Section III, we derive the new recursive relation between the adjacent-bits-channels and use this recursive relation to construct ABS polar codes. In Section IV, we present an efficient encoding algorithm for ABS polar codes. In Section V, we present the new SCL decoder for ABS polar codes. Finally, in Section VI, we provide the simulation results.

II. MAIN IDEA OF THE NEW CODE CONSTRUCTION

A. The polarization framework

Let U_1, U_2, \dots, U_n be n i.i.d. Bernoulli-1/2 random variables. Let \mathbf{G}_n be an $n \times n$ invertible matrix over the binary field. Define $(X_1, X_2, \dots, X_n) = (U_1, U_2, \dots, U_n)\mathbf{G}_n$. We transmit each X_i through a BMS channel W and denote the channel output vector as (Y_1, Y_2, \dots, Y_n) . In this framework, (U_1, U_2, \dots, U_n) is the message vector, \mathbf{G}_n is the encoding matrix, and (X_1, X_2, \dots, X_n) is the codeword vector. We use

a successive decoder to recover the message vector from the channel output vector. More precisely, we decode the coordinates in the message vector one by one from U_1 to U_n . When decoding U_i , the successive decoder knows the values of all the previous message bits U_1, \dots, U_{i-1} and all the channel outputs Y_1, \dots, Y_n . Note that the codeword vector (X_1, X_2, \dots, X_n) depends on the matrix \mathbf{G}_n , and the channel output vector (Y_1, Y_2, \dots, Y_n) depends on both the matrix \mathbf{G}_n and the BMS channel W , although we omit the dependence from their notation. Next we define

$$H_i(\mathbf{G}_n, W) := H(U_i | U_1, \dots, U_{i-1}, Y_1, \dots, Y_n) \text{ for } 1 \leq i \leq n, \quad (1)$$

where $H(\cdot | \cdot)$ is the conditional entropy. $H_i(\mathbf{G}_n, W)$ measures the reliability of the i th message bit under the successive decoder when we use the encoding matrix \mathbf{G}_n and transmit the codeword vector through the BMS channel W . Since \mathbf{G}_n is an invertible matrix, we have

$$H_1(\mathbf{G}_n, W) + H_2(\mathbf{G}_n, W) + \dots + H_n(\mathbf{G}_n, W) = n(1 - I(W)), \quad (2)$$

where $I(W)$ is the channel capacity of W . We say that a family of matrices $\{\mathbf{G}_n\}$ is polarizing over a BMS channel W if $H_i(\mathbf{G}_n, W)$ is close to either 0 or 1 for almost all $i \in \{1, 2, \dots, n\}$ as $n \rightarrow \infty$. In order to quantify the polarization level of a given encoding matrix \mathbf{G}_n over a BMS channel W , we define

$$\Gamma(\mathbf{G}_n, W) = \frac{1}{n} \sum_{i=1}^n H_i(\mathbf{G}_n, W)(1 - H_i(\mathbf{G}_n, W)).$$

According to the definition above, a family of matrices $\{\mathbf{G}_n\}$ is polarizing over W if and only if $\Gamma(\mathbf{G}_n, W) \rightarrow 0$ as $n \rightarrow \infty$. A family of polarizing matrix $\{\mathbf{G}_n\}$ over a BMS channel W allows us to construct capacity-achieving codes as follows: We include the i th row of \mathbf{G}_n in the generator matrix if and only if $H_i(\mathbf{G}_n, W)$ is very close to 0. The condition $H_i(\mathbf{G}_n, W) \approx 0$ guarantees that the decoding error of the constructed codes approaches 0 under the successive decoder. We can further use (2) to show that the code rate of the constructed codes approaches $I(W)$. To see this, we first assume the extreme case where $\Gamma(\mathbf{G}_n, W) = 0$, i.e., $H_i(\mathbf{G}_n, W)$ is either 0 or 1 for all $1 \leq i \leq n$. Then by (2) we know that the dimension of the constructed polar code is precisely $nI(W)$, i.e., the code rate is $R = I(W)$. For the realistic case of $\Gamma(\mathbf{G}_n, W) \rightarrow 0$ as $n \rightarrow \infty$, one can show that the gap to capacity $I(W) - R$ also decreases to 0 as $n \rightarrow \infty$. Moreover, the smaller $\Gamma(\mathbf{G}_n, W)$ is, the smaller gap to capacity we have.

In the standard polar code construction [1], we construct the family of matrices $\{\mathbf{G}_{2^m}^{\text{polar}}\}_{m=1}^{\infty}$ recursively using the following relation:

$$\mathbf{G}_2^{\text{polar}} := \begin{bmatrix} 1 & 0 \\ 1 & 1 \end{bmatrix} \text{ and } \mathbf{G}_n^{\text{polar}} = \mathbf{G}_{n/2}^{\text{polar}} \otimes \mathbf{G}_2^{\text{polar}} \text{ for } n = 2^m \geq 4,$$

where \otimes is the Kronecker product and $m > 1$ is a positive integer. It was shown in [1] that $\{\mathbf{G}_{2^m}^{\text{polar}}\}_{m=1}^{\infty}$ is polarizing over every BMS channel W , and the codes constructed from these matrices can be efficiently decoded. In this paper, our objective is to construct another family of polarizing matrices $\{\mathbf{G}_{2^m}^{\text{ABS}}\}_{m=1}^{\infty}$ satisfying the following two conditions: (1) $\Gamma(\mathbf{G}_{2^m}^{\text{ABS}}, W) < \Gamma(\mathbf{G}_{2^m}^{\text{polar}}, W)$, i.e., the matrices $\mathbf{G}_{2^m}^{\text{ABS}}$ polarize even faster than $\mathbf{G}_{2^m}^{\text{polar}}$; (2) the codes constructed from $\{\mathbf{G}_{2^m}^{\text{ABS}}\}_{m=1}^{\infty}$ can also be efficiently decoded. The first condition allows us to construct a new family of codes with smaller gap to capacity and better finite-length performance than standard polar codes.

B. Swapping unordered adjacent bits accelerates polarization

The key observation in the standard polar code construction is that $\Gamma(\mathbf{G}_n, W)$ decreases as we perform the Kronecker product $\mathbf{G}_{2n} = \mathbf{G}_n \otimes \mathbf{G}_2^{\text{polar}}$. More precisely, we always have

$$\Gamma(\mathbf{G}_n \otimes \mathbf{G}_2^{\text{polar}}, W) < \Gamma(\mathbf{G}_n, W)$$

for every invertible matrix \mathbf{G}_n as long as $I(W)$ is not equal to 0 or 1. Therefore, the Kronecker product $\mathbf{G}_{2n} = \mathbf{G}_n \otimes \mathbf{G}_2^{\text{polar}}$ deepens the polarization at the cost of increasing the code length by a factor of 2.

In this paper, we observe that there is another method to deepen the polarization without increasing the code length, and this simple observation forms the foundation of our new code construction. Given a matrix \mathbf{G}_n and a BMS channel W , we say that two adjacent message bits U_i and U_{i+1} are unordered if $H_i(\mathbf{G}_n, W) \leq H_{i+1}(\mathbf{G}_n, W)$. This inequality means that U_i is more reliable than U_{i+1} under the successive decoder although U_i is decoded before U_{i+1} . Our key observation is that in this case, switching the decoding order of U_i and U_{i+1} deepens the polarization. Intuitively, this is because switching the decoding order of these two bits makes the reliable bit even more reliable and the noisy bit even noisier.

Note that switching the decoding order of U_i and U_{i+1} is equivalent to swapping the i th row and the $(i+1)$ th row of \mathbf{G}_n . More specifically, let us define a new matrix $\overline{\mathbf{G}}_n$ as the matrix obtained from swapping the i th row and the $(i+1)$ th row of \mathbf{G}_n and keeping all the other rows the same as \mathbf{G}_n . Following the framework in Section II-A, let $(\overline{U}_1, \overline{U}_2, \dots, \overline{U}_n)$ be the message vector associated with the new matrix $\overline{\mathbf{G}}_n$, where $\overline{U}_1, \dots, \overline{U}_n$ are n i.i.d. Bernoulli-1/2 random variables. Let $(\overline{X}_1, \dots, \overline{X}_n) = (\overline{U}_1, \dots, \overline{U}_n)\overline{\mathbf{G}}_n$ be the codeword vector transmitted through the BMS channel W and let $(\overline{Y}_1, \dots, \overline{Y}_n)$ be the corresponding channel output vector. By definition (1), we have

$$H_j(\overline{\mathbf{G}}_n, W) = H(\overline{U}_j | \overline{U}_1, \dots, \overline{U}_{j-1}, \overline{Y}_1, \dots, \overline{Y}_n) \text{ for } 1 \leq j \leq n.$$

By the relation between the matrices $\overline{\mathbf{G}}_n$ and \mathbf{G}_n , we have

$$H_j(\mathbf{G}_n, W) = H_j(\overline{\mathbf{G}}_n, W) \text{ for all } j \in \{1, 2, \dots, n\} \setminus \{i, i+1\}, \quad (3)$$

$$\begin{aligned} H_i(\mathbf{G}_n, W) &= H(\overline{U}_{i+1} | \overline{U}_1, \dots, \overline{U}_{i-1}, \overline{Y}_1, \dots, \overline{Y}_n) \\ &\geq H(\overline{U}_{i+1} | \overline{U}_1, \dots, \overline{U}_{i-1}, \overline{U}_i, \overline{Y}_1, \dots, \overline{Y}_n) = H_{i+1}(\overline{\mathbf{G}}_n, W), \end{aligned} \quad (4)$$

$$\begin{aligned} H_{i+1}(\mathbf{G}_n, W) &= H(\overline{U}_i | \overline{U}_1, \dots, \overline{U}_{i-1}, \overline{U}_{i+1}, \overline{Y}_1, \dots, \overline{Y}_n) \\ &\leq H(\overline{U}_i | \overline{U}_1, \dots, \overline{U}_{i-1}, \overline{Y}_1, \dots, \overline{Y}_n) = H_i(\overline{\mathbf{G}}_n, W). \end{aligned} \quad (5)$$

Now suppose that U_i and U_{i+1} are unordered, i.e., $H_i(\mathbf{G}_n, W) \leq H_{i+1}(\mathbf{G}_n, W)$. Combining this inequality with (4)–(5), we obtain

$$H_{i+1}(\overline{\mathbf{G}}_n, W) \leq H_i(\mathbf{G}_n, W) \leq H_{i+1}(\mathbf{G}_n, W) \leq H_i(\overline{\mathbf{G}}_n, W). \quad (6)$$

Moreover,

$$H_i(\mathbf{G}_n, W) + H_{i+1}(\mathbf{G}_n, W) = H_i(\overline{\mathbf{G}}_n, W) + H_{i+1}(\overline{\mathbf{G}}_n, W) = H(\overline{U}_i, \overline{U}_{i+1} | \overline{U}_1, \dots, \overline{U}_{i-1}, \overline{Y}_1, \dots, \overline{Y}_n).$$

This equality together with (6) implies that

$$\begin{aligned} &(H_i(\mathbf{G}_n, W))^2 + (H_{i+1}(\mathbf{G}_n, W))^2 \\ &= \frac{1}{2} \left((H_i(\mathbf{G}_n, W) + H_{i+1}(\mathbf{G}_n, W))^2 + (H_i(\mathbf{G}_n, W) - H_{i+1}(\mathbf{G}_n, W))^2 \right) \\ &\leq \frac{1}{2} \left((H_i(\overline{\mathbf{G}}_n, W) + H_{i+1}(\overline{\mathbf{G}}_n, W))^2 + (H_i(\overline{\mathbf{G}}_n, W) - H_{i+1}(\overline{\mathbf{G}}_n, W))^2 \right) \\ &= (H_i(\overline{\mathbf{G}}_n, W))^2 + (H_{i+1}(\overline{\mathbf{G}}_n, W))^2. \end{aligned}$$

Therefore,

$$\begin{aligned} &H_i(\overline{\mathbf{G}}_n, W)(1 - H_i(\overline{\mathbf{G}}_n, W)) + H_{i+1}(\overline{\mathbf{G}}_n, W)(1 - H_{i+1}(\overline{\mathbf{G}}_n, W)) \\ &\leq H_i(\mathbf{G}_n, W)(1 - H_i(\mathbf{G}_n, W)) + H_{i+1}(\mathbf{G}_n, W)(1 - H_{i+1}(\mathbf{G}_n, W)). \end{aligned}$$

Combining this with (3), we conclude that $\Gamma(\overline{\mathbf{G}}_n, W) \leq \Gamma(\mathbf{G}_n, W)$. This formally justifies that switching the decoding order of two unordered adjacent bits deepens polarization.

C. Our new code construction and its connection to RM codes

We view the operation of taking the Kronecker product $\mathbf{G}_n^{\text{polar}} = \mathbf{G}_{n/2}^{\text{polar}} \otimes \mathbf{G}_2^{\text{polar}}$ in the standard polar code construction as one layer of polar transform. Then the construction of a standard polar code with code length $n = 2^m$ consists of m consecutive layers of polar transforms. In light of the discussion in Section II-B, we add a permutation layer after each polar transform layer in our ABS polar code construction. More precisely, we replace the recursive relation $\mathbf{G}_n^{\text{polar}} = \mathbf{G}_{n/2}^{\text{polar}} \otimes \mathbf{G}_2^{\text{polar}}$ in the standard polar code construction with

$$\mathbf{G}_n^{\text{ABS}} = \mathbf{P}_n^{\text{ABS}}(\mathbf{G}_{n/2}^{\text{ABS}} \otimes \mathbf{G}_2^{\text{polar}}), \quad (7)$$

where the matrix $\mathbf{P}_n^{\text{ABS}}$ is an $n \times n$ permutation matrix. In this case, $\mathbf{G}_n^{\text{ABS}}$ is a row permutation of the Kronecker product $\mathbf{G}_{n/2}^{\text{ABS}} \otimes \mathbf{G}_2^{\text{polar}}$. The permutation associated with $\mathbf{P}_n^{\text{ABS}}$ is a composition of multiple swaps of unordered adjacent bits. The starting point of the recursive relation (7) is $\mathbf{G}_1^{\text{ABS}} = [1]$, the identity matrix of size 1×1 .

Before we present how to choose $\mathbf{P}_n^{\text{ABS}}$ in (7), let us point out an interesting connection between our new code and RM codes. In fact, RM codes can also be constructed using a similar recursive relation:

$$\mathbf{G}_n^{\text{RM}} = \mathbf{P}_n^{\text{RM}}(\mathbf{G}_{n/2}^{\text{RM}} \otimes \mathbf{G}_2^{\text{polar}}). \quad (8)$$

Here \mathbf{P}_n^{RM} is an $n \times n$ permutation matrix which reorders the rows of $\mathbf{G}_{n/2}^{\text{RM}} \otimes \mathbf{G}_2^{\text{polar}}$ according to their Hamming weights. In other words, \mathbf{G}_n^{RM} is a row permutation of $\mathbf{G}_{n/2}^{\text{RM}} \otimes \mathbf{G}_2^{\text{polar}}$, and the Hamming weights of the rows of \mathbf{G}_n^{RM} are monotonically increasing from the first row to the last row. It was shown in [10] that the family of matrices $\{\mathbf{G}_n^{\text{RM}}\}$ is polarizing over every BMS channel W , i.e., $H_i(\mathbf{G}_n^{\text{RM}}, W)$ is close to either 0 or 1 for almost all $i \in \{1, 2, \dots, n\}$ as $n \rightarrow \infty$. It was further conjectured¹ in [10] that $\{H_i(\mathbf{G}_n^{\text{RM}}, W)\}_{i=1}^n$ is decreasing for every BMS channel W , i.e.,

$$H_1(\mathbf{G}_n^{\text{RM}}, W) \geq H_2(\mathbf{G}_n^{\text{RM}}, W) \geq \dots \geq H_n(\mathbf{G}_n^{\text{RM}}, W). \quad (9)$$

If this conjecture were true, then we can immediately conclude that RM codes achieve capacity of BMS channels. Indeed, RM codes choose rows with heaviest Hamming weight in \mathbf{G}_n^{RM} to form the generator matrices. Since the rows of \mathbf{G}_n^{RM} are sorted according to their Hamming weights, RM codes simply pick the rows with large row indices. By (9), these rows correspond to the most reliable bits under the successive decoder. Moreover, since almost all the conditional entropy in (9) are close to either 0 or 1, the conditional entropy of the most reliable bits must be close to 0, and the number of such bits is close to $nI(W)$ as $n \rightarrow \infty$.

The conjecture (9) not only constitutes a sufficient condition for RM codes to achieve capacity but also indicates that RM codes polarize even faster than polar codes. To see this, let us define the set $\mathcal{RP}(\mathbf{G}_n^{\text{polar}}) = \{\overline{\mathbf{G}}_n : \overline{\mathbf{G}}_n \text{ is a row permutation of } \mathbf{G}_n^{\text{polar}}\}$. Then by definition, $\mathbf{G}_n^{\text{RM}} \in \mathcal{RP}(\mathbf{G}_n^{\text{polar}})$. If the conjecture (9) were true, then we can show that \mathbf{G}_n^{RM} has the highest level of polarization among all the row permutations of $\mathbf{G}_n^{\text{polar}}$, i.e.,

$$\Gamma(\mathbf{G}_n^{\text{RM}}, W) \leq \Gamma(\overline{\mathbf{G}}_n, W) \text{ for every } \overline{\mathbf{G}}_n \in \mathcal{RP}(\mathbf{G}_n^{\text{polar}}).$$

This is because the conjecture (9) implies that \mathbf{G}_n^{RM} is the only row permutation of $\mathbf{G}_n^{\text{polar}}$ which does not have any unordered adjacent bits. For any other row permutation $\overline{\mathbf{G}}_n \in \mathcal{RP}(\mathbf{G}_n^{\text{polar}})$, there is at least one pair of unordered adjacent bits. According to the discussion in Section II-B, by swapping the two adjacent rows corresponding to this pair of unordered adjacent bits, we obtain another row permutation of $\mathbf{G}_n^{\text{polar}}$ with deeper polarization. If we start with a matrix $\overline{\mathbf{G}}_n \in \mathcal{RP}(\mathbf{G}_n^{\text{polar}})$ and keep swapping unordered adjacent rows², then eventually we will obtain \mathbf{G}_n^{RM} . Since each swap only deepens polarization, \mathbf{G}_n^{RM} has the highest level of polarization among all the row permutations of $\mathbf{G}_n^{\text{polar}}$. In particular, this implies

¹The authors of [10] provided some theoretical analysis and simulation results to support this conjecture.

²We say that two adjacent rows are unordered if the corresponding bits are unordered.

that RM codes polarize even faster than polar codes. Faster polarization further implies that RM codes have a smaller gap to capacity than polar codes with the same parameters, which was suggested to be the case by both theoretical analysis [8], [9] and simulation results [6], [7].

Although RM codes are believed to have better performance than polar codes under the Maximum Likelihood (ML) decoder, the problem of designing an efficient decoder whose performance is almost the same as the ML decoder still remains open for RM codes, except for a certain range of parameters. In particular, the performance of currently known decoding algorithms for RM codes [7], [11]–[13] is close to the ML decoder only in the short code length or the low code rate regimes. In contrast, the performance of the Successive Cancellation List (SCL) decoder with list size 32 is almost the same as the ML decoder for polar codes.

Our new code construction is a balanced point between RM codes and polar codes. On the one hand, the recursive relation (7) of our new code is similar to the recursion (8) of RM codes in the sense that both codes add a permutation layer after each polar transform layer to accelerate polarization. On the other hand, we only use a relatively small number of swaps in the permutation matrix $\mathbf{P}_n^{\text{ABS}}$ while the permutation matrix \mathbf{P}_n^{RM} for RM codes involves a large number of swaps. As a consequence, the overall structure of our new code is still close to the standard polar codes, and it allows a modified SCL decoder to efficiently decode.

In order to explain how to choose $\mathbf{P}_n^{\text{ABS}}$ in (7), we introduce the notation $\sigma_{i \leftrightarrow j}^{(n)}$ to denote the permutation that swaps i and j while mapping all the other elements to themselves. The superscript in $\sigma_{i \leftrightarrow j}^{(n)}$ means that it is a permutation on $\{1, 2, \dots, n\}$. We denote the permutation associated with $\mathbf{P}_n^{\text{ABS}}$ as π_n . In our code construction, π_n is a composition of multiple $\sigma_{i \leftrightarrow i+1}^{(n)}$ for multiple values of i . More precisely, π_n can be written as

$$\pi_n = \sigma_{i_1 \leftrightarrow i_1+1}^{(n)} \circ \sigma_{i_2 \leftrightarrow i_2+1}^{(n)} \circ \sigma_{i_3 \leftrightarrow i_3+1}^{(n)} \circ \dots \circ \sigma_{i_s \leftrightarrow i_s+1}^{(n)}, \quad (10)$$

where s is the total number of swaps in π_n . The choice of s depends on the value of n , and we will explain how to choose s in Section III. In the ABS polar code construction, we require that i_1, i_2, \dots, i_s in (10) satisfy the following condition:

$$i_2 \geq i_1 + 4, \quad i_3 \geq i_2 + 4, \quad i_4 \geq i_3 + 4, \quad \dots, \quad i_s \geq i_{s-1} + 4. \quad (11)$$

This condition guarantees that the swapped elements are fully separated, and it is the foundation of efficient code construction and efficient decoding for ABS polar codes. More specifically, the condition (11) allows us to efficiently track the evolution of every pair of adjacent bits through different layers of polar transforms in a recursive way. We will explain the details about this in Section III. As a final remark, we note that one needs to choose m permutation matrices $\mathbf{P}_2^{\text{ABS}}, \mathbf{P}_4^{\text{ABS}}, \mathbf{P}_8^{\text{ABS}}, \dots, \mathbf{P}_n^{\text{ABS}}$ in the construction of an ABS polar code with code length $n = 2^m$.

III. CODE CONSTRUCTION OF ABS POLAR CODES

The construction of ABS polar codes with code length $n = 2^m$ consists of two main steps. The first step is to pick the permutation matrices $\mathbf{P}_2^{\text{ABS}}, \mathbf{P}_4^{\text{ABS}}, \mathbf{P}_8^{\text{ABS}}, \dots, \mathbf{P}_n^{\text{ABS}}$ in the recursive relation (7), as mentioned at the end of the previous section. After picking these permutation matrices, the second step is to find which bits are information bits and which bits are frozen bits. Although the second step is also needed in the construction of standard polar codes [1], [14], the techniques used in this paper are quite different. In the standard polar code construction, we can directly track the evolution of bit-channels in a recursive way. However, in the ABS polar code construction, it is not possible to identify a recursive relation between bit-channels directly because we swap certain pairs of adjacent bits in the code construction. Instead, we find a recursive relation between pairs of adjacent bits from different layers of polar transforms. After obtaining the joint distribution of every pair of adjacent bits, we are able to calculate the transition probability of the bit-channels and locate the information bits and the frozen bits.

The organization of this section is as follows: In Section III-A, we first recall how to track the evolution of bit-channels in standard polar codes using the basic 2×2 transform. In Section III-B, we introduce

a new transform and use it to establish a recursive relation between pairs of adjacent bits for standard polar codes. The purpose of Section III-B is to illustrate the application of the new transform in a familiar setting. In Section III-C, we use the new transform to track the evolution of adjacent bits in the ABS polar codes. The result in Section III-C accomplishes the second step of the ABS polar code construction, i.e., it allows us to locate the information bits and the frozen bits when the permutation matrices $\mathbf{P}_2^{\text{ABS}}, \mathbf{P}_4^{\text{ABS}}, \mathbf{P}_8^{\text{ABS}}, \dots, \mathbf{P}_n^{\text{ABS}}$ in the recursive relation (7) are known. Next, in Section III-D, we explain how to pick these permutation matrices in the ABS polar code construction. Recall that the quantization operation is needed in the standard polar code construction [14] because the output alphabet size of the bit-channels grows exponentially with n . The same issue also arises in the ABS polar code construction, and we will discuss this in Section III-E. Finally, we put everything together and summarize the code construction algorithm for ABS polar codes in Section III-F.

A. Tracking the evolution of bit-channels in standard polar codes using the 2×2 transform

Let us first recall the 2×2 transform in the standard polar code construction.

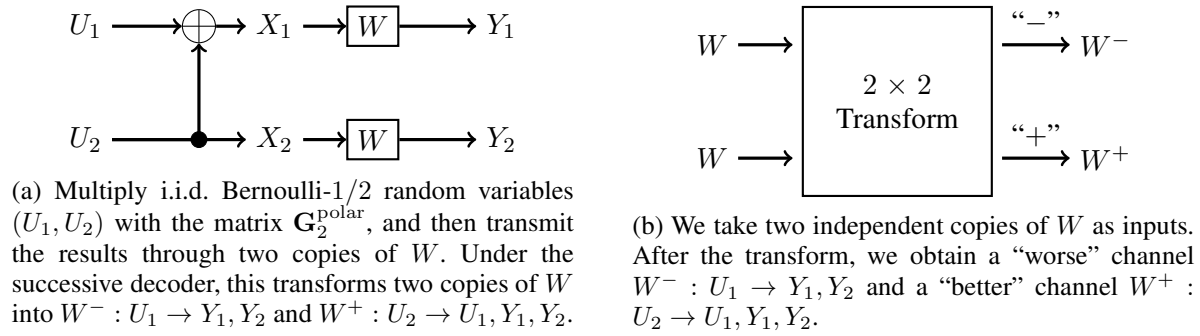


Fig. 1: The 2×2 basic polar transform

Given a BMS channel $W : \{0, 1\} \rightarrow \mathcal{Y}$, the transition probabilities of $W^- : \{0, 1\} \rightarrow \mathcal{Y}^2$ and $W^+ : \{0, 1\} \rightarrow \{0, 1\} \times \mathcal{Y}^2$ in Fig. 1 are given by

$$\begin{aligned} W^-(y_1, y_2 | u_1) &= \frac{1}{2} \sum_{u_2 \in \{0, 1\}} W(y_1 | u_1 + u_2) W(y_2 | u_2) \quad \text{for } u_1 \in \{0, 1\} \text{ and } y_1, y_2 \in \mathcal{Y}, \\ W^+(u_1, y_1, y_2 | u_2) &= \frac{1}{2} W(y_1 | u_1 + u_2) W(y_2 | u_2) \quad \text{for } u_1, u_2 \in \{0, 1\} \text{ and } y_1, y_2 \in \mathcal{Y}. \end{aligned} \quad (12)$$

The basic 2×2 transform plays a fundamental role in the standard polar code construction because it allows us to efficiently track the evolution of bit-channels in a recursive way. More specifically, the bit-channels induced by the matrix $\mathbf{G}_n^{\text{polar}}$ are defined in Fig. 2 below. It is well known that the bit-channels associated with $\mathbf{G}_n^{\text{polar}}$ and the bit-channels associated with $\mathbf{G}_{n/2}^{\text{polar}}$ satisfy the following recursive relation:

$$W_{2i-1}^{(n)} = (W_i^{(n/2)})^- \quad \text{and} \quad W_{2i}^{(n)} = (W_i^{(n/2)})^+ \quad \text{for } 1 \leq i \leq n/2. \quad (13)$$

Both the code construction and the decoding algorithm of standard polar codes rely on this recursive relation.

B. Tracking the evolution of adjacent bits in standard polar codes using a new transform

In the construction of ABS polar codes, we need to track the joint distribution of every pair of adjacent bits, not just the distribution of every single bit given the previous bits and channel outputs. To that end, we introduce a new transform, named as the Double-Bits (DB) polar transform. All the channels involved in the DB polar transform have 4-ary inputs. To distinguish between binary-input channels and 4-ary-input

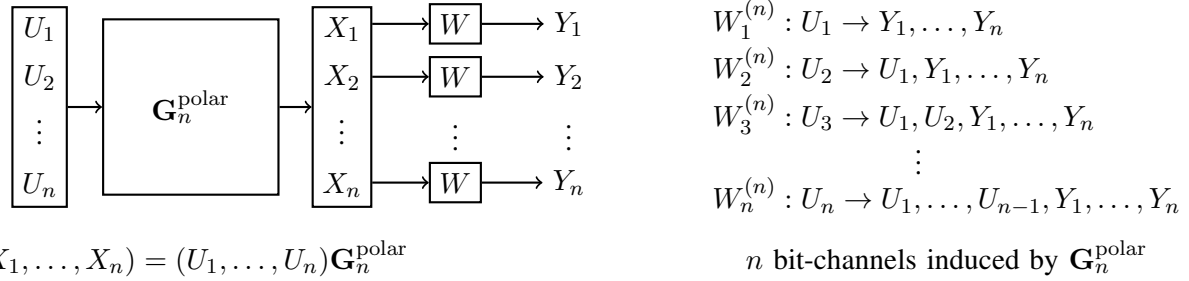
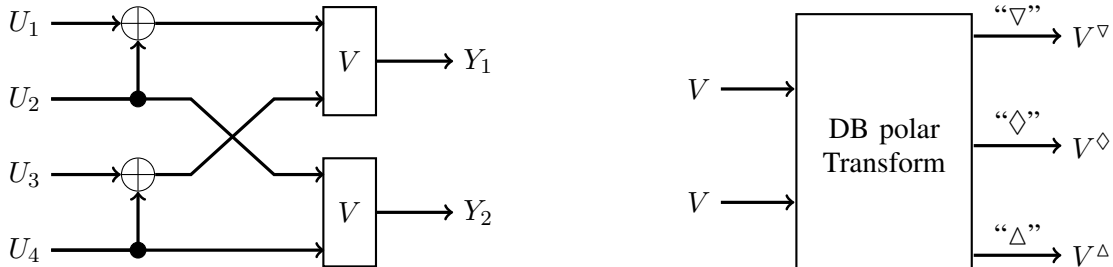


Fig. 2: U_1, \dots, U_n are $n = 2^m$ i.i.d. Bernoulli-1/2 random variables. $(X_1, \dots, X_n) = (U_1, \dots, U_n)\mathbf{G}_n^{\text{polar}}$ is the codeword vector, and (Y_1, \dots, Y_n) is the channel output vector. The n bit-channels induced by $\mathbf{G}_n^{\text{polar}}$ are listed on the right side of the figure. $W_i^{(n)}$ is the bit-channel mapping from U_i to $U_1, \dots, U_{i-1}, Y_1, \dots, Y_n$.

channels, we use W to denote the former channels and use V to denote latter channels³. The details of the DB polar transform are illustrated in Fig. 3. Given a 4-ary-input channel $V : \{0, 1\}^2 \rightarrow \mathcal{Y}$, the transition probabilities of $V^\nabla : \{0, 1\}^2 \rightarrow \mathcal{Y}^2$, $V^\diamond : \{0, 1\}^2 \rightarrow \{0, 1\} \times \mathcal{Y}^2$, and $V^\Delta : \{0, 1\}^2 \rightarrow \{0, 1\}^2 \times \mathcal{Y}^2$ in Fig. 3 are given by

$$\begin{aligned}
 V^\nabla(y_1, y_2 | u_1, u_2) &= \frac{1}{4} \sum_{u_3, u_4 \in \{0, 1\}} V(y_1 | u_1 + u_2, u_3 + u_4) V(y_2 | u_2, u_4) \\
 &\quad \text{for } u_1, u_2 \in \{0, 1\} \text{ and } y_1, y_2 \in \mathcal{Y}, \\
 V^\diamond(u_1, y_1, y_2 | u_2, u_3) &= \frac{1}{4} \sum_{u_4 \in \{0, 1\}} V(y_1 | u_1 + u_2, u_3 + u_4) V(y_2 | u_2, u_4) \\
 &\quad \text{for } u_1, u_2, u_3 \in \{0, 1\} \text{ and } y_1, y_2 \in \mathcal{Y}, \\
 V^\Delta(u_1, u_2, y_1, y_2 | u_3, u_4) &= \frac{1}{4} V(y_1 | u_1 + u_2, u_3 + u_4) V(y_2 | u_2, u_4) \\
 &\quad \text{for } u_1, u_2, u_3, u_4 \in \{0, 1\} \text{ and } y_1, y_2 \in \mathcal{Y}.
 \end{aligned} \tag{14}$$



(a) U_1, U_2, U_3, U_4 are i.i.d. Bernoulli-1/2 random variables. The channel $V : \{0, 1\}^2 \rightarrow \mathcal{Y}$ takes two bits as its inputs, i.e., V has 4-ary inputs. Under the successive decoder, we have the following three channels: (1) $V^\nabla : U_1, U_2 \rightarrow Y_1, Y_2$; (2) $V^\diamond : U_2, U_3 \rightarrow U_1, Y_1, Y_2$; (3) $V^\Delta : U_3, U_4 \rightarrow U_1, U_2, Y_1, Y_2$.

(b) Two independent copies of V are transformed into three channels $V^\nabla, V^\diamond, V^\Delta$. These three channels also have 4-ary inputs. Note that the inputs of V^∇ and V^\diamond have one-bit overlap, and the inputs of V^\diamond and V^Δ also have one-bit overlap.

Fig. 3: The Double-Bits (DB) polar transform

³More precisely, W and its variations such as $W^+, W^-, W_i^{(n)}$ are used for binary-input channels; V and its variations such as $V^\nabla, V^\diamond, V^\Delta, V_i^{(n)}$ are used for channels with 4-ary inputs.

The role of the DB polar transform in the construction of ABS polar codes is the same as the role of the 2×2 basic polar transform in the standard polar code construction. Instead of jumping directly into the ABS polar code construction, let us first use standard polar codes to illustrate how to track the evolution of adjacent bits recursively using the DB polar transform. In order to calculate the joint distribution of adjacent bits, we introduce the notion of adjacent-bits-channels, which is the counterpart of the bit-channels used for tracking the distribution of every single bit. We still use the setting in Fig. 2, where we defined the bit-channels. For the matrix $\mathbf{G}_n^{\text{polar}}$ and a BMS channel W , we define $n - 1$ adjacent-bits-channels $V_1^{(n)}, V_2^{(n)}, \dots, V_{n-1}^{(n)}$ as follows:

$$V_i^{(n)} : U_i, U_{i+1} \rightarrow U_1, \dots, U_{i-1}, Y_1, \dots, Y_n \quad \text{for } 1 \leq i \leq n - 1,$$

where $U_1, \dots, U_n, Y_1, \dots, Y_n$ are defined in Fig. 2. By definition, $V_1^{(n)}, V_2^{(n)}, \dots, V_{n-1}^{(n)}$ take two bits as their inputs, i.e., all of them have 4-ary inputs. Moreover, these adjacent-bits-channels depend on the BMS channel W , although we omit this dependence in the notation.

The following lemma allows us to calculate $V_1^{(n)}, V_2^{(n)}, \dots, V_{n-1}^{(n)}$ recursively from $V_1^{(n/2)}, V_2^{(n/2)}, \dots, V_{n/2-1}^{(n/2)}$.

Lemma 1. *Let $n \geq 4$. We have*

$$V_{2i-1}^{(n)} = (V_i^{(n/2)})^\nabla, \quad V_{2i}^{(n)} = (V_i^{(n/2)})^\diamond, \quad V_{2i+1}^{(n)} = (V_i^{(n/2)})^\Delta \quad \text{for } 1 \leq i \leq n/2 - 1. \quad (15)$$

The proof of Lemma 1 is given in Appendix A. The relation (15) is similar in nature to the relation (13), and the proof of (15) also uses the same method as the proof of (13). There is, however, one difference between these two recursive relations: The “+” and “-” transforms of different bit-channels are distinct while the “ ∇ ”, “ \diamond ” and “ Δ ” transforms of different adjacent-bits-channels may overlap. More precisely, the $n/2$ sets $\{(W_i^{(n/2)})^-, (W_i^{(n/2)})^+\}_{i=1}^{n/2}$ are disjoint while the two sets $\{(V_i^{(n/2)})^\nabla, (V_i^{(n/2)})^\diamond, (V_i^{(n/2)})^\Delta\}$ and $\{(V_{i+1}^{(n/2)})^\nabla, (V_{i+1}^{(n/2)})^\diamond, (V_{i+1}^{(n/2)})^\Delta\}$ have the following element in their intersection for every $1 \leq i \leq n/2 - 2$:

$$V_{2i+1}^{(n)} = (V_i^{(n/2)})^\Delta = (V_{i+1}^{(n/2)})^\nabla. \quad (16)$$

This gives us two methods of calculating $V_{2i+1}^{(n)}$ recursively for $1 \leq i \leq n/2 - 2$.

Lemma 1 tells us how to calculate $\{V_i^{(n)}\}_{i=1}^{n-1}$ from $\{V_i^{(n/2)}\}_{i=1}^{n/2-1}$ recursively for $n \geq 4$. The last question we need to answer is how to calculate the adjacent-bits-channel $V_1^{(2)}$ from the BMS channel W , because $V_1^{(2)}$ is the starting point of the recursive relation in Lemma 1. Fortunately, this is an easy task. Let us go back to the setting in Fig. 1. Given a BMS channel W , the adjacent-bits-channel $V_1^{(2)}$ is simply the channel mapping from U_1, U_2 to Y_1, Y_2 . More precisely, we have

$$V_1^{(2)}(y_1, y_2 | u_1, u_2) = W(y_1 | u_1 + u_2)W(y_2 | u_2). \quad (17)$$

After obtaining the transition probabilities of the adjacent-bits-channels $\{V_i^{(n)}\}_{i=1}^{n-1}$, it is straightforward to calculate the transition probabilities of the bit-channels $\{W_i^{(n)}\}_{i=1}^n$. More precisely, we have

$$\begin{aligned} W_i^{(n)}(y_1, y_2, \dots, y_n, u_1, u_2, \dots, u_{i-1} | u_i) &= \frac{1}{2} \sum_{u_{i+1} \in \{0,1\}} V_i^{(n)}(y_1, y_2, \dots, y_n, u_1, u_2, \dots, u_{i-1} | u_i, u_{i+1}), \\ W_{i+1}^{(n)}(y_1, y_2, \dots, y_n, u_1, u_2, \dots, u_i | u_{i+1}) &= \frac{1}{2} V_i^{(n)}(y_1, y_2, \dots, y_n, u_1, u_2, \dots, u_{i-1} | u_i, u_{i+1}) \end{aligned} \quad (18)$$

for $1 \leq i \leq n - 1$.

As a final remark, we note that the output alphabet size of the adjacent-bits-channels $\{V_i^{(n)}\}_{i=1}^{n-1}$ grows exponentially with n . Therefore, accurate calculations of $\{V_i^{(n)}\}_{i=1}^{n-1}$ are intractable. We need to quantize the output alphabets by merging output symbols with similar posterior distributions. Recall that

in the standard polar code construction [14], we also need the quantization operation to calculate an approximation of the bit-channels $\{W_i^{(n)}\}_{i=1}^n$. Our quantization method is different from the one used in [14] because the adjacent-bits-channels have 4-ary inputs while the bit-channels have binary inputs. We will present our quantization method later in Section III-E.

C. Tracking the evolution of adjacent bits in ABS polar codes

As discussed at the beginning of this section, the construction of ABS polar codes consists of two main steps. The first step is to pick the permutation matrices $\mathbf{P}_2^{\text{ABS}}, \mathbf{P}_4^{\text{ABS}}, \mathbf{P}_8^{\text{ABS}}, \dots, \mathbf{P}_n^{\text{ABS}}$ in the recursive relation (7), and the second step is to find which bits are information bits and which bits are frozen bits after picking these permutation matrices. In this subsection, we explain how to accomplish the second step. More precisely, we define the bit-channels and the adjacent-bits-channels for ABS polar codes in Fig. 4. The task of this subsection is to show how to calculate the capacity of the bit-channels $\{W_i^{(n),\text{ABS}}\}_{i=1}^n$ when the permutation matrices $\mathbf{P}_2^{\text{ABS}}, \mathbf{P}_4^{\text{ABS}}, \mathbf{P}_8^{\text{ABS}}, \dots, \mathbf{P}_n^{\text{ABS}}$ in (7) are known. Then the information bits are simply the U_i 's satisfying that $I(W_i^{(n),\text{ABS}}) \approx 1$, where $I(\cdot)$ is the channel capacity. Unlike the standard polar codes, there does not exist a recursive relation between the bit-channels $\{W_i^{(n),\text{ABS}}\}_{i=1}^n$ and $\{W_i^{(n/2),\text{ABS}}\}_{i=1}^{n/2}$ for ABS polar codes. Instead, we derive a recursive relation between the adjacent-bits-channels $\{V_i^{(n),\text{ABS}}\}_{i=1}^{n-1}$ and $\{V_i^{(n/2),\text{ABS}}\}_{i=1}^{n/2-1}$. After that, the transition probabilities of $\{W_i^{(n),\text{ABS}}\}_{i=1}^n$ can be calculated from the transition probabilities of $\{V_i^{(n),\text{ABS}}\}_{i=1}^{n-1}$.

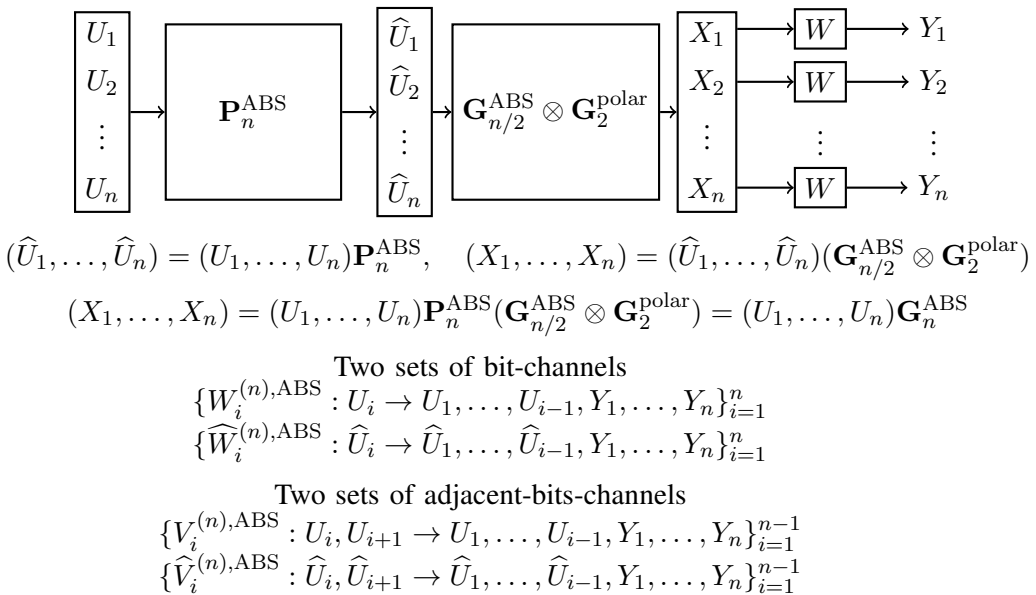
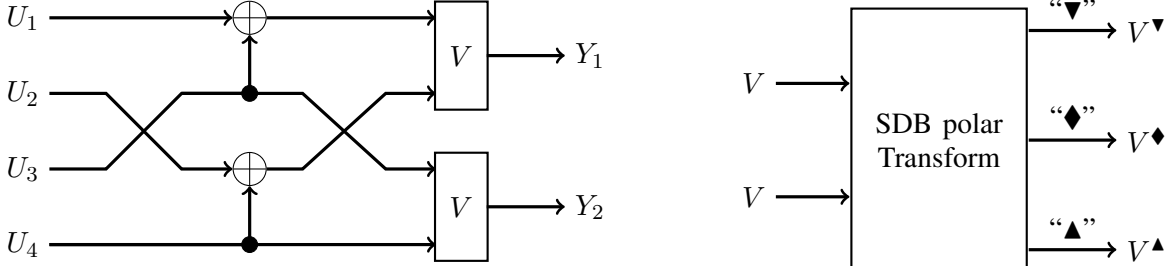


Fig. 4: U_1, \dots, U_n are $n = 2^m$ i.i.d. Bernoulli-1/2 random variables. $(X_1, \dots, X_n) = (U_1, \dots, U_n) \mathbf{G}_n^{\text{ABS}}$ is the codeword vector, and (Y_1, \dots, Y_n) is the channel output vector. We view each Kronecker product with $\mathbf{G}_2^{\text{polar}}$ as one layer of polar transform and view each multiplication with a permutation matrix as one layer of permutation. Then $\mathbf{G}_n^{\text{ABS}}$ is obtained from m layers of polar transforms and m layers of permutations while $\mathbf{G}_{n/2}^{\text{ABS}} \otimes \mathbf{G}_2^{\text{polar}}$ is obtained from m layers of polar transforms and $m - 1$ layers of permutations. Therefore, $\{W_i^{(n),\text{ABS}}\}_{i=1}^n$ and $\{V_i^{(n),\text{ABS}}\}_{i=1}^{n-1}$ are the bit-channels and adjacent-bits-channels seen by the successive decoder after m layers of polar transforms and m layers of permutations. Similarly, $\{\widehat{W}_i^{(n),\text{ABS}}\}_{i=1}^n$ and $\{\widehat{V}_i^{(n),\text{ABS}}\}_{i=1}^{n-1}$ are the bit-channels and adjacent-bits-channels seen by the successive decoder after m layers of polar transforms and $m - 1$ layers of permutations.

In order to derive the recursive relation between the adjacent-bits-channels for ABS polar codes, we need another new transform named as the Swapped-Double-Bits (SDB) polar transform in addition to

the DB polar transform defined in (14). The details of the SDB polar transform are illustrated in Fig. 5. In fact, the SDB polar transform is very similar to the DB polar transform. By comparing Fig. 3a and Fig. 5a, we can see that the only difference between these two transforms is the order of U_2 and U_3 . Given a 4-ary-input channel $V : \{0, 1\}^2 \rightarrow \mathcal{Y}$, the transition probabilities of $V^\blacktriangledown : \{0, 1\}^2 \rightarrow \mathcal{Y}^2$, $V^\blacklozenge : \{0, 1\}^2 \rightarrow \{0, 1\} \times \mathcal{Y}^2$, and $V^\blacktriangle : \{0, 1\}^2 \rightarrow \{0, 1\}^2 \times \mathcal{Y}^2$ in Fig. 5 are given by

$$\begin{aligned}
V^\blacktriangledown(y_1, y_2 | u_1, u_2) &= \frac{1}{4} \sum_{u_3, u_4 \in \{0, 1\}} V(y_1 | u_1 + u_3, u_2 + u_4) V(y_2 | u_3, u_4) \\
&\quad \text{for } u_1, u_2 \in \{0, 1\} \text{ and } y_1, y_2 \in \mathcal{Y}, \\
V^\blacklozenge(u_1, y_1, y_2 | u_2, u_3) &= \frac{1}{4} \sum_{u_4 \in \{0, 1\}} V(y_1 | u_1 + u_3, u_2 + u_4) V(y_2 | u_3, u_4) \\
&\quad \text{for } u_1, u_2, u_3 \in \{0, 1\} \text{ and } y_1, y_2 \in \mathcal{Y}, \\
V^\blacktriangle(u_1, u_2, y_1, y_2 | u_3, u_4) &= \frac{1}{4} V(y_1 | u_1 + u_3, u_2 + u_4) V(y_2 | u_3, u_4) \\
&\quad \text{for } u_1, u_2, u_3, u_4 \in \{0, 1\} \text{ and } y_1, y_2 \in \mathcal{Y}.
\end{aligned} \tag{19}$$



(a) U_1, U_2, U_3, U_4 are i.i.d. Bernoulli-1/2 random variables. The channel $V : \{0, 1\}^2 \rightarrow \mathcal{Y}$ takes two bits as its inputs, i.e., V has 4-ary inputs. Under the successive decoder, we have the following three channels: (1) $V^\blacktriangledown : U_1, U_2 \rightarrow Y_1, Y_2$; (2) $V^\blacklozenge : U_2, U_3 \rightarrow U_1, Y_1, Y_2$; (3) $V^\blacktriangle : U_3, U_4 \rightarrow U_1, U_2, Y_1, Y_2$.

(b) Two independent copies of V are transformed into three channels $V^\blacktriangledown, V^\blacklozenge, V^\blacktriangle$. These three channels also have 4-ary inputs. Note that the inputs of V^\blacktriangledown and V^\blacklozenge have one-bit overlap, and the inputs of V^\blacklozenge and V^\blacktriangle also have one-bit overlap.

Fig. 5: The Swapped-Double-Bits (SDB) polar transform

Recall that at the end of Section II-C, we denote the permutation associated with $\mathbf{P}_n^{\text{ABS}}$ as π_n , and we write π_n in the form of (10). Moreover, we require that i_1, i_2, \dots, i_s in (10) satisfy the condition (11) because otherwise there does not exist a recursive relation between the adjacent-bits-channels $\{V_i^{(n),\text{ABS}}\}_{i=1}^{n-1}$ and $\{V_i^{(n/2),\text{ABS}}\}_{i=1}^{n/2-1}$. We will give a detailed explanation about this later in Remark 1. Here we point out another property of i_1, i_2, \dots, i_s in (10): they must all be even numbers. To see this, let us go back to the setting in Fig. 4. The role of π_n is to decide which pairs of adjacent bits to swap in the vector $(\widehat{U}_1, \widehat{U}_2, \dots, \widehat{U}_n)$ defined in Fig. 4. According to the discussion in Section II-B, we swap the adjacent bits \widehat{U}_i and \widehat{U}_{i+1} only if they are unordered, i.e., if \widehat{U}_i is more reliable than \widehat{U}_{i+1} under the successive decoder. In other words, we swap the adjacent bits \widehat{U}_i and \widehat{U}_{i+1} only if $I(\widehat{W}_i^{(n),\text{ABS}}) \geq I(\widehat{W}_{i+1}^{(n),\text{ABS}})$, where the bit-channels $\widehat{W}_i^{(n),\text{ABS}}$ and $\widehat{W}_{i+1}^{(n),\text{ABS}}$ are also defined in Fig. 4. Since $\{\widehat{W}_i^{(n),\text{ABS}}\}_{i=1}^n$ are obtained from the 2×2 basic polar transform of $\{W_i^{(n/2),\text{ABS}}\}_{i=1}^{n/2}$, they satisfy the following relation:

$$\widehat{W}_{2i-1}^{(n),\text{ABS}} = (W_i^{(n/2),\text{ABS}})^- \quad \text{and} \quad \widehat{W}_{2i}^{(n),\text{ABS}} = (W_i^{(n/2),\text{ABS}})^+ \quad \text{for } 1 \leq i \leq n/2.$$

Therefore,

$$I(\widehat{W}_{2i-1}^{(n),\text{ABS}}) \leq I(W_i^{(n/2),\text{ABS}}) \leq I(\widehat{W}_{2i}^{(n),\text{ABS}}),$$

so we should not swap \widehat{U}_{2i-1} and \widehat{U}_{2i} for any $1 \leq i \leq n/2$. Thus we conclude that i_1, i_2, \dots, i_s in (10) must all be even numbers. In light of this, let us replace i_1, i_2, \dots, i_s in (10) with $2j_1, 2j_2, \dots, 2j_s$. Then we obtain

$$\pi_n = \sigma_{2j_1 \leftrightarrow 2j_1+1}^{(n)} \circ \sigma_{2j_2 \leftrightarrow 2j_2+1}^{(n)} \circ \sigma_{2j_3 \leftrightarrow 2j_3+1}^{(n)} \circ \cdots \circ \sigma_{2j_s \leftrightarrow 2j_s+1}^{(n)}, \quad (20)$$

and the condition (11) can be written as

$$j_2 \geq j_1 + 2, \quad j_3 \geq j_2 + 2, \quad j_4 \geq j_3 + 2, \quad \dots, \quad j_s \geq j_{s-1} + 2. \quad (21)$$

Now we are ready to state the recursive relation between $\{V_i^{(n),\text{ABS}}\}_{i=1}^{n-1}$ and $\{V_i^{(n/2),\text{ABS}}\}_{i=1}^{n/2-1}$.

Lemma 2. *Let $n \geq 4$. Let π_n be the permutation associated with $\mathbf{P}_n^{\text{ABS}}$. We write π_n in the form of (20) and require that j_1, j_2, \dots, j_s in (20) satisfy (21). For $1 \leq i \leq n/2 - 1$, we have the following results:*

Case i) *If $i \in \{j_1, j_2, \dots, j_s\}$, then*

$$V_{2i-1}^{(n),\text{ABS}} = (V_i^{(n/2),\text{ABS}})^\nabla, \quad V_{2i}^{(n),\text{ABS}} = (V_i^{(n/2),\text{ABS}})^\diamond, \quad V_{2i+1}^{(n),\text{ABS}} = (V_i^{(n/2),\text{ABS}})^\blacktriangle.$$

Case ii) *If $i \in \{j_1 - 1, j_2 - 1, \dots, j_s - 1\}$, then*

$$V_{2i-1}^{(n),\text{ABS}} = (V_i^{(n/2),\text{ABS}})^\nabla, \quad V_{2i}^{(n),\text{ABS}} = (V_i^{(n/2),\text{ABS}})^\diamond.$$

Case iii) *If $i \in \{j_1 + 1, j_2 + 1, \dots, j_s + 1\}$, then*

$$V_{2i}^{(n),\text{ABS}} = (V_i^{(n/2),\text{ABS}})^\diamond, \quad V_{2i+1}^{(n),\text{ABS}} = (V_i^{(n/2),\text{ABS}})^\triangle.$$

Case iv) *If $i \notin \{j_1 - 1, j_2 - 1, \dots, j_s - 1\} \cup \{j_1, j_2, \dots, j_s\} \cup \{j_1 + 1, j_2 + 1, \dots, j_s + 1\}$, then*

$$V_{2i-1}^{(n),\text{ABS}} = (V_i^{(n/2),\text{ABS}})^\nabla, \quad V_{2i}^{(n),\text{ABS}} = (V_i^{(n/2),\text{ABS}})^\diamond, \quad V_{2i+1}^{(n),\text{ABS}} = (V_i^{(n/2),\text{ABS}})^\triangle.$$

The proof of this lemma is omitted because it is essentially the same as the proof of Lemma 1. Here we point out one difference between Lemma 1 and Lemma 2. Lemma 1 tells us that $V_{2i+1}^{(n)}$ can be recursively calculated in two different ways for every $1 \leq i \leq n/2 - 2$; see (16). However, for $i \in \{j_1 - 1, j_2 - 1, \dots, j_s - 1\} \cup \{j_1, j_2, \dots, j_s\}$, there is only one way to calculate $V_{2i+1}^{(n),\text{ABS}}$ recursively. More precisely, if $i \in \{j_1 - 1, j_2 - 1, \dots, j_s - 1\}$, then $V_{2i+1}^{(n),\text{ABS}}$ can only be calculated from $V_{2i+1}^{(n),\text{ABS}} = (V_{i+1}^{(n/2),\text{ABS}})^\nabla$, and the relation $V_{2i+1}^{(n),\text{ABS}} = (V_i^{(n/2),\text{ABS}})^\triangle$ does not hold. Similarly, if $i \in \{j_1, j_2, \dots, j_s\}$, then $V_{2i+1}^{(n),\text{ABS}}$ can only be calculated from $V_{2i+1}^{(n),\text{ABS}} = (V_i^{(n/2),\text{ABS}})^\blacktriangle$, and the relation $V_{2i+1}^{(n),\text{ABS}} = (V_{i+1}^{(n/2),\text{ABS}})^\nabla$ does not hold.

Remark 1. *The condition (21) is necessary for us to derive a recursive relation between $\{V_i^{(n),\text{ABS}}\}_{i=1}^{n-1}$ and $\{V_i^{(n/2),\text{ABS}}\}_{i=1}^{n/2-1}$. Recall the definition of $\widehat{U}_1, \dots, \widehat{U}_n$ in Fig. 4. Suppose that the condition (21) does not hold. Then there exists an integer i such that we swap the adjacent bits \widehat{U}_{2i} and \widehat{U}_{2i+1} , and we also swap \widehat{U}_{2i+2} and \widehat{U}_{2i+3} . After that, \widehat{U}_{2i} and \widehat{U}_{2i+3} become adjacent bits. In order to calculate the joint distribution of \widehat{U}_{2i} and \widehat{U}_{2i+3} , we need to know the joint distribution of three adjacent bits in the previous layer. However, $\{V_i^{(n/2),\text{ABS}}\}_{i=1}^{n/2-1}$ only give us the joint distributions of two adjacent bits in the previous layer. Therefore, without (21), there does not exist a recursive relation between $\{V_i^{(n),\text{ABS}}\}_{i=1}^{n-1}$ and $\{V_i^{(n/2),\text{ABS}}\}_{i=1}^{n/2-1}$.*

Since we require $n \geq 4$ in Lemma 2, the starting point of the recursive relation in Lemma 2 is $V_1^{(2),\text{ABS}}$. It is easy to see that the permutation matrix $\mathbf{P}_2^{\text{ABS}}$ is the identity matrix. Therefore, given a BMS channel W , the transition probability of $V_1^{(2),\text{ABS}}$ is given by

$$V_1^{(2),\text{ABS}}(y_1, y_2 | u_1, u_2) = W(y_1 | u_1 + u_2)W(y_2 | u_2). \quad (22)$$

Note that this is the same as (17) for standard polar codes.

After obtaining the transition probabilities of the adjacent-bits-channels $\{V_i^{(n),\text{ABS}}\}_{i=1}^{n-1}$, we can use (18) to calculate the transition probabilities of the bit-channels $\{W_i^{(n),\text{ABS}}\}_{i=1}^n$. We only need to replace $W_i^{(n)}, W_{i+1}^{(n)}, V_i^{(n)}$ in (18) with $W_i^{(n),\text{ABS}}, W_{i+1}^{(n),\text{ABS}}, V_i^{(n),\text{ABS}}$. Once the transition probabilities of $\{W_i^{(n),\text{ABS}}\}_{i=1}^n$ are known, we are able to determine which bits are information bits and which bits are frozen bits.

D. Constructing the permutation matrices $\mathbf{P}_2^{\text{ABS}}, \mathbf{P}_4^{\text{ABS}}, \mathbf{P}_8^{\text{ABS}}, \dots, \mathbf{P}_n^{\text{ABS}}$ in (7)

We construct the permutation matrices in (7) one by one, starting from $\mathbf{P}_2^{\text{ABS}}$. Therefore, the matrices $\mathbf{P}_2^{\text{ABS}}, \mathbf{P}_4^{\text{ABS}}, \mathbf{P}_8^{\text{ABS}}, \dots, \mathbf{P}_{n/2}^{\text{ABS}}$ are already known when we construct $\mathbf{P}_n^{\text{ABS}}$. The method described in Section III-C allows us to calculate the transition probabilities of the adjacent-bits-channels $\{V_i^{(n/2),\text{ABS}}\}_{i=1}^{n/2-1}$ from $\mathbf{P}_2^{\text{ABS}}, \mathbf{P}_4^{\text{ABS}}, \mathbf{P}_8^{\text{ABS}}, \dots, \mathbf{P}_{n/2}^{\text{ABS}}$. As a consequence, we know the transition probabilities of $\{V_i^{(n/2),\text{ABS}}\}_{i=1}^{n/2-1}$ when constructing $\mathbf{P}_n^{\text{ABS}}$. Constructing the permutation matrix $\mathbf{P}_n^{\text{ABS}}$ is equivalent to constructing/choosing the corresponding permutation π_n . This is further equivalent to constructing the set $\mathcal{S}^* = \{j_1, j_2, \dots, j_s\}$, where the elements j_1, j_2, \dots, j_s come from (20) and satisfy the condition (21).

Before presenting how to construct the set \mathcal{S}^* , let us introduce some notation. Suppose that $V : \{0, 1\}^2 \rightarrow \mathcal{Y}$ is an adjacent-bits-channel with 4-ary inputs. Define two bit-channels $V_{\text{first}} : \{0, 1\} \rightarrow \mathcal{Y}$ and $V_{\text{second}} : \{0, 1\} \rightarrow \{0, 1\} \times \mathcal{Y}$ as

$$V_{\text{first}}(y|u_1) = \frac{1}{2} \sum_{u_2 \in \{0, 1\}} V(y|u_1, u_2) \quad \text{and} \quad V_{\text{second}}(y, u_1|u_2) = \frac{1}{2} V(y|u_1, u_2).$$

Comparing this with (18), we can see that if V is $V_i^{(n)}$, then V_{first} is simply $W_i^{(n)}$, and V_{second} is $W_{i+1}^{(n)}$. Similarly, if V is $V_i^{(n),\text{ABS}}$, then V_{first} is simply $W_i^{(n),\text{ABS}}$, and V_{second} is $W_{i+1}^{(n),\text{ABS}}$. Next we define

$$\begin{aligned} I_{\text{first}}(V) &:= I(V_{\text{first}}) \quad \text{and} \quad I_{\text{second}}(V) := I(V_{\text{second}}), \\ g(V) &:= I_{\text{first}}(V)(1 - I_{\text{first}}(V)) + I_{\text{second}}(V)(1 - I_{\text{second}}(V)). \end{aligned}$$

The function $g(V)$ measures the polarization level of the two bit-channels induced by V . In particular, $g(V) \approx 0$ means that the capacity of both bit-channels is very close to either 0 or 1. Finally, for $1 \leq i \leq n/2 - 1$, we define

$$\text{Score}(i) := g((V_i^{(n/2),\text{ABS}})^\diamond) - g((V_i^{(n/2),\text{ABS}})^\blacklozenge).$$

The interpretation of $\text{Score}(i)$ is as follows: According to Lemma 2, if $i \in \mathcal{S}^*$, then $V_{2i}^{(n),\text{ABS}} = (V_i^{(n/2),\text{ABS}})^\blacklozenge$; if $i \notin \mathcal{S}^*$, then $V_{2i}^{(n),\text{ABS}} = (V_i^{(n/2),\text{ABS}})^\diamond$. Therefore, $g((V_i^{(n/2),\text{ABS}})^\blacklozenge)$ measures the polarization level of the two bit-channels $W_{2i}^{(n),\text{ABS}}$ and $W_{2i+1}^{(n),\text{ABS}}$ when we include i in the set \mathcal{S}^* . Similarly, $g((V_i^{(n/2),\text{ABS}})^\diamond)$ measures the polarization level of the two bit-channels $W_{2i}^{(n),\text{ABS}}$ and $W_{2i+1}^{(n),\text{ABS}}$ when we do not include i in the set \mathcal{S}^* . If $\text{Score}(i) > 0$, then including i in the set \mathcal{S}^* accelerates polarization. If $\text{Score}(i) < 0$, then including i in the set \mathcal{S}^* slows down polarization, and in this case we should not include i in \mathcal{S}^* .

If we ignore the condition (21), then we can simply choose the set \mathcal{S}^* to be $\mathcal{S}^* = \{i : \text{Score}(i) > 0\}$. However, as discussed in Remark 1, the condition (21) is crucial for us to calculate the transition probabilities of the adjacent-bits-channels, so it must be satisfied. As a consequence, we need to find a set $\mathcal{S}^* \subseteq \{1, 2, \dots, n/2 - 1\}$ to maximize $\sum_{i \in \mathcal{S}^*} \text{Score}(i)$ under the constraint that the distance between any two distinct elements of \mathcal{S}^* must be at least 2. In other words, we need to solve the following optimization problem:

$$\begin{aligned} \mathcal{S}^* &= \operatorname{argmax}_{\mathcal{S} \subseteq \{1, 2, \dots, n/2 - 1\}} \sum_{i \in \mathcal{S}} \text{Score}(i) \\ \text{subject to: } &|i_1 - i_2| \geq 2 \text{ for all } i_1, i_2 \in \mathcal{S} \text{ such that } i_1 \neq i_2. \end{aligned} \tag{23}$$

This problem can be solved using a dynamic programming method. For $1 \leq j \leq n/2 - 1$, define

$$\begin{aligned} \mathcal{S}_j^* &= \operatorname{argmax}_{\mathcal{S} \subseteq \{1, 2, \dots, j\}} \sum_{i \in \mathcal{S}} \operatorname{Score}(i) \\ \text{subject to: } &|i_1 - i_2| \geq 2 \text{ for all } i_1, i_2 \in \mathcal{S} \text{ such that } i_1 \neq i_2, \\ M_j &= \max_{\mathcal{S} \subseteq \{1, 2, \dots, j\}} \sum_{i \in \mathcal{S}} \operatorname{Score}(i) \\ \text{subject to: } &|i_1 - i_2| \geq 2 \text{ for all } i_1, i_2 \in \mathcal{S} \text{ such that } i_1 \neq i_2. \end{aligned}$$

By definition, we can see that $M_1 \leq M_2 \leq M_3 \leq \dots \leq M_{n/2-1}$. The sets $\mathcal{S}_1^*, \mathcal{S}_2^*$ and the maximum values M_1, M_2 can be calculated as follows: If $\operatorname{Score}(1) > 0$, then $\mathcal{S}_1^* = \{1\}$ and $M_1 = \operatorname{Score}(1)$. If $\operatorname{Score}(1) \leq 0$, then $\mathcal{S}_1^* = \emptyset$ and $M_1 = 0$. If $\operatorname{Score}(2) > M_1$, then $\mathcal{S}_2^* = \{2\}$ and $M_2 = \operatorname{Score}(2)$. If $\operatorname{Score}(2) \leq M_1$, then $\mathcal{S}_2^* = \mathcal{S}_1^*$ and $M_2 = M_1$. For $j \geq 3$, the set \mathcal{S}_j^* and the maximum value M_j can be calculated recursively as follows: If $\operatorname{Score}(j) + M_{j-2} > M_{j-1}$, then $\mathcal{S}_j^* = \mathcal{S}_{j-2}^* \cup \{j\}$ and $M_j = \operatorname{Score}(j) + M_{j-2}$. If $\operatorname{Score}(j) + M_{j-2} \leq M_{j-1}$, then $\mathcal{S}_j^* = \mathcal{S}_{j-1}^*$ and $M_j = M_{j-1}$. This dynamic programming algorithm allows us to calculate \mathcal{S}_j^* for every $1 \leq j \leq n/2 - 1$. In particular, we are able to calculate $\mathcal{S}_{n/2-1}^* = \mathcal{S}^*$, which is the set we want to construct. Once we know the set $\mathcal{S}^* = \{j_1, j_2, \dots, j_s\}$, we can immediately write out the permutation π_n according to (20) and obtain the corresponding permutation matrix \mathbf{P}^{ABS} .

As a final remark, we note that $\mathbf{P}_2^{\text{ABS}}$ is always the identity matrix. However, for $n \geq 4$, the permutation matrix $\mathbf{P}_n^{\text{ABS}}$ depends on the underlying BMS channel W .

E. Quantization of the output alphabet

Algorithm 1: QuantizeChannel(μ, V)

Input: an upper bound μ on the output alphabet size after quantization; an adjacent-bits-channel V with outputs y_1, y_2, \dots, y_M

Output: quantized channel \tilde{V} with outputs $\{\tilde{y}_{i_1, i_2, i_3} : 0 \leq i_1, i_2, i_3 \leq b\}$

```

1 if  $M \leq \mu$  then
2   Set  $\tilde{V}$  to be the same as  $V$ 
3 else
4    $b \leftarrow \lfloor \mu^{1/3} \rfloor - 1$ 
5   Set  $\tilde{V}(\tilde{y}_{i_1, i_2, i_3} | (u_1, u_2)) = 0$  for all  $0 \leq i_1, i_2, i_3 \leq b$  and all  $u_1, u_2 \in \{0, 1\}$ 
6   ▷ Initialize all the transition probabilities of  $\tilde{V}$  as 0
7   for  $j = 1, 2, \dots, M$  do
8      $sum \leftarrow V(y_j | (0, 0)) + V(y_j | (0, 1)) + V(y_j | (1, 0)) + V(y_j | (1, 1))$ 
9      $p_1 \leftarrow \frac{V(y_j | (0, 0))}{sum}, \quad p_2 \leftarrow \frac{V(y_j | (0, 1))}{sum}, \quad p_3 \leftarrow \frac{V(y_j | (1, 0))}{sum}$ 
10    ▷ Calculate the posterior probability of  $y_j$ 
11     $i_1 \leftarrow \lfloor bp_1 \rfloor, \quad i_2 \leftarrow \lfloor bp_2 \rfloor, \quad i_3 \leftarrow \lfloor bp_3 \rfloor$ 
12     $\tilde{V}(\tilde{y}_{i_1, i_2, i_3} | (u_1, u_2)) \leftarrow \tilde{V}(\tilde{y}_{i_1, i_2, i_3} | (u_1, u_2)) + V(y_j | (u_1, u_2))$  for all  $u_1, u_2 \in \{0, 1\}$ 
13    ▷ Merge  $y_j$  into  $\tilde{y}_{i_1, i_2, i_3}$ 
14 return  $\tilde{V}$ 

```

An important step in the construction of standard polar codes is to quantize the output alphabets of the bit-channels $\{W_i^{(n)}\}_{i=1}^n$ because the output alphabet size grows exponentially with the code length n . The most widely used quantization method for binary-input standard polar codes was given in [14], where the main idea is to merge output symbols with similar posterior distributions using a greedy algorithm. This greedy algorithm was later generalized to construct polar codes with non-binary input

alphabets [15]–[17]. The time complexity of the greedy quantization algorithm is $O(\mu^2 \log \mu)$, where μ is the maximum size of the output alphabet after quantization. Since there are $2n - 1$ bit-channels we need to quantize in the code construction procedure, the overall time complexity of standard polar code construction is $O(n\mu^2 \log \mu)$.

In the ABS polar code construction, the output alphabet size of the adjacent-bits-channels $\{V_i^{(n)}\}_{i=1}^{n-1}$ also grows exponentially with n , and the quantization operations are also needed. Since the adjacent-bits-channels have 4-ary inputs, we can simply use the greedy quantization algorithms proposed in [15]–[17] for polar codes with non-binary inputs. However, in practical implementations, we found that these greedy algorithms for non-binary inputs usually involve implicit large constants in their time complexity. Therefore, we propose a new quantization algorithm to merge the output symbols of the adjacent-bits-channels $\{V_i^{(n)}\}_{i=1}^{n-1}$. The time complexity of our new quantization algorithm is $O(\mu^2)$, which is smaller than that of the greedy algorithms in [15]–[17]. Since there are $\Theta(n)$ adjacent-bits-channels we need to quantize in the ABS polar code construction, its overall time complexity is $O(n\mu^2)$.

Our new quantization algorithm works as follows. Given an upper bound μ on the output alphabet size after quantization, we define $b = \lfloor \mu^{1/3} \rfloor - 1$. For an adjacent-bits-channel V , we write its 4 inputs as $(0, 0), (0, 1), (1, 0), (1, 1)$, and we write its outputs as y_1, y_2, \dots, y_M , where M is the output alphabet size of V . We use \tilde{V} to denote the channel after output quantization. The 4 inputs of \tilde{V} are the same as the original channel V , and the outputs of \tilde{V} are written as $\{\tilde{y}_{i_1, i_2, i_3} : 0 \leq i_1, i_2, i_3 \leq b\}$. Clearly, the output alphabet size of \tilde{V} is no larger than μ . With the above notation in mind, we present our quantization algorithm in Algorithm 1. In our implementation, we pick $\mu = 250000$.

F. Summary of the ABS polar code construction

In Section III-C, we showed how to calculate the transition probabilities of the adjacent-bits-channels $\{V_i^{(n), \text{ABS}}\}_{i=1}^{n-1}$ when the permutation matrices $\mathbf{P}_2^{\text{ABS}}, \mathbf{P}_4^{\text{ABS}}, \mathbf{P}_8^{\text{ABS}}, \dots, \mathbf{P}_n^{\text{ABS}}$ in (7) are known. In Section III-D, we showed how to construct the permutation matrix $\mathbf{P}_n^{\text{ABS}}$ when the transition probabilities of $\{V_i^{(n/2), \text{ABS}}\}_{i=1}^{n/2-1}$ are available. In Section III-E, we proposed Algorithm 1 to quantize the output alphabets of the adjacent-bits-channels. Now we are in a position to put everything together and present

the code construction algorithm for ABS polar codes in Algorithm 2.

Algorithm 2: ABSConstruct(n, k, W)

Input: code length $n = 2^m \geq 4$, code dimension k , and the BMS channel W
Output: the permutation matrices $\mathbf{P}_2^{\text{ABS}}, \mathbf{P}_4^{\text{ABS}}, \mathbf{P}_8^{\text{ABS}}, \dots, \mathbf{P}_n^{\text{ABS}}$, and the index set \mathcal{A} of the information bits

- 1 Quantize the output alphabet of W using the method in [14] \triangleright This step is needed when the output alphabet size of W is very large, e.g., when W has a continuous output alphabet.
- 2 Set $\mathbf{P}_2^{\text{ABS}}$ to be the identity matrix
- 3 Calculate the transition probability of $V_1^{(2),\text{ABS}}$ from W using (22)
- 4 Quantize the output alphabet of $V_1^{(2),\text{ABS}}$ using Algorithm 1
- 5 **for** $n_0 = 4, 8, 16, \dots, n$ **do**
 - 6 Construct $\mathbf{P}_{n_0}^{\text{ABS}}$ from $\{V_i^{(n_0/2),\text{ABS}}\}_{i=1}^{n_0/2-1}$ using the method in Section III-D
 - 7 Calculate the transition probabilities of $\{V_i^{(n_0),\text{ABS}}\}_{i=1}^{n_0-1}$ from $\mathbf{P}_{n_0}^{\text{ABS}}$ and $\{V_i^{(n_0/2),\text{ABS}}\}_{i=1}^{n_0/2-1}$ using Lemma 2
 - 8 Quantize the output alphabets of $\{V_i^{(n_0),\text{ABS}}\}_{i=1}^{n_0-1}$ using Algorithm 1
 - 9 Calculate the transition probabilities of $\{W_i^{(n),\text{ABS}}\}_{i=1}^n$ from the transition probabilities of $\{V_i^{(n),\text{ABS}}\}_{i=1}^{n-1}$.
 - 10 Sort the capacity of the bit-channels $\{W_i^{(n),\text{ABS}}\}_{i=1}^n$ to obtain $I(W_{i_1}^{(n),\text{ABS}}) \geq I(W_{i_2}^{(n),\text{ABS}}) \geq \dots \geq I(W_{i_n}^{(n),\text{ABS}})$, where $\{i_1, i_2, \dots, i_n\}$ is a permutation of $\{1, 2, \dots, n\}$
 - 11 $\mathcal{A} \leftarrow \{i_1, i_2, \dots, i_k\}$
 - 12 **return** $\mathbf{P}_2^{\text{ABS}}, \mathbf{P}_4^{\text{ABS}}, \mathbf{P}_8^{\text{ABS}}, \dots, \mathbf{P}_n^{\text{ABS}}, \mathcal{A}$

IV. THE ENCODING ALGORITHM FOR ABS POLAR CODES

In this section, we present the encoding algorithm of ABS polar codes. Suppose that we have constructed an (n, k) ABS polar code with permutation matrices $\mathbf{P}_2^{\text{ABS}}, \mathbf{P}_4^{\text{ABS}}, \mathbf{P}_8^{\text{ABS}}, \dots, \mathbf{P}_n^{\text{ABS}}$ and the index set $\mathcal{A} = \{i_1, i_2, \dots, i_k\}$ of the information bits. We present the encoding algorithm of this code in Algorithm 3 below.

Algorithm 3: Encode((m_1, m_2, \dots, m_k))

Input: the message vector $(m_1, m_2, \dots, m_k) \in \{0, 1\}^k$
Output: the codeword $(c_1, c_2, \dots, c_n) \in \{0, 1\}^n$, where $n = 2^m$ is the code length

- 1 Initialize (c_1, c_2, \dots, c_n) as the all-zero vector
- 2 $(c_{i_1}, c_{i_2}, \dots, c_{i_k}) \leftarrow (m_1, m_2, \dots, m_k)$ \triangleright Recall that i_1, i_2, \dots, i_k are the indices of the information bits.
- 3 **for** $i = 0, 1, 2, 3, \dots, m-1$ **do**
 - 4 **for** $t = 2^i$ **do**
 - 5 $t \leftarrow 2^i$
 - 6 $n_0 \leftarrow 2^{m-i}$
 - 7 **for** $h = 1, 2, 3, \dots, t$ **do**
 - 8 $(c_h, c_{h+t}, c_{h+2t}, c_{h+3t}, \dots, c_{h+(n_0-1)t}) \leftarrow (c_h, c_{h+t}, c_{h+2t}, c_{h+3t}, \dots, c_{h+(n_0-1)t}) \mathbf{P}_{n_0}^{\text{ABS}}$
 - 9 \triangleright Line 8 is the only difference between the encoding algorithms for ABS polar codes and standard polar codes
 - 10 **for** $j = 0, 1, 2, 3, \dots, n_0/2-1$ **do**
 - 11 $c_{h+2jt} \leftarrow c_{h+2jt} + c_{h+2jt+t}$
 - 12 \triangleright The addition between c_{h+2jt} and $c_{h+2jt+t}$ is over the binary field
 - 13 **return** (c_1, c_2, \dots, c_n)

Without Line 8, Algorithm 3 is the same as the encoding algorithm of standard polar codes, whose time complexity is $O(n \log(n))$. In line 8, we perform a permutation on n_0 elements. According to our code construction, each of these n_0 elements is swapped at most once, so the number of operations involved in this permutation is no more than $n_0 = 2^{m-i}$. From the for loop in Line 7, we can see that Line 8 is executed $t = 2^i$ times for each $i \in \{0, 1, \dots, m-1\}$. In other words, for each fixed value of i , Line 8 induces at most $n_0 * t = 2^m = n$ operations. Therefore, the total number of operations induced by Line 8 is upper bounded by $n * m = n \log(n)$. Thus we conclude that the encoding complexity of ABS polar codes is still $O(n \log(n))$.

Proposition 1. *The encoding time complexity of ABS polar codes is $O(n \log(n))$.*

V. NEW SCL DECODER FOR ABS POLAR CODES

In this section, we present a new SCL decoder for ABS polar codes. The organization of this section is as follows: In Section V-A, we recap the classic SCL decoder for standard polar codes based on the 2×2 polar transform. The purpose of doing so is to get ourselves familiar with the recursive structure, which is shared by both the classic SCL decoder and our new SCL decoder. The SCL decoder presented in Section V-A is based on the one proposed in [18]. While the classic SCL decoder is based on the 2×2 polar transform, our new SCL decoder is based on the DB polar transform and the SDB polar transform; see Fig. 3 and Fig. 5 for the definitions of these two transforms. Instead of jumping directly into the decoding of ABS polar codes, we first present a new SCL decoder for standard polar codes based on the DB polar transform in Section V-B. This new SCL decoder for standard polar codes already contains most of the new ingredients in the SCL decoder for ABS polar codes, and it helps us learn these new ingredients in a familiar setting. Finally, in Section V-C, we present our new SCL decoder for ABS polar codes.

A. SCL decoder for standard polar codes based on the 2×2 polar transform

In this subsection, we recap the classic SCL decoder proposed in [18] for standard polar codes. Let us first introduce the data structure used in the SCL decoder. Suppose that the code length is $n = 2^m$, and the current list size of the SCL decoder is L^* . We associate each candidate in the list with a list element. Then there are L^* list elements in total, and we write them as $d[1], d[2], \dots, d[L^*]$. Each list element $d[j]$ has the following fields:

$$\begin{aligned} p_0[i] &= (p_0[i][1], p_0[i][2], \dots, p_0[i][2^i]), \quad i = 0, 1, 2, \dots, m, \\ p_1[i] &= (p_1[i][1], p_1[i][2], \dots, p_1[i][2^i]), \quad i = 0, 1, 2, \dots, m, \\ r[i] &= (r[i][1], r[i][2], \dots, r[i][2^i]), \quad i = 0, 1, 2, \dots, m, \\ &\text{score.} \end{aligned} \tag{24}$$

Among these fields, $p_0[i], p_1[i]$ and $r[i]$ are arrays of length 2^i for $0 \leq i \leq m$. The arrays $p_0[i]$ and $p_1[i]$ record the posterior probabilities of each bit, so their entries $p_0[i][j]$ and $p_1[i][j]$ are real numbers between 0 and 1 for $1 \leq j \leq 2^i$. The array $r[i]$ records the decoding results, so its entry $r[i][j]$ is either 0 or 1 for $1 \leq j \leq 2^i$. Finally, the last field *score* is a real number that records the current posterior probability of the list element. When the current list size is larger than the prescribed upper bound L , we prune the list according to the value of *score*.

Following the notation in Fig. 2, we use (X_1, \dots, X_n) and (Y_1, \dots, Y_n) to denote the random codeword vector and the random channel output vector, respectively. We use (y_1, \dots, y_n) to denote a realization of the random vector (Y_1, \dots, Y_n) . Given a realization (y_1, \dots, y_n) , we record the corresponding posterior probabilities in the arrays $p_0[m]$ and $p_1[m]$, whose entries are listed in (24). More precisely, we set

$$p_0[m][j] = \mathbb{P}(X_j = 0 | Y_j = y_j) \quad \text{and} \quad p_1[m][j] = \mathbb{P}(X_j = 1 | Y_j = y_j) \quad \text{for } 1 \leq j \leq n. \tag{25}$$

Note that we can also use the transition probability of the underlying BMS channel W to express $p_0[m][j]$ and $p_1[m][j]$ as follows:

$$p_0[m][j] = \frac{W(y_j|0)}{W(y_j|0) + W(y_j|1)} \quad \text{and} \quad p_1[m][j] = \frac{W(y_j|1)}{W(y_j|0) + W(y_j|1)}.$$

The next step is to calculate the arrays $p_0[m-1]$ and $p_1[m-1]$ from $p_0[m]$ and $p_1[m]$ as follows:

$$\begin{aligned} p_0[m-1][j] &= p_0[m][j] * p_0[m][j+n/2] + p_1[m][j] * p_1[m][j+n/2] \quad \text{and} \\ p_1[m-1][j] &= p_0[m][j] * p_1[m][j+n/2] + p_1[m][j] * p_0[m][j+n/2] \quad \text{for } 1 \leq j \leq n/2. \end{aligned} \quad (26)$$

The arrays $p_0[m-1]$ and $p_1[m-1]$ record the posterior probabilities of the components in the vector $(X_1 + X_{n/2+1}, X_2 + X_{n/2+2}, X_3 + X_{n/2+3}, \dots, X_{n/2} + X_n)$, and they further allow us to decode this vector. We denote the decoding result as $(\hat{x}_1 + \hat{x}_{n/2+1}, \hat{x}_2 + \hat{x}_{n/2+2}, \dots, \hat{x}_{n/2} + \hat{x}_n)$, and we put it in the first half of the array $r[m]$. More precisely, we set

$$r[m][j] = \hat{x}_j + \hat{x}_{n/2+j} \quad \text{for } 1 \leq j \leq n/2,$$

where the addition is over the binary field. After that, we update the arrays $p_0[m-1]$ and $p_1[m-1]$ as follows: For $1 \leq j \leq n/2$, if $r[m][j] = 0$, then we set

$$\begin{aligned} p_0[m-1][j] &= \frac{p_0[m][j] * p_0[m][j+n/2]}{p_0[m][j] * p_0[m][j+n/2] + p_1[m][j] * p_1[m][j+n/2]}, \\ p_1[m-1][j] &= \frac{p_1[m][j] * p_1[m][j+n/2]}{p_0[m][j] * p_0[m][j+n/2] + p_1[m][j] * p_1[m][j+n/2]}; \end{aligned} \quad (27)$$

if $r[m][j] = 1$, then we set

$$\begin{aligned} p_0[m-1][j] &= \frac{p_1[m][j] * p_0[m][j+n/2]}{p_0[m][j] * p_1[m][j+n/2] + p_1[m][j] * p_0[m][j+n/2]}, \\ p_1[m-1][j] &= \frac{p_0[m][j] * p_1[m][j+n/2]}{p_0[m][j] * p_1[m][j+n/2] + p_1[m][j] * p_0[m][j+n/2]}. \end{aligned} \quad (28)$$

This time the arrays $p_0[m-1]$ and $p_1[m-1]$ record the posterior probabilities of the components in the vector $(X_{n/2+1}, X_{n/2+2}, X_{n/2+3}, \dots, X_n)$, and they also allow us to decode this vector. We denote the decoding result as $(\hat{x}_{n/2+1}, \hat{x}_{n/2+2}, \dots, \hat{x}_n)$, and we put it in the second half of the array $r[m]$. More precisely, we set

$$r[m][j] = \hat{x}_j \quad \text{for } n/2 + 1 \leq j \leq n.$$

The final step is to add the second half of $r[m]$ to the first half. In this way, we obtain the decoding result in $r[m]$.

As we can see from the above description, the SCL decoder has a recursive structure. In order to decode a length- n code, we only need to decode two subcodes of length $n/2$. Similarly, in order to decode a length- $n/2$ subcode, we only need to decode two subcodes of length $n/4$. This recursive procedure continues until we reach subcodes of length 1, which are the information bits and frozen bits. If we encounter a frozen bit, then we simply calculate its posterior probability and use it to update the field *score* in every list element. If we encounter an information bit, then we expand the current list size by a factor of 2. If the list size is larger than the prescribed upper bound L after the expansion, then we prune the list according to the value of *score*.

The SCL decoder described above is formally presented in Algorithms 4–6. In this recursive decoding procedure, we need to decode many different subcodes with different code length. The first input parameter n^* of the `Decoder1` function in Algorithm 4 is the length of the subcode currently being decoded. When we use the SCL decoder to decode a channel output vector (y_1, y_2, \dots, y_n) , we initialize the list with a single list element `d[1]`. Only the following three fields in `d[1]` need to be assigned with initial values: We initialize `d[1].score` as 0, and we initialize the two arrays `d[1].p0[m]` and `d[1].p1[m]` according to (25).

More precisely, when initializing these two arrays, we replace $p_0[m][j]$ with $\mathbf{d}[1].p_0[m][j]$ and replace $p_1[m][j]$ with $\mathbf{d}[1].p_1[m][j]$ in (25). After that, we only need to call the function `Decoder1`($n, L, (\mathbf{d}[1])$), and it will return L list elements $\mathbf{d}[1], \mathbf{d}[2], \dots, \mathbf{d}[L]$ containing L decoding results of (y_1, y_2, \dots, y_n) . For $1 \leq i \leq L$, the array $\mathbf{d}[i].r[m]$ is the decoding result recorded in the list element $\mathbf{d}[i]$.

Remark 2. *The calculations in Equation (26) and Lines 4–5 of Algorithm 4 correspond to the “–” transform in Fig. 1. The calculations in Equations (27)–(28) and Lines 15–20 of Algorithm 4 correspond to the “+” transform in Fig. 1. This is why we say that the SCL decoder presented in this subsection is based on the 2×2 basic polar transform.*

More precisely, let us use the setting in Fig. 1 to explain this connection in detail. Let $U_1, U_2, X_1, X_2, Y_1, Y_2$ be the random variables defined in Fig. 1a. We first explain the connection between Equation (26) and the “–” transform. If $p_0[m][j] = \mathbb{P}(X_1 = 0|Y_1 = y_1), p_1[m][j] = \mathbb{P}(X_1 = 1|Y_1 = y_1), p_0[m][j + n/2] = \mathbb{P}(X_2 = 0|Y_2 = y_2), p_1[m][j + n/2] = \mathbb{P}(X_2 = 1|Y_2 = y_2)$, then $p_0[m - 1][j] = \mathbb{P}(U_1 = 0|Y_1 = y_1, Y_2 = y_2), p_1[m - 1][j] = \mathbb{P}(U_1 = 1|Y_1 = y_1, Y_2 = y_2)$. The calculations in Lines 4–5 of Algorithm 4 are essentially the same as Equation (26).

Next we explain the connection between Equations (27)–(28) and the “+” transform. If $p_0[m][j] = \mathbb{P}(X_1 = 0|Y_1 = y_1), p_1[m][j] = \mathbb{P}(X_1 = 1|Y_1 = y_1), p_0[m][j + n/2] = \mathbb{P}(X_2 = 0|Y_2 = y_2), p_1[m][j + n/2] = \mathbb{P}(X_2 = 1|Y_2 = y_2)$, then $p_0[m - 1][j] = \mathbb{P}(U_2 = 0|Y_1 = y_1, Y_2 = y_2, U_1 = r[m][j]), p_1[m - 1][j] = \mathbb{P}(U_2 = 1|Y_1 = y_1, Y_2 = y_2, U_1 = r[m][j])$. The calculations in Lines 15–20 of Algorithm 4 are essentially the same as Equations (27)–(28).

Algorithm 4: Decoder1($n^*, L, (d[1], d[2], \dots, d[L^*])$)

Input: $n^* = 2^{m^*}$ is the length of the subcode currently being decoded; L is the upper bound on the list size; $d[1], d[2], \dots, d[L^*]$ are the list elements in the current list, where L^* is the current list size

Output: updated list elements $(d[1], d[2], \dots, d[L'])$, where L' is the updated list size after decoding

```

1 if  $n^* > 1$  then
2    $m^* \leftarrow \log_2(n^*)$                                       $\triangleright m^*$  is an integer
3   for  $i = 1, 2, \dots, L^*$  do
4     for  $j = 1, 2, \dots, n^*/2$  do
5        $d[i].p_0[m^* - 1][j] \leftarrow$ 
6        $d[i].p_0[m^*][j] * d[i].p_0[m^*][j + n/2] + d[i].p_1[m^*][j] * d[i].p_1[m^*][j + n/2]$ 
7        $d[i].p_1[m^* - 1][j] \leftarrow$ 
8        $d[i].p_0[m^*][j] * d[i].p_1[m^*][j + n/2] + d[i].p_1[m^*][j] * d[i].p_0[m^*][j + n/2]$ 
9      $(d[1], d[2], \dots, d[L']) \leftarrow \text{Decoder1}(n^*/2, L, (d[1], d[2], \dots, d[L^*]))$ 
10     $\triangleright (d[1], d[2], \dots, d[L'])$  is the updated list after decoding the subcode of length  $n^*/2$ 
11     $\triangleright$  The updated list size  $L'$  can be different from the original list size  $L^*$ 
12   for  $i = 1, 2, \dots, L'$  do
13     for  $j = 1, 2, \dots, n^*/2$  do
14        $d[i].r[m^*][j] \leftarrow d[i].r[m^* - 1][j]$ 
15      $\triangleright$  Copy the decoding results to the first half of  $r[m^*]$ 
16   for  $i = 1, 2, \dots, L'$  do
17     for  $j = 1, 2, \dots, n^*/2$  do
18       if  $r[m^*][j] = 0$  then
19          $d[i].p_0[m^* - 1][j] \leftarrow \frac{d[i].p_0[m^*][j]*d[i].p_0[m^*][j+n/2]}{d[i].p_0[m^*][j]*d[i].p_0[m^*][j+n/2]+d[i].p_1[m^*][j]*d[i].p_1[m^*][j+n/2]}$ 
20          $d[i].p_1[m^* - 1][j] \leftarrow \frac{d[i].p_1[m^*][j]*d[i].p_1[m^*][j+n/2]}{d[i].p_0[m^*][j]*d[i].p_0[m^*][j+n/2]+d[i].p_1[m^*][j]*d[i].p_1[m^*][j+n/2]}$ 
21       else
22          $d[i].p_0[m^* - 1][j] \leftarrow \frac{d[i].p_1[m^*][j]*d[i].p_0[m^*][j+n/2]}{d[i].p_0[m^*][j]*d[i].p_1[m^*][j+n/2]+d[i].p_1[m^*][j]*d[i].p_0[m^*][j+n/2]}$ 
23          $d[i].p_1[m^* - 1][j] \leftarrow \frac{d[i].p_0[m^*][j]*d[i].p_1[m^*][j+n/2]}{d[i].p_0[m^*][j]*d[i].p_1[m^*][j+n/2]+d[i].p_1[m^*][j]*d[i].p_0[m^*][j+n/2]}$ 
24      $(d[1], d[2], \dots, d[L']) \leftarrow \text{Decoder1}(n^*/2, L, (d[1], d[2], \dots, d[L']))$ 
25      $\triangleright (d[1], d[2], \dots, d[L'])$  is the updated list after decoding the second subcode of length  $n^*/2$ 
26   for  $i = 1, 2, \dots, L'$  do
27     for  $j = 1, 2, \dots, n^*/2$  do
28        $d[i].r[m^*][j + n^*/2] \leftarrow d[i].r[m^* - 1][j]$ 
29        $d[i].r[m^*][j] \leftarrow d[i].r[m^*][j] + d[i].r[m^*][j + n^*/2]$ 
30      $\triangleright$  The decoding results are recorded in the array  $d[i].r[m^*]$ 
31   else
32     if this is a frozen bit then
33        $(d[1], d[2], \dots, d[L']) \leftarrow \text{Decode_Frozen_Bit}(L, (d[1], d[2], \dots, d[L^*]))$ 
34        $\triangleright$  The function is defined in Algorithm 5. Here the updated list size is  $L' = L^*$ 
35     else
36        $(d[1], d[2], \dots, d[L']) \leftarrow \text{Decode_Information_Bit}(L, (d[1], d[2], \dots, d[L^*]))$ 
37        $\triangleright$  The function is defined in Algorithm 6. Here the updated list size is  $L' = \min(2L^*, L)$ 
38   return  $(d[1], d[2], \dots, d[L'])$ 

```

Algorithm 5: Decode_Frozen_Bit($L, (d[1], d[2], \dots, d[L^*])$)

Input: L is the upper bound on the list size; $d[1], d[2], \dots, d[L^*]$ are the list elements in the current list, where L^* is the current list size

Output: updated list elements $(d[1], d[2], \dots, d[L^*])$

- 1 **for** $i = 1, 2, \dots, L^*$ **do**
- 2 $d[i].r[0][1] \leftarrow 0$ ▷ Frozen bits always take value 0.
- 3 $d[i].score \leftarrow d[i].score + \log(d[i].p_0[0][1])$
- 4 ▷ $d[i].p_0[0][1]$ is the posterior probability of this frozen bit being equal to 0
- 5 **return** $(d[1], d[2], \dots, d[L^*])$

Algorithm 6: Decode_Information_Bit($L, (d[1], d[2], \dots, d[L^*])$)

Input: L is the upper bound on the list size; $d[1], d[2], \dots, d[L^*]$ are the list elements in the current list, where L^* is the current list size

Output: updated list elements $(d[1], d[2], \dots, d[L'])$, where $L' = \min(2L^*, L)$ is the updated list size after decoding

- 1 Creat L^* new list elements $d[L^* + 1], d[L^* + 2], \dots, d[2L^*]$
- 2 Initialize $d[L^* + i]$ to be the same as $d[i]$ for every $i = 1, 2, \dots, L^*$
- 3 **for** $i = 1, 2, \dots, L^*$ **do**
- 4 $d[i].r[0][1] \leftarrow 0$ ▷ Assign value 0 to this information bit
- 5 $d[i].score \leftarrow d[i].score + \log(d[i].p_0[0][1])$
- 6 ▷ $d[i].p_0[0][1]$ is the posterior probability of this information bit being equal to 0
- 7 $d[L^* + i].r[0][1] \leftarrow 1$ ▷ Assign value 1 to this information bit
- 8 $d[L^* + i].score \leftarrow d[L^* + i].score + \log(d[L^* + i].p_1[0][1])$
- 9 ▷ $d[L^* + i].p_1[0][1]$ is the posterior probability of this information bit being equal to 1
- 10 **if** $2L^* > L$ **then**
- 11 Reorder the list elements $d[1], d[2], \dots, d[2L^*]$ such that $d[1].score \geq d[2].score \geq \dots \geq d[2L^*].score$
- 12 Only keep the first L list elements and discard all the others
- 13 $L' \leftarrow \min(2L^*, L)$
- 14 **return** $(d[1], d[2], \dots, d[L'])$

B. SCL decoder for standard polar codes based on the Double-Bits polar transform

In this subsection, we present a new SCL decoder for standard polar codes based on the Double-Bits polar transform in Fig. 3. Suppose that the code length is $n = 2^m$, and the current list size of the SCL decoder is L^* . We again write the L^* list elements as $d[1], d[2], \dots, d[L^*]$. For the SCL decoder presented in this subsection, each list element $d[j]$ has the following fields:

$$\begin{aligned}
 p_{0,0}[i] &= (p_{0,0}[i][1], p_{0,0}[i][2], \dots, p_{0,0}[i][2^i]), \quad i = 0, 1, 2, \dots, m-1, \\
 p_{0,1}[i] &= (p_{0,1}[i][1], p_{0,1}[i][2], \dots, p_{0,1}[i][2^i]), \quad i = 0, 1, 2, \dots, m-1, \\
 p_{1,0}[i] &= (p_{1,0}[i][1], p_{1,0}[i][2], \dots, p_{1,0}[i][2^i]), \quad i = 0, 1, 2, \dots, m-1, \\
 p_{1,1}[i] &= (p_{1,1}[i][1], p_{1,1}[i][2], \dots, p_{1,1}[i][2^i]), \quad i = 0, 1, 2, \dots, m-1, \\
 r_1[i] &= (r_1[i][1], r_1[i][2], \dots, r_1[i][2^i]), \quad i = 0, 1, 2, \dots, m-1, \\
 r_2[i] &= (r_2[i][1], r_2[i][2], \dots, r_2[i][2^i]), \quad i = 0, 1, 2, \dots, m-1, \\
 final &= (final[1], final[2], \dots, final[n]), \\
 score.
 \end{aligned} \tag{29}$$

Note that the fields here are different from the fields in the previous subsection; see (24). Among these fields, $p_{0,0}[i], p_{0,1}[i], p_{1,0}[i], p_{1,1}[i], r_1[i], r_2[i]$ are arrays of length 2^i for $0 \leq i \leq m-1$. The

arrays $p_{0,0}[i], p_{0,1}[i], p_{1,0}[i], p_{1,1}[i]$ record the posterior probabilities of each bit, so their entries $p_{0,0}[i][j], p_{0,1}[i][j], p_{1,0}[i][j], p_{1,1}[i][j]$ are real numbers between 0 and 1 for $1 \leq j \leq 2^i$. The arrays $r_1[i]$ and $r_2[i]$ record the intermediate decoding results, so their entries $r_1[i][j]$ and $r_2[i][j]$ are either 0 or 1 for $1 \leq j \leq 2^i$. The field *final* is an array of length n that records the final decoding result in each list element. Therefore, its entries $final[1], final[2], \dots, final[n]$ are either 0 or 1. The last field *score* is a real number that records the current posterior probability of the list element. When the current list size is larger than the prescribed upper bound L , we prune the list according to the value of *score*.

The SCL decoder in this subsection also has a recursive structure. In order to decode a length- n code, we also decode several subcodes of length $n/2$. In order to decode subcodes of length $n/2$, we further decompose them into length- $n/4$ subcodes. However, the SCL decoder in this subsection is different from the one in the previous subsection in the following aspects: First, when decoding a subcode of length $2n^* = 2^{m^*+1}$, we divide its $2n^*$ coordinates into $n^* = 2^{m^*}$ pairs. The entries $p_{0,0}[m^*][j], p_{0,1}[m^*][j], p_{1,0}[m^*][j], p_{1,1}[m^*][j]$ are the posterior probabilities of the two bits in the j th pair for $1 \leq j \leq n^*$. More precisely, $p_{0,0}[m^*][j]$ is the posterior probability that both bits take value 0; $p_{0,1}[m^*][j]$ is the posterior probability that the first bit is 0 and the second bit is 1; $p_{1,0}[m^*][j]$ is the posterior probability that the first bit is 1 and the second bit is 0; $p_{1,1}[m^*][j]$ is the posterior probability that both bits take value 1. Moreover, for $1 \leq j \leq n^*$, $r_1[m^*][j]$ is used for recording the decoding result of the first bit in the j th pair, and $r_2[m^*][j]$ is used for recording the decoding result of the second bit in the j th pair. Second, when decoding a subcode of length $2n^*$, we need to decode three further subcodes of length n^* in the new SCL decoder, where these three further subcodes are obtained from the ∇ transform, the \diamond transform and the Δ transform defined in Fig. 3. In contrast, we only need to decode two further subcodes of length n^* in the standard SCL decoder, where those two subcodes correspond to the “+” transform and the “-” transform defined in Fig. 1. Third, the new SCL decoder presented in Algorithm 7 has an input parameter *mode* which does not appear in the standard SCL decoder in Algorithm 4. The parameter *mode* only takes two possible values—either 1 or 2. It tells us how many bits we need to decode in each pair of bits. If *mode* = 1, then we only need to decode the first bit in each pair; if *mode* = 2, then we need to decode both bits. One might wonder why we only need to decode the first bit in certain cases. This is because for a channel V with 4-ary inputs, the inputs of V^∇ and V^\diamond have one-bit overlap, and the inputs of V^\diamond and V^Δ also have one-bit overlap, as discussed in Fig. 3.

The function `Decoder2` presented in Algorithm 7 is the SCL decoder for standard polar codes based on the Double-Bits polar transform. The function `Calculate_∇_Transform` in Line 3 of Algorithm 7 is given in Algorithm 8. The function `Calculate_◊_Transform` in Line 8 of Algorithm 7 is given in Algorithm 9. The function `Calculate_Δ_Transform` in Line 14 is given in Algorithm 10. The function `Decode_First_Bit` in Line 33 is given in Algorithm 11. The function `Decode_Both_Bits` in Line 35 is defined in Algorithm 12.

Below we give a detailed explanation about Algorithm 7. As mentioned above, when decoding a subcode consisting of $n^* = 2^{m^*}$ pairs of bits, we need to decode three further subcodes consisting of $n^*/2$ pairs of bits, and these three further subcodes are obtained from the ∇ transform, the \diamond transform, and the Δ transform, respectively. In Line 3 of Algorithm 7, we calculate the posterior probabilities of the first subcode corresponding to the ∇ transform. In Line 4, we decode the first subcode, and the decoding results are stored in the array $d[i].r_1[m^* - 1]$ for each list element $d[i]$. In Line 5–7, we copy the decoding results of the first subcode from the array $d[i].r_1[m^* - 1]$ to the first half of $d[i].r_1[m^*]$. This step is needed because the results in $d[i].r_1[m^* - 1]$ will be overwritten when we decode the second subcode. Next we calculate the posterior probabilities of the second subcode corresponding to the \diamond transform in Line 8. In Line 9–12, we decode the second subcode and copy the decoding results to the second half of $d[i].r_1[m^*]$ for each list element $d[i]$. The input parameter *mode* in the function `Decoder2` is the number of bits we need to decode in each pair. No matter *mode* is 1 or 2, we only need to decode the first bit in each pair from the first two subcodes. In fact, when *mode* = 1, that is all we need. We decode the third subcode corresponding to the Δ transform only when *mode* = 2, and in this case, we decode both bits in each pair from the third subcode. Line 13–19 shows how to decode the third subcode

when $mode = 2$. Since we only need to decode the first bit in each pair of bits for both the first and the second subcodes, we set the input parameter $mode$ of the `Decoder2` function to be 1 in both Line 4 and Line 9. On the other hand, we set $mode$ to be 2 in Line 15 because we need to decode both bits in each pair for the third subcode. After obtaining the decoding results of the three subcodes, we perform the 2×2 basic polar transform in Line 20–25. When $n^* = n/2$, we further calculate the final decoding results and store them in the array $d[i].final$ for each list element $d[i]$. This is done in Line 26–30. We deal with the case $n^* = 1$ in Line 31–35, where we can directly decode each pair of bits using the posterior probabilities $p_{0,0}[0][1], p_{0,1}[0][1], p_{1,0}[0][1], p_{1,1}[0][1]$. As a final remark, each time we execute the function `Decoder2`, the decoding list gets updated, and the list size might change. For example, in Line 4 of Algorithm 7, the list size changes from L^* to L'' after executing the function `Decoder2`; in Line 9, the list size changes from L'' to L''' ; in Line 15, the list size changes from L''' to L'''' .

Now let us explain how to use the function `Decoder2` in Algorithm 7 to decode a standard polar code with code length $n = 2^m$ over a BMS channel W . Given a channel output vector (y_1, y_2, \dots, y_n) , we initialize the list with a single list element $d[1]$. Only the following five fields in $d[1]$ need to be assigned with initial values: We initialize $d[1].score$ as 0, and we initialize the four arrays $d[1].p_{0,0}[m-1], d[1].p_{0,1}[m-1], d[1].p_{1,0}[m-1], d[1].p_{1,1}[m-1]$ as follows: For $1 \leq j \leq n/2$, define

$$\begin{aligned} sum_j = & W(y_j|0)W(y_{j+n/2}|0) + W(y_j|0)W(y_{j+n/2}|1) \\ & + W(y_j|1)W(y_{j+n/2}|0) + W(y_j|1)W(y_{j+n/2}|1), \end{aligned} \quad (30)$$

and we set

$$\begin{aligned} d[1].p_{0,0}[m-1][j] &= \frac{W(y_j|0)W(y_{j+n/2}|0)}{sum_j}, & d[1].p_{0,1}[m-1][j] &= \frac{W(y_j|1)W(y_{j+n/2}|1)}{sum_j}, \\ d[1].p_{1,0}[m-1][j] &= \frac{W(y_j|1)W(y_{j+n/2}|0)}{sum_j}, & d[1].p_{1,1}[m-1][j] &= \frac{W(y_j|0)W(y_{j+n/2}|1)}{sum_j}. \end{aligned} \quad (31)$$

The meaning of the above assignments can be explained using the setup in Fig. 1. Let U_1, U_2, Y_1, Y_2 be the random variables defined in Fig. 1. Then the above assignments are equivalent to

$$\begin{aligned} d[1].p_{0,0}[m-1][j] &= \mathbb{P}(U_1 = 0, U_2 = 0 | Y_1 = y_j, Y_2 = y_{j+n/2}), \\ d[1].p_{0,1}[m-1][j] &= \mathbb{P}(U_1 = 0, U_2 = 1 | Y_1 = y_j, Y_2 = y_{j+n/2}), \\ d[1].p_{1,0}[m-1][j] &= \mathbb{P}(U_1 = 1, U_2 = 0 | Y_1 = y_j, Y_2 = y_{j+n/2}), \\ d[1].p_{1,1}[m-1][j] &= \mathbb{P}(U_1 = 1, U_2 = 1 | Y_1 = y_j, Y_2 = y_{j+n/2}). \end{aligned}$$

After the initialization, we only need to call the function `Decoder2`($n/2, 2, L, (d[1])$), and it will return L list elements $d[1], d[2], \dots, d[L]$ containing L decoding results of (y_1, y_2, \dots, y_n) . For $1 \leq i \leq L$, the array $d[i].final$ is the decoding result recorded in the list element $d[i]$. Note that we set the input parameter $n^* = n/2$, **not** $n^* = n$. This is because in `Decoder2`, n^* is the number of pairs in the code/subcode currently being decoded, and the number of pairs is simply half the code length. Moreover, we set another input parameter $mode = 2$ in order to decode both bits in each pair.

Algorithm 7: Decoder2(n^* , mode, L , ($d[1], d[2], \dots, d[L^*]$))

Input: $n^* = 2^{m^*}$ is the number of pairs in the subcode currently being decoded; $mode$ is the number of bits we need to decode in each pair; L is the upper bound on the list size; $d[1], d[2], \dots, d[L^*]$ are the list elements in the current list, where L^* is the current list size

Output: updated list elements ($d[1], d[2], \dots, d[L']$), where L' is the updated list size after decoding

```

1 if  $n^* > 1$  then
2    $m^* \leftarrow \log_2(n^*)$   $\triangleright m^*$  is an integer
3   ( $d[1], d[2], \dots, d[L^*]$ )  $\leftarrow$  Calculate $_{\nabla}$ Transform( $m^*$ , ( $d[1], d[2], \dots, d[L^*]$ ))
4   ( $d[1], d[2], \dots, d[L'']$ )  $\leftarrow$  Decoder2( $n^*/2, 1, L$ , ( $d[1], d[2], \dots, d[L^*]$ ))
5   for  $i = 1, 2, \dots, L''$  do
6     for  $j = 1, 2, \dots, n^*/2$  do
7        $d[i].r_1[m^*][j] \leftarrow d[i].r_1[m^* - 1][j]$ 
8   ( $d[1], d[2], \dots, d[L'']$ )  $\leftarrow$  Calculate $_{\Diamond}$ Transform( $m^*$ , ( $d[1], d[2], \dots, d[L'']$ ))
9   ( $d[1], d[2], \dots, d[L''']$ )  $\leftarrow$  Decoder2( $n^*/2, 1, L$ , ( $d[1], d[2], \dots, d[L'']$ ))
10  for  $i = 1, 2, \dots, L'''$  do
11    for  $j = 1, 2, \dots, n^*/2$  do
12       $d[i].r_1[m^*][j + n^*/2] \leftarrow d[i].r_1[m^* - 1][j]$ 
13  if  $mode = 2$  then
14    ( $d[1], d[2], \dots, d[L''']$ )  $\leftarrow$  Calculate $_{\Delta}$ Transform( $m^*$ , ( $d[1], d[2], \dots, d[L''']$ ))
15    ( $d[1], d[2], \dots, d[L'''']$ )  $\leftarrow$  Decoder2( $n^*/2, 2, L$ , ( $d[1], d[2], \dots, d[L''']$ ))
16    for  $i = 1, 2, \dots, L''''$  do
17      for  $j = 1, 2, \dots, n^*/2$  do
18         $d[i].r_2[m^*][j] \leftarrow d[i].r_1[m^* - 1][j]$ 
19         $d[i].r_2[m^*][j + n^*/2] \leftarrow d[i].r_2[m^* - 1][j]$ 
20  if  $mode = 1$  then  $L' \leftarrow L''$ . if  $mode = 2$  then  $L' \leftarrow L''''$ .
21  for  $i = 1, 2, \dots, L'$  do
22    for  $j = 1, 2, \dots, n^*/2$  do
23       $d[i].r_1[m^*][j] \leftarrow d[i].r_1[m^*][j] + d[i].r_1[m^*][j + n^*/2]$ 
24      if  $mode = 2$  then
25         $d[i].r_2[m^*][j] \leftarrow d[i].r_2[m^*][j] + d[i].r_2[m^*][j + n^*/2]$ 
26  if  $n^* = n/2$  then
27    for  $i = 1, 2, \dots, L'$  do
28      for  $j = 1, 2, \dots, n/2$  do
29         $d[i].final[j] \leftarrow d[i].r_1[m^*][j] + d[i].r_2[m^*][j]$ 
30         $d[i].final[j + n/2] \leftarrow d[i].r_2[m^*][j]$ 
31  if  $n^* = 1$  then
32    if  $mode = 1$  then
33      ( $d[1], d[2], \dots, d[L']$ )  $\leftarrow$  DecodeFirstBit( $L$ , ( $d[1], d[2], \dots, d[L^*]$ ))
34    if  $mode = 2$  then
35      ( $d[1], d[2], \dots, d[L']$ )  $\leftarrow$  DecodeBothBits( $L$ , ( $d[1], d[2], \dots, d[L^*]$ ))
36  return ( $d[1], d[2], \dots, d[L']$ )

```

Algorithm 8: Calculate_∇_Transform(m^* , (d[1], d[2], ..., d[L^*]))

Input: the first input m^* indicates that we calculate the arrays with index $m^* - 1$ from the arrays with index m^* ; d[1], d[2], ..., d[L^*] are the list elements in the current list, where L^* is the current list size

Output: updated list elements (d[1], d[2], ..., d[L^*])

```

1  $n' \leftarrow 2^{m^*-1}$ 
2 for  $i = 1, 2, \dots, L^*$  do
3   for  $j = 1, 2, \dots, n'$  do
4      $d[i].p_{0,0}[m^*-1][j] \leftarrow$ 
       $d[i].p_{0,0}[m^*][j] * d[i].p_{0,0}[m^*][j+n'] + d[i].p_{0,0}[m^*][j] * d[i].p_{0,1}[m^*][j+n'] +$ 
       $d[i].p_{0,1}[m^*][j] * d[i].p_{0,0}[m^*][j+n'] + d[i].p_{0,1}[m^*][j] * d[i].p_{0,1}[m^*][j+n']$ 
5      $d[i].p_{0,1}[m^*-1][j] \leftarrow$ 
       $d[i].p_{1,0}[m^*][j] * d[i].p_{1,0}[m^*][j+n'] + d[i].p_{1,0}[m^*][j] * d[i].p_{1,1}[m^*][j+n'] +$ 
       $d[i].p_{1,1}[m^*][j] * d[i].p_{1,0}[m^*][j+n'] + d[i].p_{1,1}[m^*][j] * d[i].p_{1,1}[m^*][j+n']$ 
6      $d[i].p_{1,0}[m^*-1][j] \leftarrow$ 
       $d[i].p_{1,0}[m^*][j] * d[i].p_{0,0}[m^*][j+n'] + d[i].p_{1,0}[m^*][j] * d[i].p_{0,1}[m^*][j+n'] +$ 
       $d[i].p_{1,1}[m^*][j] * d[i].p_{0,0}[m^*][j+n'] + d[i].p_{1,1}[m^*][j] * d[i].p_{0,1}[m^*][j+n']$ 
7      $d[i].p_{1,1}[m^*-1][j] \leftarrow$ 
       $d[i].p_{0,0}[m^*][j] * d[i].p_{1,0}[m^*][j+n'] + d[i].p_{0,0}[m^*][j] * d[i].p_{1,1}[m^*][j+n'] +$ 
       $d[i].p_{0,1}[m^*][j] * d[i].p_{1,0}[m^*][j+n'] + d[i].p_{0,1}[m^*][j] * d[i].p_{1,1}[m^*][j+n']$ 
8 return (d[1], d[2], ..., d[ $L^*$ ])

```

Algorithm 9: Calculate_◊_Transform(m^* , (d[1], d[2], ..., d[L^*]))

Input: the first input m^* indicates that we calculate the arrays with index $m^* - 1$ from the arrays with index m^* ; d[1], d[2], ..., d[L^*] are the list elements in the current list, where L^* is the current list size

Output: updated list elements (d[1], d[2], ..., d[L^*])

```

1  $n' \leftarrow 2^{m^*-1}$ 
2 for  $i = 1, 2, \dots, L^*$  do
3   for  $j = 1, 2, \dots, n'$  do
4     if  $d[i].r_1[m^*][j] = 0$  then
5        $q_{0,0} \leftarrow d[i].p_{0,0}[m^*][j] * d[i].p_{0,0}[m^*][j+n'] + d[i].p_{0,1}[m^*][j] * d[i].p_{0,1}[m^*][j+n']$ 
6        $q_{0,1} \leftarrow d[i].p_{0,0}[m^*][j] * d[i].p_{0,1}[m^*][j+n'] + d[i].p_{0,1}[m^*][j] * d[i].p_{0,0}[m^*][j+n']$ 
7        $q_{1,0} \leftarrow d[i].p_{1,0}[m^*][j] * d[i].p_{1,0}[m^*][j+n'] + d[i].p_{1,1}[m^*][j] * d[i].p_{1,1}[m^*][j+n']$ 
8        $q_{1,1} \leftarrow d[i].p_{1,0}[m^*][j] * d[i].p_{1,1}[m^*][j+n'] + d[i].p_{1,1}[m^*][j] * d[i].p_{1,0}[m^*][j+n']$ 
9     if  $d[i].r_1[m^*][j] = 1$  then
10       $q_{0,0} \leftarrow d[i].p_{1,0}[m^*][j] * d[i].p_{0,0}[m^*][j+n'] + d[i].p_{1,1}[m^*][j] * d[i].p_{0,1}[m^*][j+n']$ 
11       $q_{0,1} \leftarrow d[i].p_{1,0}[m^*][j] * d[i].p_{0,1}[m^*][j+n'] + d[i].p_{1,1}[m^*][j] * d[i].p_{0,0}[m^*][j+n']$ 
12       $q_{1,0} \leftarrow d[i].p_{0,0}[m^*][j] * d[i].p_{1,0}[m^*][j+n'] + d[i].p_{0,1}[m^*][j] * d[i].p_{1,1}[m^*][j+n']$ 
13       $q_{1,1} \leftarrow d[i].p_{0,0}[m^*][j] * d[i].p_{1,1}[m^*][j+n'] + d[i].p_{0,1}[m^*][j] * d[i].p_{1,0}[m^*][j+n']$ 
14      $sum \leftarrow q_{0,0} + q_{0,1} + q_{1,0} + q_{1,1}$ 
15      $d[i].p_{0,0}[m^*-1][j] \leftarrow q_{0,0}/sum, \quad d[i].p_{0,1}[m^*-1][j] \leftarrow q_{0,1}/sum$ 
16      $d[i].p_{1,0}[m^*-1][j] \leftarrow q_{1,0}/sum, \quad d[i].p_{1,1}[m^*-1][j] \leftarrow q_{1,1}/sum$ 
17 return (d[1], d[2], ..., d[ $L^*$ ])

```

Algorithm 10: Calculate_Δ_Transform(m^* , (d[1], d[2], ..., d[L^*]))

Input: the first input m^* indicates that we calculate the arrays with index $m^* - 1$ from the arrays with index m^* ; d[1], d[2], ..., d[L^*] are the list elements in the current list, where L^* is the current list size

Output: updated list elements (d[1], d[2], ..., d[L^*])

```

1   $n' \leftarrow 2^{m^*-1}$ 
2  for  $i = 1, 2, \dots, L^*$  do
3    for  $j = 1, 2, \dots, n'$  do
4      if  $d[i].r_1[m^*][j] = 0$  and  $d[i].r_1[m^*][j + n'] = 0$  then
5         $sum \leftarrow d[i].p_{0,0}[m^*][j] * d[i].p_{0,0}[m^*][j + n'] + d[i].p_{0,0}[m^*][j] * d[i].p_{0,1}[m^*][j + n'] + d[i].p_{0,1}[m^*][j] * d[i].p_{0,0}[m^*][j + n'] + d[i].p_{0,1}[m^*][j] * d[i].p_{0,1}[m^*][j + n']$ 
6         $d[i].p_{0,0}[m^* - 1][j] \leftarrow d[i].p_{0,0}[m^*][j] * d[i].p_{0,0}[m^*][j + n'] / sum$ 
7         $d[i].p_{0,1}[m^* - 1][j] \leftarrow d[i].p_{0,1}[m^*][j] * d[i].p_{0,1}[m^*][j + n'] / sum$ 
8         $d[i].p_{1,0}[m^* - 1][j] \leftarrow d[i].p_{0,1}[m^*][j] * d[i].p_{0,0}[m^*][j + n'] / sum$ 
9         $d[i].p_{1,1}[m^* - 1][j] \leftarrow d[i].p_{0,0}[m^*][j] * d[i].p_{0,1}[m^*][j + n'] / sum$ 
10      if  $d[i].r_1[m^*][j] = 0$  and  $d[i].r_1[m^*][j + n'] = 1$  then
11         $sum \leftarrow d[i].p_{1,0}[m^*][j] * d[i].p_{1,0}[m^*][j + n'] + d[i].p_{1,0}[m^*][j] * d[i].p_{1,1}[m^*][j + n'] + d[i].p_{1,1}[m^*][j] * d[i].p_{1,0}[m^*][j + n'] + d[i].p_{1,1}[m^*][j] * d[i].p_{1,1}[m^*][j + n']$ 
12         $d[i].p_{0,0}[m^* - 1][j] \leftarrow d[i].p_{1,0}[m^*][j] * d[i].p_{1,0}[m^*][j + n'] / sum$ 
13         $d[i].p_{0,1}[m^* - 1][j] \leftarrow d[i].p_{1,1}[m^*][j] * d[i].p_{1,1}[m^*][j + n'] / sum$ 
14         $d[i].p_{1,0}[m^* - 1][j] \leftarrow d[i].p_{1,1}[m^*][j] * d[i].p_{1,0}[m^*][j + n'] / sum$ 
15         $d[i].p_{1,1}[m^* - 1][j] \leftarrow d[i].p_{1,0}[m^*][j] * d[i].p_{1,1}[m^*][j + n'] / sum$ 
16      if  $d[i].r_1[m^*][j] = 1$  and  $d[i].r_1[m^*][j + n'] = 0$  then
17         $sum \leftarrow d[i].p_{1,0}[m^*][j] * d[i].p_{0,0}[m^*][j + n'] + d[i].p_{1,0}[m^*][j] * d[i].p_{0,1}[m^*][j + n'] + d[i].p_{1,1}[m^*][j] * d[i].p_{0,0}[m^*][j + n'] + d[i].p_{1,1}[m^*][j] * d[i].p_{0,1}[m^*][j + n']$ 
18         $d[i].p_{0,0}[m^* - 1][j] \leftarrow d[i].p_{1,0}[m^*][j] * d[i].p_{0,0}[m^*][j + n'] / sum$ 
19         $d[i].p_{0,1}[m^* - 1][j] \leftarrow d[i].p_{1,1}[m^*][j] * d[i].p_{0,1}[m^*][j + n'] / sum$ 
20         $d[i].p_{1,0}[m^* - 1][j] \leftarrow d[i].p_{1,1}[m^*][j] * d[i].p_{0,0}[m^*][j + n'] / sum$ 
21         $d[i].p_{1,1}[m^* - 1][j] \leftarrow d[i].p_{1,0}[m^*][j] * d[i].p_{0,1}[m^*][j + n'] / sum$ 
22      if  $d[i].r_1[m^*][j] = 1$  and  $d[i].r_1[m^*][j + n'] = 1$  then
23         $sum \leftarrow d[i].p_{0,0}[m^*][j] * d[i].p_{1,0}[m^*][j + n'] + d[i].p_{0,0}[m^*][j] * d[i].p_{1,1}[m^*][j + n'] + d[i].p_{0,1}[m^*][j] * d[i].p_{1,0}[m^*][j + n'] + d[i].p_{0,1}[m^*][j] * d[i].p_{1,1}[m^*][j + n']$ 
24         $d[i].p_{0,0}[m^* - 1][j] \leftarrow d[i].p_{0,0}[m^*][j] * d[i].p_{1,0}[m^*][j + n'] / sum$ 
25         $d[i].p_{0,1}[m^* - 1][j] \leftarrow d[i].p_{0,1}[m^*][j] * d[i].p_{1,1}[m^*][j + n'] / sum$ 
26         $d[i].p_{1,0}[m^* - 1][j] \leftarrow d[i].p_{0,1}[m^*][j] * d[i].p_{1,0}[m^*][j + n'] / sum$ 
27         $d[i].p_{1,1}[m^* - 1][j] \leftarrow d[i].p_{0,0}[m^*][j] * d[i].p_{1,1}[m^*][j + n'] / sum$ 
28  return (d[1], d[2], ..., d[ $L^*$ ])

```

Algorithm 11: Decode_First_Bit($L, (d[1], d[2], \dots, d[L^*])$)

Input: L is the upper bound on the list size; $d[1], d[2], \dots, d[L^*]$ are the list elements in the current list, where L^* is the current list size

Output: updated list elements $(d[1], d[2], \dots, d[L'])$, where L' is the updated list size after decoding

```

1 if the first bit is a frozen bit then
2   for  $i = 1, 2, \dots, L^*$  do
3      $d[i].r_1[0][1] \leftarrow 0$                                 ▷ Frozen bits always take value 0
4      $d[i].score \leftarrow d[i].score + \log(d[i].p_{0,0}[0][1] + d[i].p_{0,1}[0][1])$ 
5     ▷  $d[i].p_{0,0}[0][1] + d[i].p_{0,1}[0][1]$  is the posterior probability of the first bit taking value 0
6    $L' \leftarrow L^*$                                          ▷ In this case, the list size does not change
7 if the first bit is an information bit then
8   Create  $L^*$  new list elements  $d[L^* + 1], d[L^* + 2], \dots, d[2L^*]$ 
9   Initialize  $d[L^* + i]$  to be the same as  $d[i]$  for every  $i = 1, 2, \dots, L^*$ 
10  for  $i = 1, 2, \dots, L^*$  do
11     $d[i].r_1[0][1] \leftarrow 0$                                 ▷ Assign value 0 to this information bit
12     $d[i].score \leftarrow d[i].score + \log(d[i].p_{0,0}[0][1] + d[i].p_{0,1}[0][1])$ 
13     $d[L^* + i].r_1[0][1] \leftarrow 1$                             ▷ Assign value 1 to this information bit
14     $d[L^* + i].score \leftarrow d[L^* + i].score + \log(d[L^* + i].p_{1,0}[0][1] + d[L^* + i].p_{1,1}[0][1])$ 
15  if  $2L^* > L$  then
16    Reorder the list elements  $d[1], d[2], \dots, d[2L^*]$  such that
       $d[1].score \geq d[2].score \geq \dots \geq d[2L^*].score$ 
17    Only keep the first  $L$  list elements and discard all the others
18   $L' \leftarrow \min(2L^*, L)$ 
19 return  $(d[1], d[2], \dots, d[L'])$ 

```

Algorithm 12: Decode_Both_Bits($L, (d[1], d[2], \dots, d[L^*])$)

Input: L is the upper bound on the list size; $d[1], d[2], \dots, d[L^*]$ are the list elements in the current list, where L^* is the current list size

Output: updated list elements $(d[1], d[2], \dots, d[L'])$, where L' is the updated list size after decoding

```

1 if both bits are frozen bits then
2   for  $i = 1, 2, \dots, L^*$  do
3      $d[i].r_1[0][1] \leftarrow 0, d[i].r_2[0][1] \leftarrow 0$            ▷ Frozen bits always take value 0
4      $d[i].score \leftarrow d[i].score + \log(d[i].p_{0,0}[0][1])$ 
5     ▷  $d[i].p_{0,0}[0][1]$  is the posterior probability of both bits taking value 0
6    $L' \leftarrow L^*$                                          ▷ In this case, the list size does not change
7 if the first bit is a frozen bit and the second bit is an information bit then
8   Create  $L^*$  new list elements  $d[L^* + 1], d[L^* + 2], \dots, d[2L^*]$ 
9   Initialize  $d[L^* + i]$  to be the same as  $d[i]$  for every  $i = 1, 2, \dots, L^*$ 
10  for  $i = 1, 2, \dots, L^*$  do
11     $d[i].r_1[0][1] \leftarrow 0, d[i].r_2[0][1] \leftarrow 0$ 
12     $d[i].score \leftarrow d[i].score + \log(d[i].p_{0,0}[0][1])$ 
13     $d[L^* + i].r_1[0][1] \leftarrow 0, d[L^* + i].r_2[0][1] \leftarrow 1$ 
14     $d[L^* + i].score \leftarrow d[L^* + i].score + \log(d[L^* + i].p_{0,1}[0][1])$ 
15  if  $2L^* > L$  then
16    Reorder the list elements  $d[1], d[2], \dots, d[2L^*]$  such that
17       $d[1].score \geq d[2].score \geq \dots \geq d[2L^*].score$ 
18    Only keep the first  $L$  list elements and discard all the others
19     $L' \leftarrow \min(2L^*, L)$ 
20  if the first bit is an information bit and the second bit is a frozen bit then
21    Create  $L^*$  new list elements  $d[L^* + 1], d[L^* + 2], \dots, d[2L^*]$ 
22    Initialize  $d[L^* + i]$  to be the same as  $d[i]$  for every  $i = 1, 2, \dots, L^*$ 
23    for  $i = 1, 2, \dots, L^*$  do
24       $d[i].r_1[0][1] \leftarrow 0, d[i].r_2[0][1] \leftarrow 0$ 
25       $d[i].score \leftarrow d[i].score + \log(d[i].p_{0,0}[0][1])$ 
26       $d[L^* + i].r_1[0][1] \leftarrow 1, d[L^* + i].r_2[0][1] \leftarrow 0$ 
27       $d[L^* + i].score \leftarrow d[L^* + i].score + \log(d[L^* + i].p_{1,0}[0][1])$ 
28  if  $2L^* > L$  then
29    Reorder the list elements  $d[1], d[2], \dots, d[2L^*]$  such that
30       $d[1].score \geq d[2].score \geq \dots \geq d[2L^*].score$ 
31    Only keep the first  $L$  list elements and discard all the others
32     $L' \leftarrow \min(2L^*, L)$ 
33  if both bits are information bits then
34     $L' \leftarrow \min(4L^*, L)$ 
35     $(d[1], d[2], \dots, d[L']) \leftarrow \text{Decode_Both_Info_Bits}(L, (d[1], d[2], \dots, d[L^*]))$ 
36    ▷ The function Decode_Both_Info_Bits is given in Algorithm 13
37  return  $(d[1], d[2], \dots, d[L'])$ 

```

Algorithm 13: Decode_Both_Info_Bits($L, (d[1], d[2], \dots, d[L^*])$)

Input: L is the upper bound on the list size; $d[1], d[2], \dots, d[L^*]$ are the list elements in the current list, where L^* is the current list size

Output: updated list elements $(d[1], d[2], \dots, d[L'])$, where $L' = \min(4L^*, L)$ is the updated list size after decoding

- 1 Create $3L^*$ new list elements $d[L^* + 1], d[L^* + 2], d[L^* + 3], \dots, d[4L^*]$
- 2 Initialize $d[L^* + i], d[2L^* + i], d[3L^* + i]$ to be the same as $d[i]$ for every $i = 1, 2, \dots, L^*$
- 3 **for** $i = 1, 2, \dots, L^*$ **do**
- 4 $d[i].r_1[0][1] \leftarrow 0, d[i].r_2[0][1] \leftarrow 0$
- 5 $d[i].score \leftarrow d[i].score + \log(d[i].p_{0,0}[0][1])$
- 6 $d[L^* + i].r_1[0][1] \leftarrow 0, d[L^* + i].r_2[0][1] \leftarrow 1$
- 7 $d[L^* + i].score \leftarrow d[L^* + i].score + \log(d[L^* + i].p_{0,1}[0][1])$
- 8 $d[2L^* + i].r_1[0][1] \leftarrow 1, d[2L^* + i].r_2[0][1] \leftarrow 0$
- 9 $d[2L^* + i].score \leftarrow d[2L^* + i].score + \log(d[2L^* + i].p_{1,0}[0][1])$
- 10 $d[3L^* + i].r_1[0][1] \leftarrow 1, d[3L^* + i].r_2[0][1] \leftarrow 1$
- 11 $d[3L^* + i].score \leftarrow d[3L^* + i].score + \log(d[3L^* + i].p_{1,1}[0][1])$
- 12 **if** $4L^* > L$ **then**
- 13 Reorder the list elements $d[1], d[2], d[3], \dots, d[4L^*]$ such that
 $d[1].score \geq d[2].score \geq \dots \geq d[4L^*].score$
- 14 Only keep the first L list elements and discard all the others
- 15 $L' \leftarrow \min(4L^*, L)$
- 16 **return** $(d[1], d[2], \dots, d[L'])$

C. SCL decoder for ABS polar codes

In this subsection, we present the new SCL decoder for ABS polar codes. This decoder is based on the DB polar transform in Fig. 3 and the SDB polar transform in Fig. 5. Suppose that the code length is $n = 2^m$, and the current list size of the SCL decoder is L^* . We again write the L^* list elements as $d[1], d[2], \dots, d[L^*]$. For the SCL decoder presented in this subsection, each list element $d[j]$ has the following fields:

$$\begin{aligned}
 p_{0,0}[i] &= (p_{0,0}[i][1], p_{0,0}[i][2], \dots, p_{0,0}[i][2^i]), \quad i = 0, 1, 2, \dots, m-1, \\
 p_{0,1}[i] &= (p_{0,1}[i][1], p_{0,1}[i][2], \dots, p_{0,1}[i][2^i]), \quad i = 0, 1, 2, \dots, m-1, \\
 p_{1,0}[i] &= (p_{1,0}[i][1], p_{1,0}[i][2], \dots, p_{1,0}[i][2^i]), \quad i = 0, 1, 2, \dots, m-1, \\
 p_{1,1}[i] &= (p_{1,1}[i][1], p_{1,1}[i][2], \dots, p_{1,1}[i][2^i]), \quad i = 0, 1, 2, \dots, m-1, \\
 r_1[i] &= (r_1[i][1], r_1[i][2], \dots, r_1[i][2^i]), \quad i = 0, 1, 2, \dots, m-1, \\
 r_2[i] &= (r_2[i][1], r_2[i][2], \dots, r_2[i][2^i]), \quad i = 0, 1, 2, \dots, m-1, \\
 cache[i] &= (cache[i][1], cache[i][2], \dots, cache[i][2^i]), \quad i = 0, 1, 2, \dots, m-1, \\
 final &= (final[1], final[2], \dots, final[n]), \\
 score.
 \end{aligned}$$

Apart from $cache[0], cache[1], \dots, cache[m-1]$, all the other fields have already appeared in (29). The roles of these fields are explained right after (29), so we do not repeat them here. The new fields $cache[0], cache[1], \dots, cache[m-1]$ are arrays that record the intermediate decoding results. More specifically, $cache[i]$ is an array of length 2^i , and its entries $cache[i][1], cache[i][2], \dots, cache[i][2^i]$ are either 0 or 1. Note that the role of $cache[i]$ is very similar to the role of $r_1[i]$ and $r_2[i]$ because they are all used for recording the intermediate decoding results. In fact, $cache[i]$ can be viewed as a backup for $r_1[i]$. When decoding swapped adjacent bits, $r_1[i]$ does not have enough room to store all the intermediate

decoding results, and we use $cache[i]$ to provide some extra storage room in this case. Since we do not swap any adjacent bits in standard polar codes, the arrays $cache[0], cache[1], \dots, cache[m-1]$ are not needed in Section V-B.

The function `ABS_Decoder` presented in Algorithm 14 is the new SCL decoder for ABS polar codes. The functions `Swapped_mode1`, `Preswapped_mode1`, `Notswapped_mode1` in Line 5,7,9 of Algorithm 14 are given in Algorithms 15–17. The functions `Swapped_mode2`, `Preswapped_mode2`, `Notswapped_mode2` in Line 12,14,16 of Algorithm 14 are given in Algorithms 18–20. The functions `Calculate_▼_Transform`, `Calculate_◆_Transform`, `Calculate_▲_Transform` in Algorithm 15 and Algorithm 18 are given in Algorithms 21–23.

A major difference between the function `ABS_Decoder` for ABS polar codes and the function `Decoder2` for standard polar codes is that `ABS_Decoder` has an extra input parameter idx . The parameter idx is the index of the adjacent-bits-channel whose inputs are currently being decoded. The value of idx determines whether we use the DB polar transform or the SDB polar transform to calculate the posterior probabilities of the next layer; see Line 4–9 and Line 11–16 of Algorithm 14. The pseudocode in Line 4–9 and Line 11–16 of Algorithm 14 is based on Lemma 2.

Now let us explain how to use the function `ABS_Decoder` in Algorithm 14 to decode an ABS polar code with code length $n = 2^m$ over a BMS channel W . Given a channel output vector (y_1, y_2, \dots, y_n) , we initialize the list with a single list element $d[1]$. Only the following five fields in $d[1]$ need to be assigned with initial values: We initialize $d[1].score$ as 0, and we initialize the four arrays $d[1].p_{0,0}[m-1], d[1].p_{0,1}[m-1], d[1].p_{1,0}[m-1], d[1].p_{1,1}[m-1]$ using (30)–(31) in Section V-B. After the initialization, we only need to call the function `ABS_Decoder`($n/2, 2, 1, L, (d[1])$), and it will return L list elements $d[1], d[2], \dots, d[L]$ containing L decoding results of (y_1, y_2, \dots, y_n) . For $1 \leq i \leq L$, the array $d[i].final$ is the decoding result recorded in the list element $d[i]$. Note that the choices of the input parameters $n^* = n/2$ and $mode = 2$ are the same as those for the function `Decoder2` in Section V-B. The extra input parameter idx is set to be 1 because it is the index of the adjacent-bits-channel $V_1^{(2),ABS}$.

Since the overall recursive structure of the `ABS_Decoder` for ABS polar codes is the same as the classic SCL decoder in Algorithm 4 for standard polar codes, it is easy to see that the time complexity of `ABS_Decoder` is also $O(Ln \log(n))$.

Proposition 2. *The time complexity of the new SCL decoder for ABS polar codes is $O(Ln \log(n))$.*

Algorithm 14: ABS_Decoder(n^* , mode, idx, L, (d[1], d[2], ..., d[L*]))

Input: $n^* = 2^{m^*}$ is the number of pairs in the subcode currently being decoded; mode is the number of bits we need to decode in each pair; idx is the index of the adjacent-bits-channel whose inputs are currently being decoded; L is the upper bound on the list size; d[1], d[2], ..., d[L*] are the list elements in the current list, where L^* is the current list size

Output: updated list elements (d[1], d[2], ..., d[L']), where L' is the updated list size after decoding

```

1 if  $n^* > 1$  then
2    $n_1 \leftarrow 2n/n^*$ 
3   if mode = 1 then
4     if  $2idx$  and  $2idx + 1$  are swapped by the permutation matrix  $\mathbf{P}_{n_1}^{\text{ABS}}$  in (7) then
5        $(d[1], d[2], \dots, d[L']) \leftarrow \text{Swapped\_mode1}(n^*, idx, L, (d[1], d[2], \dots, d[L*]))$ 
6     else if  $2idx - 2$  and  $2idx - 1$  are swapped by the permutation matrix  $\mathbf{P}_{n_1}^{\text{ABS}}$  in (7) then
7        $(d[1], d[2], \dots, d[L']) \leftarrow \text{Preswapped\_mode1}(n^*, idx, L, (d[1], d[2], \dots, d[L*]))$ 
8     else
9        $(d[1], d[2], \dots, d[L']) \leftarrow \text{Notswapped\_mode1}(n^*, idx, L, (d[1], d[2], \dots, d[L*]))$ 
10  if mode = 2 then
11    if  $2idx$  and  $2idx + 1$  are swapped by the permutation matrix  $\mathbf{P}_{n_1}^{\text{ABS}}$  in (7) then
12       $(d[1], d[2], \dots, d[L']) \leftarrow \text{Swapped\_mode2}(n^*, idx, L, (d[1], d[2], \dots, d[L*]))$ 
13    else if  $2idx - 2$  and  $2idx - 1$  are swapped by the permutation matrix  $\mathbf{P}_{n_1}^{\text{ABS}}$  in (7) then
14       $(d[1], d[2], \dots, d[L']) \leftarrow \text{Preswapped\_mode2}(n^*, idx, L, (d[1], d[2], \dots, d[L*]))$ 
15    else
16       $(d[1], d[2], \dots, d[L']) \leftarrow \text{Notswapped\_mode2}(n^*, idx, L, (d[1], d[2], \dots, d[L*]))$ 
17  for  $i = 1, 2, \dots, L'$  do
18    for  $j = 1, 2, \dots, n^*/2$  do
19       $d[i].r_1[m^*][j] \leftarrow d[i].r_1[m^*][j] + d[i].r_1[m^*][j + n^*/2]$ 
20      if mode = 2 then
21         $d[i].r_2[m^*][j] \leftarrow d[i].r_2[m^*][j] + d[i].r_2[m^*][j + n^*/2]$ 
22  if  $n^* = n/2$  then
23    for  $i = 1, 2, \dots, L'$  do
24      for  $j = 1, 2, \dots, n/2$  do
25         $d[i].final[j] \leftarrow d[i].r_1[m^*][j] + d[i].r_2[m^*][j]$ 
26         $d[i].final[j + n/2] \leftarrow d[i].r_2[m^*][j]$ 
27 if  $n^* = 1$  then
28   if mode = 1 then
29      $(d[1], d[2], \dots, d[L']) \leftarrow \text{Decode\_First\_Bit}(L, (d[1], d[2], \dots, d[L*]))$ 
30   if mode = 2 then
31      $(d[1], d[2], \dots, d[L']) \leftarrow \text{Decode\_Both\_Bits}(L, (d[1], d[2], \dots, d[L*]))$ 
32 return (d[1], d[2], ..., d[L'])

```

Algorithm 15: Swapped_mode1(n^* , idx , L , ($d[1], d[2], \dots, d[L^*]$))

Input: $n^* = 2^{m^*}$ is the number of pairs in the subcode currently being decoded; idx is the index of the adjacent-bits-channel whose inputs are currently being decoded; L is the upper bound on the list size; $d[1], d[2], \dots, d[L^*]$ are the list elements in the current list, where L^* is the current list size

Output: updated list elements ($d[1], d[2], \dots, d[L']$), where L' is the updated list size after decoding

```

1  $m^* \leftarrow \log_2(n^*)$  ▷  $m^*$  is an integer
2 ( $d[1], d[2], \dots, d[L^*]$ )  $\leftarrow$  Calculate_▽_Transform( $m^*$ , ( $d[1], d[2], \dots, d[L^*]$ ))
3 ( $d[1], d[2], \dots, d[L'']$ )  $\leftarrow$  ABS_Decoder( $n^*/2, 1, 2idx - 1, L$ , ( $d[1], d[2], \dots, d[L^*]$ ))
4 for  $i = 1, 2, \dots, L''$  do
5   for  $j = 1, 2, \dots, n^*/2$  do
6      $d[i].r_1[m^*][j] \leftarrow d[i].r_1[m^* - 1][j]$ 
7 ( $d[1], d[2], \dots, d[L'']$ )  $\leftarrow$  Calculate_◆_Transform( $m^*$ , ( $d[1], d[2], \dots, d[L'']$ ))
8 ( $d[1], d[2], \dots, d[L'']$ )  $\leftarrow$  ABS_Decoder( $n^*/2, 1, 2idx, L$ , ( $d[1], d[2], \dots, d[L'']$ ))
9 for  $i = 1, 2, \dots, L'''$  do
10   for  $j = 1, 2, \dots, n^*/2$  do
11      $d[i].r_1[m^*][j + n^*/2] \leftarrow d[i].r_1[m^* - 1][j]$ 
12 ( $d[1], d[2], \dots, d[L''']$ )  $\leftarrow$  Calculate_▲_Transform( $m^*$ , ( $d[1], d[2], \dots, d[L''']$ ))
13 ( $d[1], d[2], \dots, d[L']$ )  $\leftarrow$  ABS_Decoder( $n^*/2, 1, 2idx + 1, L$ , ( $d[1], d[2], \dots, d[L''']$ ))
14 for  $i = 1, 2, \dots, L'$  do
15   for  $j = 1, 2, \dots, n^*/2$  do
16      $d[i].cache[m^* - 1][j] \leftarrow d[i].r_1[m^*][j + n^*/2]$ 
17      $d[i].r_1[m^*][j + n^*/2] \leftarrow d[i].r_1[m^* - 1][j]$ 
18 return ( $d[1], d[2], \dots, d[L']$ )

```

Algorithm 16: Preswapped_mode1(n^* , idx , L , ($d[1], d[2], \dots, d[L^*]$))

Input: $n^* = 2^{m^*}$ is the number of pairs in the subcode currently being decoded; idx is the index of the adjacent-bits-channel whose inputs are currently being decoded; L is the upper bound on the list size; $d[1], d[2], \dots, d[L^*]$ are the list elements in the current list, where L^* is the current list size

Output: updated list elements ($d[1], d[2], \dots, d[L']$), where L' is the updated list size after decoding

```

1  $m^* \leftarrow \log_2(n^*)$  ▷  $m^*$  is an integer
2 for  $i = 1, 2, \dots, L^*$  do
3   for  $j = 1, 2, \dots, n^*/2$  do
4      $d[i].r_1[m^*][j] \leftarrow d[i].cache[m^* - 1][j]$ 
5 ( $d[1], d[2], \dots, d[L^*]$ )  $\leftarrow$  Calculate_◊_Transform( $m^*$ , ( $d[1], d[2], \dots, d[L^*]$ ))
6 ( $d[1], d[2], \dots, d[L']$ )  $\leftarrow$  ABS_Decoder( $n^*/2, 1, 2idx, L$ , ( $d[1], d[2], \dots, d[L^*]$ ))
7 for  $i = 1, 2, \dots, L'$  do
8   for  $j = 1, 2, \dots, n^*/2$  do
9      $d[i].r_1[m^*][j + n^*/2] \leftarrow d[i].r_1[m^* - 1][j]$ 
10 return ( $d[1], d[2], \dots, d[L']$ )

```

Algorithm 17: Not_swapped_mode1($n^*, idx, L, (d[1], d[2], \dots, d[L^*])$)

Input: $n^* = 2^{m^*}$ is the number of pairs in the subcode currently being decoded; idx is the index of the adjacent-bits-channel whose inputs are currently being decoded; L is the upper bound on the list size; $d[1], d[2], \dots, d[L^*]$ are the list elements in the current list, where L^* is the current list size

Output: updated list elements $(d[1], d[2], \dots, d[L'])$, where L' is the updated list size after decoding

```

1  $m^* \leftarrow \log_2(n^*)$  ▷  $m^*$  is an integer
2  $(d[1], d[2], \dots, d[L^*]) \leftarrow \text{Calculate\_}\nabla\text{\_Transform}(m^*, (d[1], d[2], \dots, d[L^*]))$ 
3  $(d[1], d[2], \dots, d[L']) \leftarrow \text{ABS\_Decoder}(n^*/2, 1, 2idx - 1, L, (d[1], d[2], \dots, d[L^*]))$ 
4 for  $i = 1, 2, \dots, L''$  do
5   for  $j = 1, 2, \dots, n^*/2$  do
6      $d[i].r_1[m^*][j] \leftarrow d[i].r_1[m^* - 1][j]$ 
7    $(d[1], d[2], \dots, d[L'']) \leftarrow \text{Calculate\_}\diamond\text{\_Transform}(m^*, (d[1], d[2], \dots, d[L'']))$ 
8    $(d[1], d[2], \dots, d[L']) \leftarrow \text{ABS\_Decoder}(n^*/2, 1, 2idx, L, (d[1], d[2], \dots, d[L'']))$ 
9 for  $i = 1, 2, \dots, L'$  do
10   for  $j = 1, 2, \dots, n^*/2$  do
11      $d[i].r_1[m^*][j + n^*/2] \leftarrow d[i].r_1[m^* - 1][j]$ 
12 return  $(d[1], d[2], \dots, d[L'])$ 

```

Algorithm 18: Swapped_mode2($n^*, idx, L, (d[1], d[2], \dots, d[L^*])$)

Input: $n^* = 2^{m^*}$ is the number of pairs in the subcode currently being decoded; idx is the index of the adjacent-bits-channel whose inputs are currently being decoded; L is the upper bound on the list size; $d[1], d[2], \dots, d[L^*]$ are the list elements in the current list, where L^* is the current list size

Output: updated list elements $(d[1], d[2], \dots, d[L'])$, where L' is the updated list size after decoding

```

1  $m^* \leftarrow \log_2(n^*)$  ▷  $m^*$  is an integer
2  $(d[1], d[2], \dots, d[L^*]) \leftarrow \text{Calculate\_}\blacktriangledown\text{\_Transform}(m^*, (d[1], d[2], \dots, d[L^*]))$ 
3  $(d[1], d[2], \dots, d[L']) \leftarrow \text{ABS\_Decoder}(n^*/2, 1, 2idx - 1, L, (d[1], d[2], \dots, d[L^*]))$ 
4 for  $i = 1, 2, \dots, L''$  do
5   for  $j = 1, 2, \dots, n^*/2$  do
6      $d[i].r_1[m^*][j] \leftarrow d[i].r_1[m^* - 1][j]$ 
7    $(d[1], d[2], \dots, d[L'']) \leftarrow \text{Calculate\_}\blacklozenge\text{\_Transform}(m^*, (d[1], d[2], \dots, d[L'']))$ 
8    $(d[1], d[2], \dots, d[L']) \leftarrow \text{ABS\_Decoder}(n^*/2, 1, 2idx, L, (d[1], d[2], \dots, d[L'']))$ 
9 for  $i = 1, 2, \dots, L'''$  do
10   for  $j = 1, 2, \dots, n^*/2$  do
11      $d[i].r_1[m^*][j + n^*/2] \leftarrow d[i].r_1[m^* - 1][j]$ 
12  $(d[1], d[2], \dots, d[L''']) \leftarrow \text{Calculate\_}\blacktriangle\text{\_Transform}(m^*, (d[1], d[2], \dots, d[L''']))$ 
13  $(d[1], d[2], \dots, d[L']) \leftarrow \text{ABS\_Decoder}(n^*/2, 2, 2idx + 1, L, (d[1], d[2], \dots, d[L''']))$ 
14 for  $i = 1, 2, \dots, L'$  do
15   for  $j = 1, 2, \dots, n^*/2$  do
16      $d[i].r_2[m^*][j] \leftarrow d[i].r_1[m^*][j + n^*/2]$ 
17      $d[i].r_1[m^*][j + n^*/2] \leftarrow d[i].r_1[m^* - 1][j]$ 
18      $d[i].r_2[m^*][j + n^*/2] \leftarrow d[i].r_2[m^* - 1][j]$ 
19 return  $(d[1], d[2], \dots, d[L'])$ 

```

Algorithm 19: Preswapped_mode2(n^* , idx , L , ($d[1], d[2], \dots, d[L^*]$))

Input: $n^* = 2^{m^*}$ is the number of pairs in the subcode currently being decoded; idx is the index of the adjacent-bits-channel whose inputs are currently being decoded; L is the upper bound on the list size; $d[1], d[2], \dots, d[L^*]$ are the list elements in the current list, where L^* is the current list size

Output: updated list elements ($d[1], d[2], \dots, d[L']$), where L' is the updated list size after decoding

```

1  $m^* \leftarrow \log_2(n^*)$  ▷  $m^*$  is an integer
2 for  $i = 1, 2, \dots, L^*$  do
3   for  $j = 1, 2, \dots, n^*/2$  do
4      $d[i].r_1[m^*][j] \leftarrow d[i].cache[m^* - 1][j]$ 
5  $(d[1], d[2], \dots, d[L^*]) \leftarrow \text{Calculate\_}\diamond\text{\_Transform}(m^*, (d[1], d[2], \dots, d[L^*]))$ 
6  $(d[1], d[2], \dots, d[L']) \leftarrow \text{ABS\_Decoder}(n^*/2, 1, 2idx, L, (d[1], d[2], \dots, d[L^*]))$ 
7 for  $i = 1, 2, \dots, L'$  do
8   for  $j = 1, 2, \dots, n^*/2$  do
9      $d[i].r_1[m^*][j + n^*/2] \leftarrow d[i].r_1[m^* - 1][j]$ 
10  $(d[1], d[2], \dots, d[L']) \leftarrow \text{Calculate\_}\Delta\text{\_Transform}(m^*, (d[1], d[2], \dots, d[L']))$ 
11  $(d[1], d[2], \dots, d[L']) \leftarrow \text{ABS\_Decoder}(n^*/2, 2, 2idx + 1, L, (d[1], d[2], \dots, d[L']))$ 
12 for  $i = 1, 2, \dots, L'$  do
13   for  $j = 1, 2, \dots, n^*/2$  do
14      $d[i].r_2[m^*][j] \leftarrow d[i].r_1[m^* - 1][j]$ 
15      $d[i].r_2[m^*][j + n^*/2] \leftarrow d[i].r_2[m^* - 1][j]$ 
16 return ( $d[1], d[2], \dots, d[L']$ )

```

Algorithm 20: Not_swapped_mode2($n^*, idx, L, (d[1], d[2], \dots, d[L^*])$)

Input: $n^* = 2^{m^*}$ is the number of pairs in the subcode currently being decoded; idx is the index of the adjacent-bits-channel whose inputs are currently being decoded; L is the upper bound on the list size; $d[1], d[2], \dots, d[L^*]$ are the list elements in the current list, where L^* is the current list size

Output: updated list elements $(d[1], d[2], \dots, d[L'])$, where L' is the updated list size after decoding

```

1  $m^* \leftarrow \log_2(n^*)$  ▷  $m^*$  is an integer
2  $(d[1], d[2], \dots, d[L^*]) \leftarrow \text{Calculate\_}\nabla\text{\_Transform}(m^*, (d[1], d[2], \dots, d[L^*]))$ 
3  $(d[1], d[2], \dots, d[L']) \leftarrow \text{ABS\_Decoder}(n^*/2, 1, 2idx - 1, L, (d[1], d[2], \dots, d[L^*]))$ 
4 for  $i = 1, 2, \dots, L''$  do
5   for  $j = 1, 2, \dots, n^*/2$  do
6      $d[i].r_1[m^*][j] \leftarrow d[i].r_1[m^* - 1][j]$ 
7    $(d[1], d[2], \dots, d[L'']) \leftarrow \text{Calculate\_}\diamond\text{\_Transform}(m^*, (d[1], d[2], \dots, d[L'']))$ 
8    $(d[1], d[2], \dots, d[L']) \leftarrow \text{ABS\_Decoder}(n^*/2, 1, 2idx, L, (d[1], d[2], \dots, d[L'']))$ 
9 for  $i = 1, 2, \dots, L'''$  do
10   for  $j = 1, 2, \dots, n^*/2$  do
11      $d[i].r_1[m^*][j + n^*/2] \leftarrow d[i].r_1[m^* - 1][j]$ 
12  $(d[1], d[2], \dots, d[L''']) \leftarrow \text{Calculate\_}\Delta\text{\_Transform}(m^*, (d[1], d[2], \dots, d[L''']))$ 
13  $(d[1], d[2], \dots, d[L']) \leftarrow \text{ABS\_Decoder}(n^*/2, 2, 2idx + 1, L, (d[1], d[2], \dots, d[L'']))$ 
14 for  $i = 1, 2, \dots, L'$  do
15   for  $j = 1, 2, \dots, n^*/2$  do
16      $d[i].r_2[m^*][j] \leftarrow d[i].r_1[m^* - 1][j]$ 
17      $d[i].r_2[m^*][j + n^*/2] \leftarrow d[i].r_2[m^* - 1][j]$ 
18 return  $(d[1], d[2], \dots, d[L'])$ 

```

Algorithm 21: Calculate_▽_Transform(m^* , (d[1], d[2], ..., d[L^*]))

Input: the first input m^* indicates that we calculate the arrays with index $m^* - 1$ from the arrays with index m^* ; d[1], d[2], ..., d[L^*] are the list elements in the current list, where L^* is the current list size

Output: updated list elements (d[1], d[2], ..., d[L^*])

```

1  $n' \leftarrow 2^{m^*-1}$ 
2 for  $i = 1, 2, \dots, L^*$  do
3   for  $j = 1, 2, \dots, n'$  do
4      $d[i].p_{0,0}[m^*-1][j] \leftarrow$ 
       $d[i].p_{0,0}[m^*][j] * d[i].p_{0,0}[m^*][j+n'] + d[i].p_{0,1}[m^*][j] * d[i].p_{0,1}[m^*][j+n'] +$ 
       $d[i].p_{1,0}[m^*][j] * d[i].p_{1,0}[m^*][j+n'] + d[i].p_{1,1}[m^*][j] * d[i].p_{1,1}[m^*][j+n']$ 
5      $d[i].p_{0,1}[m^*-1][j] \leftarrow$ 
       $d[i].p_{0,0}[m^*][j] * d[i].p_{0,1}[m^*][j+n'] + d[i].p_{0,1}[m^*][j] * d[i].p_{0,0}[m^*][j+n'] +$ 
       $d[i].p_{1,0}[m^*][j] * d[i].p_{1,1}[m^*][j+n'] + d[i].p_{1,1}[m^*][j] * d[i].p_{1,0}[m^*][j+n']$ 
6      $d[i].p_{1,0}[m^*-1][j] \leftarrow$ 
       $d[i].p_{0,0}[m^*][j] * d[i].p_{1,0}[m^*][j+n'] + d[i].p_{1,0}[m^*][j] * d[i].p_{0,0}[m^*][j+n'] +$ 
       $d[i].p_{0,1}[m^*][j] * d[i].p_{1,1}[m^*][j+n'] + d[i].p_{1,1}[m^*][j] * d[i].p_{0,0}[m^*][j+n']$ 
7      $d[i].p_{1,1}[m^*-1][j] \leftarrow$ 
       $d[i].p_{0,0}[m^*][j] * d[i].p_{1,1}[m^*][j+n'] + d[i].p_{0,1}[m^*][j] * d[i].p_{1,0}[m^*][j+n'] +$ 
       $d[i].p_{1,0}[m^*][j] * d[i].p_{0,1}[m^*][j+n'] + d[i].p_{1,1}[m^*][j] * d[i].p_{0,0}[m^*][j+n']$ 
8 return (d[1], d[2], ..., d[ $L^*$ ])

```

Algorithm 22: Calculate_◆_Transform(m^* , (d[1], d[2], ..., d[L^*]))

Input: the first input m^* indicates that we calculate the arrays with index $m^* - 1$ from the arrays with index m^* ; d[1], d[2], ..., d[L^*] are the list elements in the current list, where L^* is the current list size

Output: updated list elements (d[1], d[2], ..., d[L^*])

```

1  $n' \leftarrow 2^{m^*-1}$ 
2 for  $i = 1, 2, \dots, L^*$  do
3   for  $j = 1, 2, \dots, n'$  do
4     if  $d[i].r_1[m^*][j] = 0$  then
5        $q_{0,0} \leftarrow d[i].p_{0,0}[m^*][j] * d[i].p_{0,0}[m^*][j+n'] + d[i].p_{0,1}[m^*][j] * d[i].p_{0,1}[m^*][j+n']$ 
6        $q_{0,1} \leftarrow d[i].p_{1,0}[m^*][j] * d[i].p_{1,0}[m^*][j+n'] + d[i].p_{1,1}[m^*][j] * d[i].p_{1,1}[m^*][j+n']$ 
7        $q_{1,0} \leftarrow d[i].p_{0,0}[m^*][j] * d[i].p_{0,1}[m^*][j+n'] + d[i].p_{0,1}[m^*][j] * d[i].p_{0,0}[m^*][j+n']$ 
8        $q_{1,1} \leftarrow d[i].p_{1,0}[m^*][j] * d[i].p_{1,1}[m^*][j+n'] + d[i].p_{1,1}[m^*][j] * d[i].p_{1,0}[m^*][j+n']$ 
9     if  $d[i].r_1[m^*][j] = 1$  then
10       $q_{0,0} \leftarrow d[i].p_{1,0}[m^*][j] * d[i].p_{0,0}[m^*][j+n'] + d[i].p_{1,1}[m^*][j] * d[i].p_{0,1}[m^*][j+n']$ 
11       $q_{0,1} \leftarrow d[i].p_{0,0}[m^*][j] * d[i].p_{1,0}[m^*][j+n'] + d[i].p_{0,1}[m^*][j] * d[i].p_{1,1}[m^*][j+n']$ 
12       $q_{1,0} \leftarrow d[i].p_{1,0}[m^*][j] * d[i].p_{0,1}[m^*][j+n'] + d[i].p_{1,1}[m^*][j] * d[i].p_{0,0}[m^*][j+n']$ 
13       $q_{1,1} \leftarrow d[i].p_{0,0}[m^*][j] * d[i].p_{1,1}[m^*][j+n'] + d[i].p_{0,1}[m^*][j] * d[i].p_{1,0}[m^*][j+n']$ 
14      $sum \leftarrow q_{0,0} + q_{0,1} + q_{1,0} + q_{1,1}$ 
15      $d[i].p_{0,0}[m^*-1][j] \leftarrow q_{0,0}/sum, \quad d[i].p_{0,1}[m^*-1][j] \leftarrow q_{0,1}/sum$ 
16      $d[i].p_{1,0}[m^*-1][j] \leftarrow q_{1,0}/sum, \quad d[i].p_{1,1}[m^*-1][j] \leftarrow q_{1,1}/sum$ 
17 return (d[1], d[2], ..., d[ $L^*$ ])

```

Algorithm 23: Calculate_△_Transform(m^* , (d[1], d[2], ..., d[L^*]))

Input: the first input m^* indicates that we calculate the arrays with index $m^* - 1$ from the arrays with index m^* ; d[1], d[2], ..., d[L^*] are the list elements in the current list, where L^* is the current list size

Output: updated list elements (d[1], d[2], ..., d[L^*])

```

1   $n' \leftarrow 2^{m^*-1}$ 
2  for  $i = 1, 2, \dots, L^*$  do
3    for  $j = 1, 2, \dots, n'$  do
4      if  $d[i].r_1[m^*][j] = 0$  and  $d[i].r_1[m^*][j + n'] = 0$  then
5         $sum \leftarrow d[i].p_{0,0}[m^*][j] * d[i].p_{0,0}[m^*][j + n'] + d[i].p_{0,1}[m^*][j] * d[i].p_{0,1}[m^*][j + n'] + d[i].p_{1,0}[m^*][j] * d[i].p_{1,0}[m^*][j + n'] + d[i].p_{1,1}[m^*][j] * d[i].p_{1,1}[m^*][j + n']$ 
6         $d[i].p_{0,0}[m^* - 1][j] \leftarrow d[i].p_{0,0}[m^*][j] * d[i].p_{0,0}[m^*][j + n'] / sum$ 
7         $d[i].p_{0,1}[m^* - 1][j] \leftarrow d[i].p_{0,1}[m^*][j] * d[i].p_{0,1}[m^*][j + n'] / sum$ 
8         $d[i].p_{1,0}[m^* - 1][j] \leftarrow d[i].p_{1,0}[m^*][j] * d[i].p_{1,0}[m^*][j + n'] / sum$ 
9         $d[i].p_{1,1}[m^* - 1][j] \leftarrow d[i].p_{1,1}[m^*][j] * d[i].p_{1,1}[m^*][j + n'] / sum$ 
10      if  $d[i].r_1[m^*][j] = 0$  and  $d[i].r_1[m^*][j + n'] = 1$  then
11         $sum \leftarrow d[i].p_{0,0}[m^*][j] * d[i].p_{0,1}[m^*][j + n'] + d[i].p_{0,1}[m^*][j] * d[i].p_{0,0}[m^*][j + n'] + d[i].p_{1,0}[m^*][j] * d[i].p_{1,1}[m^*][j + n'] + d[i].p_{1,1}[m^*][j] * d[i].p_{1,0}[m^*][j + n']$ 
12         $d[i].p_{0,0}[m^* - 1][j] \leftarrow d[i].p_{0,1}[m^*][j] * d[i].p_{0,0}[m^*][j + n'] / sum$ 
13         $d[i].p_{0,1}[m^* - 1][j] \leftarrow d[i].p_{0,0}[m^*][j] * d[i].p_{0,1}[m^*][j + n'] / sum$ 
14         $d[i].p_{1,0}[m^* - 1][j] \leftarrow d[i].p_{1,1}[m^*][j] * d[i].p_{1,0}[m^*][j + n'] / sum$ 
15         $d[i].p_{1,1}[m^* - 1][j] \leftarrow d[i].p_{1,0}[m^*][j] * d[i].p_{1,1}[m^*][j + n'] / sum$ 
16      if  $d[i].r_1[m^*][j] = 1$  and  $d[i].r_1[m^*][j + n'] = 0$  then
17         $sum \leftarrow d[i].p_{0,0}[m^*][j] * d[i].p_{1,0}[m^*][j + n'] + d[i].p_{1,0}[m^*][j] * d[i].p_{0,0}[m^*][j + n'] + d[i].p_{0,1}[m^*][j] * d[i].p_{1,1}[m^*][j + n'] + d[i].p_{1,1}[m^*][j] * d[i].p_{0,1}[m^*][j + n']$ 
18         $d[i].p_{0,0}[m^* - 1][j] \leftarrow d[i].p_{1,0}[m^*][j] * d[i].p_{0,0}[m^*][j + n'] / sum$ 
19         $d[i].p_{0,1}[m^* - 1][j] \leftarrow d[i].p_{1,1}[m^*][j] * d[i].p_{0,1}[m^*][j + n'] / sum$ 
20         $d[i].p_{1,0}[m^* - 1][j] \leftarrow d[i].p_{0,0}[m^*][j] * d[i].p_{1,0}[m^*][j + n'] / sum$ 
21         $d[i].p_{1,1}[m^* - 1][j] \leftarrow d[i].p_{0,1}[m^*][j] * d[i].p_{1,1}[m^*][j + n'] / sum$ 
22      if  $d[i].r_1[m^*][j] = 1$  and  $d[i].r_1[m^*][j + n'] = 1$  then
23         $sum \leftarrow d[i].p_{0,0}[m^*][j] * d[i].p_{1,1}[m^*][j + n'] + d[i].p_{0,1}[m^*][j] * d[i].p_{1,0}[m^*][j + n'] + d[i].p_{1,0}[m^*][j] * d[i].p_{0,1}[m^*][j + n'] + d[i].p_{1,1}[m^*][j] * d[i].p_{0,0}[m^*][j + n']$ 
24         $d[i].p_{0,0}[m^* - 1][j] \leftarrow d[i].p_{1,1}[m^*][j] * d[i].p_{0,0}[m^*][j + n'] / sum$ 
25         $d[i].p_{0,1}[m^* - 1][j] \leftarrow d[i].p_{1,0}[m^*][j] * d[i].p_{0,1}[m^*][j + n'] / sum$ 
26         $d[i].p_{1,0}[m^* - 1][j] \leftarrow d[i].p_{0,1}[m^*][j] * d[i].p_{1,0}[m^*][j + n'] / sum$ 
27         $d[i].p_{1,1}[m^* - 1][j] \leftarrow d[i].p_{0,0}[m^*][j] * d[i].p_{1,1}[m^*][j + n'] / sum$ 
28  return (d[1], d[2], ..., d[ $L^*$ ])

```

VI. SIMULATION RESULTS

We conduct extensive simulations to compare the performance of the ABS polar codes and the standard polar codes over the binary-input AWGN channel with various choices of parameters. We have tested the performance for 4 different choices of code length 256, 512, 1024, 2048. For each choice of code length, we test 3 different code rates 0.3, 0.5 and 0.7. The comparison of decoding error probability is given in

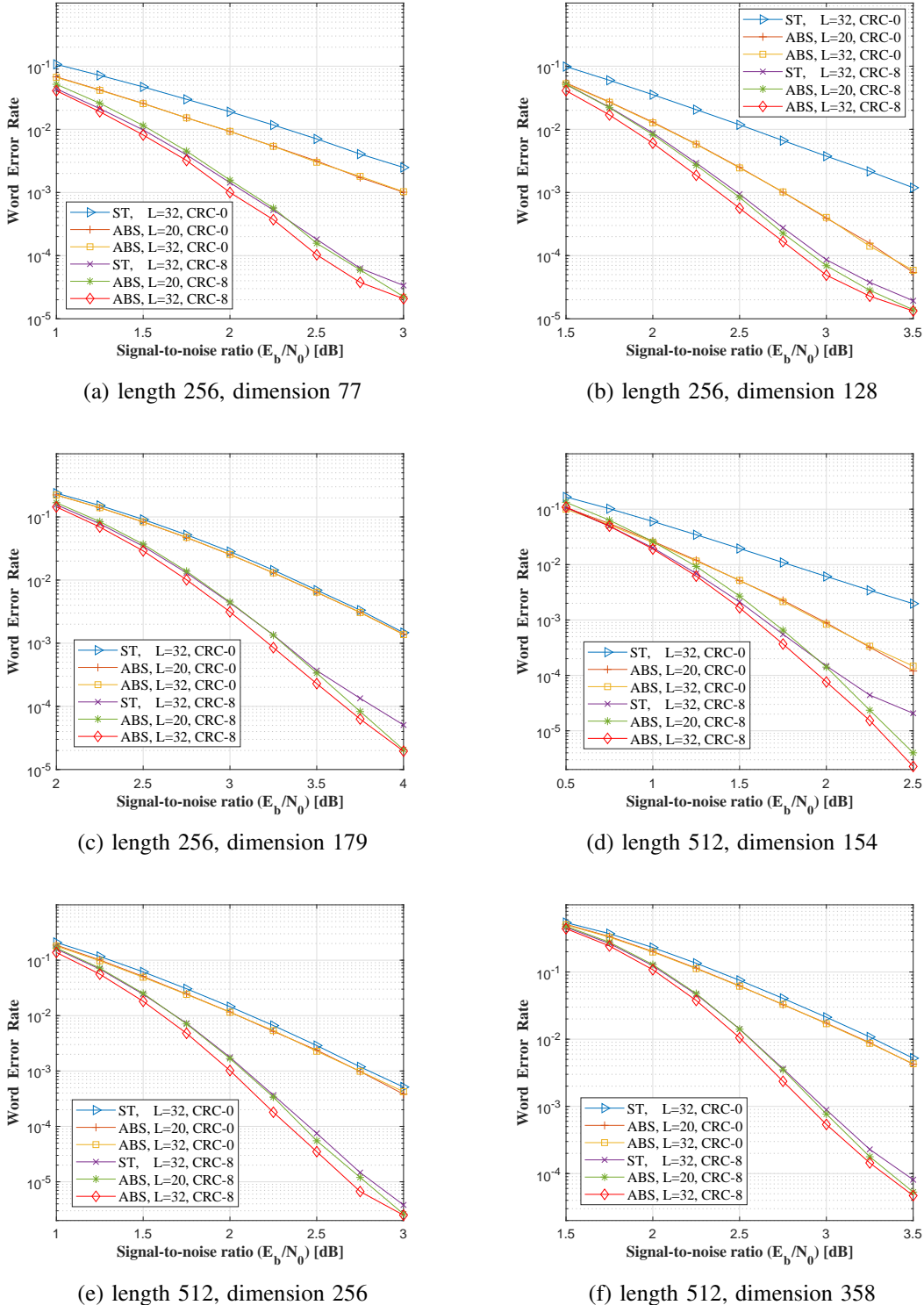


Fig. 6: Comparison between ABS polar codes and standard polar codes over the binary-input AWGN channel. The legend “ABS” refers to ABS polar codes, and “ST” refers to standard polar codes. “CRC-0” means that we do not use CRC. “CRC-8” means that the CRC length is 8. The parameter L is the list size. For standard polar codes, we always choose $L = 32$. For ABS polar codes, we test two different list sizes $L = 20$ and $L = 32$.

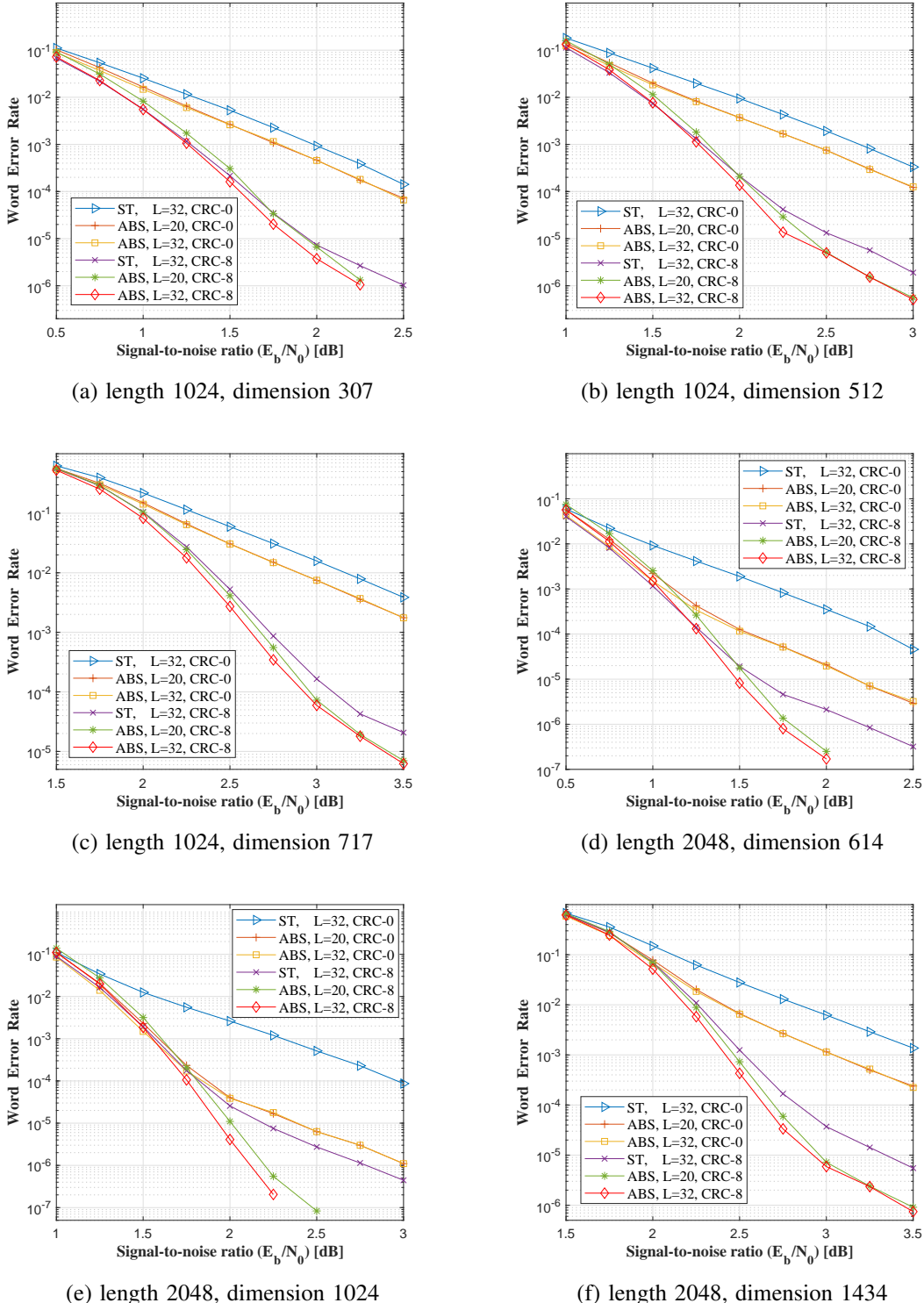


Fig. 7: Comparison between ABS polar codes and standard polar codes over the binary-input AWGN channel. The legend “ABS” refers to ABS polar codes, and “ST” refers to standard polar codes. “CRC-0” means that we do not use CRC. “CRC-8” means that the CRC length is 8. The parameter L is the list size. For standard polar codes, we always choose $L = 32$. For ABS polar codes, we test two different list sizes $L = 20$ and $L = 32$.

TABLE I: Comparison of the decoding time over the binary-input AWGN channel with $E_b/N_0 = 2$ dB. The row starting with (n, k) lists the code length and code dimension we have tested. The row starting with “ST, $L = 32$ ” lists the decoding time of the CRC-aided SCL decoder for standard polar codes with list size 32. The row starting with “ABS, $L = 20$ ” lists the decoding time of the CRC-aided SCL decoder for ABS polar codes with list size 20. The row starting with “ABS, $L = 32$ ” lists the decoding time of the CRC-aided SCL decoder for ABS polar codes with list size 32. The time unit “ms” is 10^{-3} s.

(n, k)	(256, 77)	(256, 128)	(256, 179)	(512, 154)	(512, 256)	(512, 358)
ST, $L = 32$	0.963ms	1.41ms	1.73ms	1.94ms	2.80ms	3.54ms
ABS, $L = 20$	0.816ms	1.24ms	1.47ms	1.86ms	2.66ms	3.10ms
ABS, $L = 32$	1.29ms	1.99ms	2.37ms	2.93ms	4.36ms	5.13ms

(n, k)	(1024, 307)	(1024, 512)	(1024, 717)	(2048, 614)	(2048, 1024)	(2048, 1434)
ST, $L = 32$	4.21ms	5.75ms	7.15ms	9.05ms	11.7ms	14.6ms
ABS, $L = 20$	4.32ms	5.90ms	6.67ms	10.6ms	12.6ms	14.0ms
ABS, $L = 32$	6.63ms	9.41ms	10.8ms	16.7ms	20.1ms	23.2ms

Fig. 6 and Fig. 7. Specifically, Fig. 6 contains the plots for code length 256 and 512; Fig. 7 contains the plots for code length 1024 and 2048. The comparison of decoding time is given in Table I.

In Fig. 6 and Fig. 7, for each choice of code length and code dimension, we compare the decoding error probability of the following 6 decoders: (1) SCL decoder for standard polar codes with list size 32 and no CRC; (2) SCL decoder for ABS polar codes with list size 20 and no CRC; (3) SCL decoder for ABS polar codes with list size 32 and no CRC; (4) SCL decoder for standard polar codes with list size 32 and CRC length 8; (5) SCL decoder for ABS polar codes with list size 20 and CRC length 8; (6) SCL decoder for ABS polar codes with list size 32 and CRC length 8. Note that for standard polar codes, we use the classic SCL decoder presented in Section V-A, **not** the new SCL decoder presented in Section V-B. For ABS polar codes, we use the SCL decoder presented in Section V-C.

From Fig. 6 and Fig. 7 we can see that the performance of ABS polar codes is consistently better than standard polar codes if we set the list size to be 32 for the CRC-aided SCL decoders of both codes. More specifically, for all 12 choices of (n, k) , the improvement of ABS polar codes over standard polar codes ranges from 0.15 dB to 0.6 dB. Even if we reduce the list size of ABS polar codes to be 20 and maintain the list size of standard polar codes to be 32, ABS polar codes still demonstrates better performance for all choices of parameters, and the improvement over standard polar codes is up to 0.5 dB in this case. Next let us compare the performance of ABS polar codes and standard polar codes when neither of them uses CRC. When there is no CRC, the performance of ABS polar codes with list size 20 is more or less the same as that of ABS polar codes with list size 32. Again, ABS polar codes consistently outperform standard polar codes for all 12 choices of (n, k) . This time the improvement over standard polar codes is up to 1.1 dB.

In Table I, we only compare the decoding time of the SCL decoders with CRC length 8. From Table I, we can see that the decoding time of the SCL decoder for ABS polar codes with list size 20 is more or less the same as the decoding time of the SCL decoder for standard polar codes with list size 32. More precisely, for 8 out of 12 choices of (n, k) , the SCL decoder for ABS polar codes with list size 20 runs faster. For the other 4 choices of (n, k) , the SCL decoder for standard polar codes with list size 32 runs faster. If we set the list size to be 32 for both the standard polar codes and the ABS polar codes, then Table I tells us that the decoding time of ABS polar codes is longer than that of standard polar codes by roughly 60%.

In conclusion, when we use list size 32 for the CRC-aided SCL decoders of both codes, ABS polar codes consistently outperform standard polar codes by 0.15 dB—0.6 dB, but the decoding time of ABS polar decoder is longer than that of standard polar codes by roughly 60%. If we use list size 20 for ABS polar codes and maintain the list size to be 32 for standard polar codes, then the decoding time is more or less the same for these two codes, and ABS polar codes still outperform standard polar codes for all choices of parameters. In this case, the improvement over standard polar codes is up to 0.5 dB.

As a final remark, the implementations of all the algorithms in this paper are available at the website <https://github.com/PlumJelly/ABS-Polar>

ACKNOWLEDGEMENT

In the implementation of our decoding algorithm, we have learned a lot from the GitHub project <https://github.com/kshabunov/ecclab> maintained by Kirill Shabunov. Shabunov's GitHub project mainly presents the implementation of the Reed-Muller decoder proposed in [11]. Due to the similarity between (ABS) polar codes and Reed-Muller codes, some of the accelerating techniques for Reed-Muller decoders can also be used to speed up (ABS) polar decoders.

APPENDIX A THE PROOF OF LEMMA 1

Let $(U_1, \dots, U_n), (X_1, \dots, X_n)$ and (Y_1, \dots, Y_n) be the random vectors defined in Fig. 2. Define a new vector $(\tilde{U}_1, \dots, \tilde{U}_n)$ as follows:

$$\tilde{U}_{2i-1} = U_{2i-1} + U_{2i} \text{ and } \tilde{U}_{2i} = U_{2i} \text{ for all } 1 \leq i \leq n/2.$$

Since $\mathbf{G}_n^{\text{polar}} = \mathbf{G}_{n/2}^{\text{polar}} \otimes \mathbf{G}_2^{\text{polar}}$, we have

$$\begin{aligned} (X_1, X_3, X_5, \dots, X_{n-1}) &= (\tilde{U}_1, \tilde{U}_3, \tilde{U}_5, \dots, \tilde{U}_{n-1}) \mathbf{G}_{n/2}^{\text{polar}}, \\ (X_2, X_4, X_6, \dots, X_n) &= (\tilde{U}_2, \tilde{U}_4, \tilde{U}_6, \dots, \tilde{U}_n) \mathbf{G}_{n/2}^{\text{polar}}. \end{aligned}$$

Therefore, the mapping from $\tilde{U}_{2i-1}, \tilde{U}_{2i+1}$ to $\tilde{U}_1, \tilde{U}_3, \dots, \tilde{U}_{2i-3}, Y_1, Y_3, \dots, Y_{n-1}$ is $V_i^{(n/2)}$, and the channel mapping from $\tilde{U}_{2i}, \tilde{U}_{2i+2}$ to $\tilde{U}_2, \tilde{U}_4, \dots, \tilde{U}_{2i-2}, Y_2, Y_4, \dots, Y_n$ is also $V_i^{(n/2)}$. Moreover, the two random vectors $(\tilde{U}_1, \tilde{U}_3, \dots, \tilde{U}_{n-1}, Y_1, Y_3, \dots, Y_{n-1})$ and $(\tilde{U}_2, \tilde{U}_4, \dots, \tilde{U}_n, Y_2, Y_4, \dots, Y_n)$ are independent. As a consequence,

$$\begin{aligned} &V_{2i-1}^{(n)}(y_1, y_2, \dots, y_n, u_1, u_2, \dots, u_{2i-2} | u_{2i-1}, u_{2i}) \\ &= \mathbb{P}_{Y_1, Y_2, \dots, Y_n, U_1, U_2, \dots, U_{2i-2} | U_{2i-1}, U_{2i}}(y_1, y_2, \dots, y_n, u_1, u_2, \dots, u_{2i-2} | u_{2i-1}, u_{2i}) \\ &= \frac{1}{4} \sum_{u_{2i+1}, u_{2i+2} \in \{0,1\}} \mathbb{P}_{Y_1, Y_2, \dots, Y_n, U_1, U_2, \dots, U_{2i-2} | U_{2i-1}, U_{2i}, U_{2i+1}, U_{2i+2}}(y_1, y_2, \dots, y_n, \\ &\quad u_1, u_2, \dots, u_{2i-2} | u_{2i-1}, u_{2i}, u_{2i+1}, u_{2i+2}) \\ &\stackrel{(a)}{=} \frac{1}{4} \sum_{u_{2i+1}, u_{2i+2} \in \{0,1\}} \mathbb{P}_{Y_1, Y_2, \dots, Y_n, \tilde{U}_1, \tilde{U}_2, \dots, \tilde{U}_{2i-2} | \tilde{U}_{2i-1}, \tilde{U}_{2i}, \tilde{U}_{2i+1}, \tilde{U}_{2i+2}}(y_1, y_2, \dots, y_n, \\ &\quad \tilde{u}_1, \tilde{u}_2, \dots, \tilde{u}_{2i-2} | \tilde{u}_{2i-1}, \tilde{u}_{2i}, \tilde{u}_{2i+1}, \tilde{u}_{2i+2}) \\ &= \frac{1}{4} \sum_{u_{2i+1}, u_{2i+2} \in \{0,1\}} \left(\mathbb{P}_{Y_1, Y_3, \dots, Y_{n-1}, \tilde{U}_1, \tilde{U}_3, \dots, \tilde{U}_{2i-3} | \tilde{U}_{2i-1}, \tilde{U}_{2i+1}}(y_1, y_3, \dots, y_{n-1}, \right. \\ &\quad \left. \tilde{u}_1, \tilde{u}_3, \dots, \tilde{u}_{2i-3} | \tilde{u}_{2i-1}, \tilde{u}_{2i+1}) \right. \\ &\quad \left. \cdot \mathbb{P}_{Y_2, Y_4, \dots, Y_n, \tilde{U}_2, \tilde{U}_4, \dots, \tilde{U}_{2i-2} | \tilde{U}_{2i}, \tilde{U}_{2i+2}}(y_2, y_4, \dots, y_n, \right. \\ &\quad \left. \tilde{u}_2, \tilde{u}_4, \dots, \tilde{u}_{2i-2} | \tilde{u}_{2i}, \tilde{u}_{2i+2}) \right) \\ &= \frac{1}{4} \sum_{u_{2i+1}, u_{2i+2} \in \{0,1\}} \left(V_i^{(n/2)}(y_1, y_3, \dots, y_{n-1}, \tilde{u}_1, \tilde{u}_3, \dots, \tilde{u}_{2i-3} | \tilde{u}_{2i-1}, \tilde{u}_{2i+1}) \right. \\ &\quad \left. \cdot V_i^{(n/2)}(y_2, y_4, \dots, y_n, \tilde{u}_2, \tilde{u}_4, \dots, \tilde{u}_{2i-2} | \tilde{u}_{2i}, \tilde{u}_{2i+2}) \right) \end{aligned}$$

$$\begin{aligned}
&= \frac{1}{4} \sum_{u_{2i+1}, u_{2i+2} \in \{0,1\}} \left(V_i^{(n/2)}(y_1, y_3, \dots, y_{n-1}, \tilde{u}_1, \tilde{u}_3, \dots, \tilde{u}_{2i-3} | u_{2i-1} + u_{2i}, u_{2i+1} + u_{2i+2}) \right. \\
&\quad \left. \cdot V_i^{(n/2)}(y_2, y_4, \dots, y_n, \tilde{u}_2, \tilde{u}_4, \dots, \tilde{u}_{2i-2} | u_{2i}, u_{2i+2}) \right) \\
&= (V_i^{(n/2)})^\nabla(y_1, y_2, \dots, y_n, \tilde{u}_1, \tilde{u}_2, \dots, \tilde{u}_{2i-2} | u_{2i-1}, u_{2i}),
\end{aligned}$$

where $\tilde{u}_1, \tilde{u}_2, \dots, \tilde{u}_{2i+2}$ in equality (a) are defined as $\tilde{u}_{2j-1} = u_{2j-1} + u_{2j}$ and $\tilde{u}_{2j} = u_{2j}$ for $1 \leq j \leq i+1$. Finally, by noting that there is a one-to-one mapping between $y_1, y_2, \dots, y_n, u_1, u_2, \dots, u_{2i-2}$ in the first line and $y_1, y_2, \dots, y_n, \tilde{u}_1, \tilde{u}_2, \dots, \tilde{u}_{2i-2}$ in the last line, we conclude that $V_{2i-1}^{(n)} = (V_i^{(n/2)})^\nabla$. The proofs of $V_{2i}^{(n)} = (V_i^{(n/2)})^\diamond$ and $V_{2i+1}^{(n)} = (V_i^{(n/2)})^\Delta$ are similar. We include them here for the sake of completeness.

$$\begin{aligned}
&V_{2i}^{(n)}(y_1, y_2, \dots, y_n, u_1, u_2, \dots, u_{2i-1} | u_{2i}, u_{2i+1}) \\
&= \mathbb{P}_{Y_1, Y_2, \dots, Y_n, U_1, U_2, \dots, U_{2i-1} | U_{2i}, U_{2i+1}}(y_1, y_2, \dots, y_n, u_1, u_2, \dots, u_{2i-1} | u_{2i}, u_{2i+1}) \\
&= \frac{1}{4} \sum_{u_{2i+2} \in \{0,1\}} \mathbb{P}_{Y_1, Y_2, \dots, Y_n, U_1, U_2, \dots, U_{2i-2} | U_{2i-1}, U_{2i}, U_{2i+1}, U_{2i+2}}(y_1, y_2, \dots, y_n, \\
&\quad u_1, u_2, \dots, u_{2i-2} | u_{2i-1}, u_{2i}, u_{2i+1}, u_{2i+2}) \\
&\stackrel{(a)}{=} \frac{1}{4} \sum_{u_{2i+2} \in \{0,1\}} \mathbb{P}_{Y_1, Y_2, \dots, Y_n, \tilde{U}_1, \tilde{U}_2, \dots, \tilde{U}_{2i-2} | \tilde{U}_{2i-1}, \tilde{U}_{2i}, \tilde{U}_{2i+1}, \tilde{U}_{2i+2}}(y_1, y_2, \dots, y_n, \\
&\quad \tilde{u}_1, \tilde{u}_2, \dots, \tilde{u}_{2i-2} | \tilde{u}_{2i-1}, \tilde{u}_{2i}, \tilde{u}_{2i+1}, \tilde{u}_{2i+2}) \\
&= \frac{1}{4} \sum_{u_{2i+2} \in \{0,1\}} \left(\mathbb{P}_{Y_1, Y_3, \dots, Y_{n-1}, \tilde{U}_1, \tilde{U}_3, \dots, \tilde{U}_{2i-3} | \tilde{U}_{2i-1}, \tilde{U}_{2i+1}}(y_1, y_3, \dots, y_{n-1}, \right. \\
&\quad \left. \tilde{u}_1, \tilde{u}_3, \dots, \tilde{u}_{2i-3} | \tilde{u}_{2i-1}, \tilde{u}_{2i+1}) \right. \\
&\quad \left. \cdot \mathbb{P}_{Y_2, Y_4, \dots, Y_n, \tilde{U}_2, \tilde{U}_4, \dots, \tilde{U}_{2i-2} | \tilde{U}_{2i}, \tilde{U}_{2i+2}}(y_2, y_4, \dots, y_n, \right. \\
&\quad \left. \tilde{u}_2, \tilde{u}_4, \dots, \tilde{u}_{2i-2} | \tilde{u}_{2i}, \tilde{u}_{2i+2}) \right) \\
&= \frac{1}{4} \sum_{u_{2i+2} \in \{0,1\}} \left(V_i^{(n/2)}(y_1, y_3, \dots, y_{n-1}, \tilde{u}_1, \tilde{u}_3, \dots, \tilde{u}_{2i-3} | \tilde{u}_{2i-1}, \tilde{u}_{2i+1}) \right. \\
&\quad \left. \cdot V_i^{(n/2)}(y_2, y_4, \dots, y_n, \tilde{u}_2, \tilde{u}_4, \dots, \tilde{u}_{2i-2} | \tilde{u}_{2i}, \tilde{u}_{2i+2}) \right) \\
&= \frac{1}{4} \sum_{u_{2i+2} \in \{0,1\}} \left(V_i^{(n/2)}(y_1, y_3, \dots, y_{n-1}, \tilde{u}_1, \tilde{u}_3, \dots, \tilde{u}_{2i-3} | u_{2i-1} + u_{2i}, u_{2i+1} + u_{2i+2}) \right. \\
&\quad \left. \cdot V_i^{(n/2)}(y_2, y_4, \dots, y_n, \tilde{u}_2, \tilde{u}_4, \dots, \tilde{u}_{2i-2} | u_{2i}, u_{2i+2}) \right) \\
&= (V_i^{(n/2)})^\diamond(y_1, y_2, \dots, y_n, \tilde{u}_1, \tilde{u}_2, \dots, \tilde{u}_{2i-2}, u_{2i-1}, u_{2i+1}),
\end{aligned}$$

where $\tilde{u}_1, \tilde{u}_2, \dots, \tilde{u}_{2i+2}$ in equality (a) are defined the same way as above. This proves $V_{2i}^{(n)} = (V_i^{(n/2)})^\diamond$.

$$\begin{aligned}
&V_{2i+1}^{(n)}(y_1, y_2, \dots, y_n, u_1, u_2, \dots, u_{2i} | u_{2i+1}, u_{2i+2}) \\
&= \mathbb{P}_{Y_1, Y_2, \dots, Y_n, U_1, U_2, \dots, U_{2i} | U_{2i+1}, U_{2i+2}}(y_1, y_2, \dots, y_n, u_1, u_2, \dots, u_{2i} | u_{2i+1}, u_{2i+2}) \\
&= \frac{1}{4} \mathbb{P}_{Y_1, Y_2, \dots, Y_n, U_1, U_2, \dots, U_{2i-2} | U_{2i-1}, U_{2i}, U_{2i+1}, U_{2i+2}}(y_1, y_2, \dots, y_n, \\
&\quad u_1, u_2, \dots, u_{2i-2} | u_{2i-1}, u_{2i}, u_{2i+1}, u_{2i+2}) \\
&\stackrel{(a)}{=} \frac{1}{4} \mathbb{P}_{Y_1, Y_2, \dots, Y_n, \tilde{U}_1, \tilde{U}_2, \dots, \tilde{U}_{2i-2} | \tilde{U}_{2i-1}, \tilde{U}_{2i}, \tilde{U}_{2i+1}, \tilde{U}_{2i+2}}(y_1, y_2, \dots, y_n, \\
&\quad \tilde{u}_1, \tilde{u}_2, \dots, \tilde{u}_{2i-2} | \tilde{u}_{2i-1}, \tilde{u}_{2i}, \tilde{u}_{2i+1}, \tilde{u}_{2i+2})
\end{aligned}$$

$$\begin{aligned}
&= \frac{1}{4} \mathbb{P}_{Y_1, Y_3, \dots, Y_{n-1}, \tilde{U}_1, \tilde{U}_3, \dots, \tilde{U}_{2i-3} | \tilde{U}_{2i-1}, \tilde{U}_{2i+1}}(y_1, y_3, \dots, y_{n-1}, \\
&\quad \tilde{u}_1, \tilde{u}_3, \dots, \tilde{u}_{2i-3} | \tilde{u}_{2i-1}, \tilde{u}_{2i+1}) \\
&\quad \cdot \mathbb{P}_{Y_2, Y_4, \dots, Y_n, \tilde{U}_2, \tilde{U}_4, \dots, \tilde{U}_{2i-2} | \tilde{U}_{2i}, \tilde{U}_{2i+2}}(y_2, y_4, \dots, y_n, \\
&\quad \tilde{u}_2, \tilde{u}_4, \dots, \tilde{u}_{2i-2} | \tilde{u}_{2i}, \tilde{u}_{2i+2}) \\
&= \frac{1}{4} V_i^{(n/2)}(y_1, y_3, \dots, y_{n-1}, \tilde{u}_1, \tilde{u}_3, \dots, \tilde{u}_{2i-3} | \tilde{u}_{2i-1}, \tilde{u}_{2i+1}) \\
&\quad \cdot V_i^{(n/2)}(y_2, y_4, \dots, y_n, \tilde{u}_2, \tilde{u}_4, \dots, \tilde{u}_{2i-2} | \tilde{u}_{2i}, \tilde{u}_{2i+2}) \\
&= \frac{1}{4} V_i^{(n/2)}(y_1, y_3, \dots, y_{n-1}, \tilde{u}_1, \tilde{u}_3, \dots, \tilde{u}_{2i-3} | u_{2i-1} + u_{2i}, u_{2i+1} + u_{2i+2}) \\
&\quad \cdot V_i^{(n/2)}(y_2, y_4, \dots, y_n, \tilde{u}_2, \tilde{u}_4, \dots, \tilde{u}_{2i-2} | u_{2i}, u_{2i+2}) \\
&= (V_i^{(n/2)})^\Delta(y_1, y_2, \dots, y_n, \tilde{u}_1, \tilde{u}_2, \dots, \tilde{u}_{2i-2}, u_{2i-1}, u_{2i}, u_{2i+1}, u_{2i+2}),
\end{aligned}$$

where $\tilde{u}_1, \tilde{u}_2, \dots, \tilde{u}_{2i+2}$ in equality (a) are defined the same way as above. This proves $V_{2i+1}^{(n)} = (V_i^{(n/2)})^\Delta$ and completes the proof of Lemma 1. \square

REFERENCES

- [1] E. Arikan, “Channel polarization: A method for constructing capacity-achieving codes for symmetric binary-input memoryless channels,” *IEEE Transactions on Information Theory*, vol. 55, no. 7, pp. 3051–3073, 2009.
- [2] I. Reed, “A class of multiple-error-correcting codes and the decoding scheme,” *Transactions of the IRE Professional Group on Information Theory*, vol. 4, no. 4, pp. 38–49, 1954.
- [3] D. E. Muller, “Application of boolean algebra to switching circuit design and to error detection,” *Transactions of the IRE professional group on electronic computers*, no. 3, pp. 6–12, 1954.
- [4] S. Kudekar, S. Kumar, M. Mondelli, H. D. Pfister, E. Şaşoğlu, and R. Urbanke, “Reed–Muller codes achieve capacity on erasure channels,” *IEEE Transactions on Information Theory*, vol. 63, no. 7, pp. 4298–4316, 2017.
- [5] G. Reeves and H. D. Pfister, “Reed–Muller codes achieve capacity on BMS channels,” 2021, arXiv:2110.14631.
- [6] M. Mondelli, S. H. Hassani, and R. L. Urbanke, “From polar to Reed–Muller codes: A technique to improve the finite-length performance,” *IEEE Transactions on Communications*, vol. 62, no. 9, pp. 3084–3091, 2014.
- [7] M. Ye and E. Abbe, “Recursive projection-aggregation decoding of Reed–Muller codes,” *IEEE Transactions on Information Theory*, vol. 66, no. 8, pp. 4948–4965, 2020.
- [8] S. H. Hassani, K. Alishahi, and R. Urbanke, “Finite-length scaling for polar codes,” *IEEE Transactions on Information Theory*, vol. 60, no. 10, pp. 5875–5898, 2014.
- [9] H. Hassani, S. Kudekar, O. Ordentlich, Y. Polyanskiy, and R. Urbanke, “Almost optimal scaling of Reed–Muller codes on BEC and BSC channels,” in *2018 IEEE International Symposium on Information Theory (ISIT)*, June 2018, pp. 311–315.
- [10] E. Abbe and M. Ye, “Reed–Muller codes polarize,” *IEEE Transactions on Information Theory*, vol. 66, no. 12, pp. 7311–7332, 2020.
- [11] I. Dumer and K. Shabunov, “Soft-decision decoding of Reed–Muller codes: Recursive lists,” *IEEE Transactions on Information Theory*, vol. 52, no. 3, pp. 1260–1266, 2006.
- [12] M. Lian, C. Häger, and H. D. Pfister, “Decoding Reed–Muller codes using redundant code constraints,” in *2020 IEEE International Symposium on Information Theory (ISIT)*, 2020, pp. 42–47.
- [13] M. Geiselhart, A. Elkelesh, M. Ebada, S. Cammerer, and S. ten Brink, “Automorphism ensemble decoding of Reed–Muller codes,” *IEEE Transactions on Communications*, vol. 69, no. 10, pp. 6424–6438, 2021.
- [14] I. Tal and A. Vardy, “How to construct polar codes,” *IEEE Transactions on Information Theory*, vol. 59, no. 10, pp. 6562–6582, 2013.
- [15] I. Tal, A. Sharov, and A. Vardy, “Constructing polar codes for non-binary alphabets and MACs,” in *2012 IEEE International Symposium on Information Theory Proceedings*, 2012, pp. 2132–2136.
- [16] U. Pereg and I. Tal, “Channel upgradation for non-binary input alphabets and MACs,” *IEEE Transactions on Information Theory*, vol. 63, no. 3, pp. 1410–1424, 2017.
- [17] T. C. Gulcu, M. Ye, and A. Barg, “Construction of polar codes for arbitrary discrete memoryless channels,” *IEEE Transactions on Information Theory*, vol. 64, no. 1, pp. 309–321, 2018.
- [18] I. Tal and A. Vardy, “List decoding of polar codes,” *IEEE Transactions on Information Theory*, vol. 61, no. 5, pp. 2213–2226, 2015.